ANL-83-36

ANL-83-36

COMPUTER MODEL FOR ANALYZING SODIUM COLD TRAPS

by

C. C. McPheeters and D. J. Raue

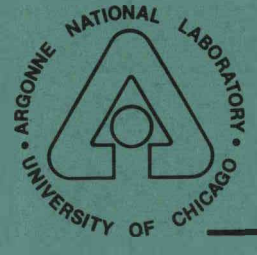

ARGONNE NATIONAL LABORATORY, ARGONNE, ILLINOIS

Operated by THE UNIVERSITY OF CHICAGO
for the U. S. DEPARTMENT OF ENERGY
under Contract W-31-109-Eng-38

DISCLAIMER

Printed in the United States of America
Available from
U. S. Department of Energy
Technical Information Center
P. O. Box 62
Oak Ridge, Tennessee 37830
Price: Printed Copy $9.50

Distribution Category:
LMFBR—Sodium Technology:
Applied Technology
(UC-79Ta)

ANL-83-36

ANL--83-36

DE83 026875

ARGONNE NATIONAL LABORATORY
9700 South Cass Avenue
Argonne, Illinois 60439

COMPUTER MODEL FOR ANALYZING SODIUM COLD TRAPS

by

C. C. McPheeters and D. J. Raue

Chemical Technology Division

May 1983

DISCLAIMER

TABLE OF CONTENTS

		Page
ABSTRACT		1
I.	INTRODUCTION	1
II.	COMPUTER MODEL DESCRIPTION	4
	A. Cold Trap Configuration	4
	B. Configuration of Cold Trap Simulation	5
	C. General Arrangement of Logic	5
	D. Calculation Methods	8
	1. Pressure Drop and Flow Correlation	8
	2. Temperature	9
	3. Impurity Concentration	9
	4. Impurity Mass Distribution	10
	E. Data Presentation Method	10
III.	COLD TRAP CASES FROM THE LITERATURE	12
	A. Billuris Cold Trap Tests	12
	B. MSA Sodium Cold Trap Tests	15
	C. Fermi Reactor Cold Trap Analysis	16
IV.	COLD TRAP EXPERIMENTS IN THIS STUDY	20
	A. Cold Trap ECT1	21
	B. CRBR Model Cold Trap	25
	C. Conclusions of Tests of Model Performance	27
VI.	PARAMETRIC STUDY OF COLD TRAP DESIGNS	28
	A. Objectives and Approach	29
	B. Results of Parametric Study	31
	C. Conclusions of Parametric Study	33
	D. Use of MASCOT in Cold Trap Design	33
ACKNOWLEDGMENTS		35
REFERENCES		35
APPENDIX.	MASCOT LISTING AND SAMPLE OUTPUT	37

LIST OF FIGURES

No.	Title	Page
1.	Schematic Representation of a Typical Sodium Cold Trap	3
2.	Five-Degree Slice of Cold Trap for Model Simulation	6
3.	The MASCOT Logic Flow Diagram	7
4.	Typical Three-Dimensional Plot of Mass Distribution	11
5.	Billuris Cold Trap for Testing Packing Materials	13
6.	Impurity Mass Distribution Calculated for the Billuris Cold Trap Compared with Experimental Results	14
7.	Cold Trap Used in the MSA Experiments	15
8.	Impurity Mass Distribution Calculated for the MSA Cold Trap Compared with the Experimental Results	17
9.	Design of the Fermi Primary System Cold Trap	18
10.	Impurity Mass Distribution Calculated for the Fermi Primary System Cold Trap Compared with the Experimental Results	19
11.	Design Configuration of ECT1	21
12.	Photograph of Bottom of ECT1 Mesh Section Moments after Removing Bottom Cap	23
13.	Impurity Mass Distribution in the ECT1 Case	24
14.	Configuration of the CRBR Model Cold Trap	25
15.	Impurity Mass Distribution Calculated and Measured in CRBR Model Cold Trap Case	27
16.	Pressure Drop across the CRBR Model Cold Trap as a Function of Quantity of Hydrogen Trapped	30
17.	Cold Trap Capacity as a Function of Annulus/Center Area Ratio and of Length/Diameter Ratio	31

LIST OF TABLES

No.	Title	Page
1.	Characteristics of the Billuris Cold Trap	13
2.	Characteristics of the MSA Cold Trap	16
3.	Characteristics of the Fermi Cold Trap	18
4.	Characteristics of the ECT1	22
5.	Results of Analyses of ECT1 Segments	24
6.	Characteristics of the CRBR Model Cold Trap	26
7.	Parameter Matrix Used in This Study	29

COMPUTER MODEL FOR ANALYZING SODIUM COLD TRAPS

by

C. C. McPheeters and D. J. Raue

ABSTRACT

Normal steam-side corrosion of steam-generator tubes in Liquid Metal Fast Breeder Reactors (LMFBRs) results in liberation of hydrogen, and most of this hydrogen diffuses through the tubes into the heat-transfer sodium and must be removed by the purification system. Cold traps are normally used to purify sodium, and they operate by cooling the sodium to temperatures near the melting point, where soluble impurities including hydrogen and oxygen precipitate as NaH and Na_2O, respectively. With the advent of large (1000 MWe) plants with correspondingly large steam generators, the rate of production of hydrogen will place a heavy burden on the purification system. Cold traps that would have lasted many years in smaller plants will become plugged with sodium hydride in about one year in the large plants. Cold trap technology is reexamined in this paper to determine where improvements in design can effect increases in impurity capacity. Cold traps currently in use in the U.S. become plugged when the impurities occupy approximately 10 to 20% of the available cold-trap volume (assuming theoretical density), while special designs have occasionally been shown to have capacities of 35 to 50% or more.

A computer model was developed to simulate the processes that occur in sodium cold traps. The Model for Analyzing Sodium Cold Traps (MASCOT) simulates any desired configuration of mesh arrangements and dimensions and calculates pressure drops and flow distributions, temperature profiles, impurity concentration profiles, and impurity mass distributions. The calculated pressure drop as a function of impurity mass content determines the capacity of the cold trap. The accuracy of the model was checked by comparing calculated mass distributions with experimentally determined mass distributions from literature publications and with results from our own cold trap experiments. The comparisons were excellent in all cases. A parametric study was performed to determine which design variables are most important in maximizing cold trap capacity. Maximum capacity can be obtained with cold traps having large annuli, relatively small center sections which are unpacked, and length-to-diameter ratios of approximately 1.5. Packing density is less important but should be low (less than 240 kg/m^3).

I. INTRODUCTION

Recirculating sodium systems, whether small experimental systems or large heat-transfer systems, must have some kind of impurity removal system in operation to prevent buildup of impurity concentrations. The impurities of

most concern in sodium systems are hydrogen and oxygen, which originate primarily from steam-generator corrosion, moisture from system-component surfaces, and leakage of air into the system. High concentrations of these impurities in sodium can result in rapid corrosion of the system components or plugging of the flow passages or both. In addition to the corrosion and plugging problems, the background hydrogen concentration must be kept low to allow sensitive detection of steam leaks into the sodium. Hydrogen meters are used for this purpose.[1]

Normal operation of 2-1/4Cr-1Mo steel as steam generator tubes results in slow, predictable corrosion of the steel by formation of an oxide layer. As the steel oxidizes, hydrogen is liberated from the reaction with water. This hydrogen preferentially enters the steel phase rather than the oxide or water phases. Once in the steel, the concentration gradient causes the hydrogen to diffuse toward and into the sodium. Observations of the hydrogen source in sodium systems operated with steam generators have shown that essentially all of the hydrogen produced by this corrosion mechanism enters the sodium rather than the steam.[2,3] The hydrogen source has been found to be $\sim 2 \times 10^{-11}$ $g \cdot s^{-1} \cdot cm^{-2}$ for this system. A large LMFBR can be expected to have a steam-generator surface area of $\sim 4 \times 10^{7}$ cm^2; thus, a typical hydrogen source rate would be ~0.8 mg/s or ~25 kg/y. This large hydrogen source rate requires that some changes be made in the conventional cold-trap design and operation, such as a significant increase in size, frequent cold-trap changes, in situ regeneration to remove the hydrogen,[4] or an increase in the capacity of the cold trap by design improvements. The Sodium Technology Program at Argonne National Laboratory has as its focus development of the technology for the latter two options, and this report addresses improvement of the cold trap design to increase capacity.

Sodium cold traps operate on the principle of differential solubility of impurities with temperature. The impurity of primary interest to the immediate problem is hydrogen; however, any impurity in sodium that has decreasing solubility with decreasing temperature should be removed by the cold trap. In the cold trap, sodium is cooled to a temperature near its freezing point. As it is cooled, the sodium flows through a bed of wire mesh and as the temperature drops, the impurities first become saturated, then supersaturated. From the supersaturated state, impurity crystals nucleate on the wire surfaces (or any other available solid surfaces), and crystals already present grow from the supersaturated solution. After passing through the wire mesh bed, the sodium is warmed up again and is returned to the main system.

Figure 1 is a schematic representation of a typical cold trap. For the purposes of this paper, the important components of the cold trap are the cooling channel where the heat is rejected, the annulus region, the center region, the bottom region, and the divider wall. Wire mesh packing is usually placed in either the annulus region or the center section or both. Some special designs have been tested in which no packing of any kind was included, and this case was included as a small part of this study. The temperature of the cold trap must be carefully controlled to assure that the saturation temperature occurs in the annulus region of the cold trap, where a large volume is available for the impurity crystals to precipitate and grow.

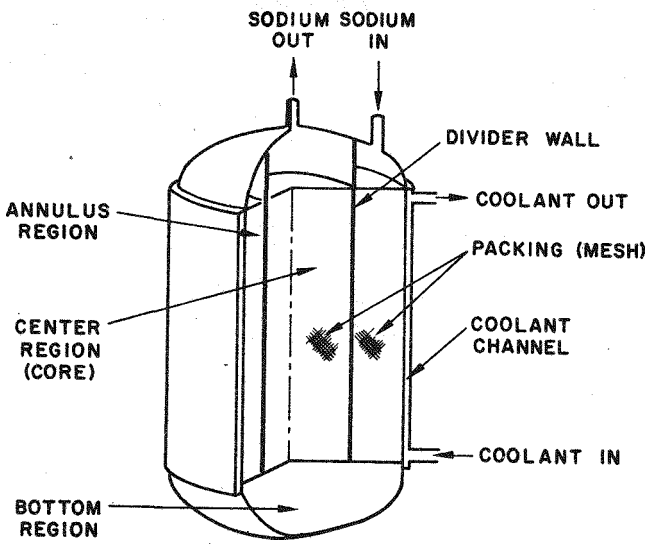

Fig. 1. Schematic Representation of a Typical Sodium Cold Trap

Design of cold traps has evolved over the years by gradual development of certain empirical design rules. The design process has traditionally included these steps: (1) the impurity source rates are determined, (2) the desired maximum impurity level is established for the system, (3) from these two numbers and an estimated cold trap efficiency, the required sodium flow rate is determined, (4) from experience and from the work of Gray et al.,[5] a requirement of a minimum residence time of 5 min in the cold trap is imposed, and the cold trap volume is calculated, (5) the length-to-diameter ratio is assumed to be in the range of 1 to 2, (6) the annulus and center region cross-sectional areas are assumed to be equal, (7) the wire mesh packing density is set at ∿240 to 320 kg/m^3 (15 to 20 lb/ft^3), (8) a heat exchanger is designed to be capable of cooling the sodium from the system temperature to the desired cold trap inlet temperature, and (9) the cooling surfaces on the outside of the cold trap are designed to handle the required heat rejection. Following this procedure and applying the appropriate safety factors, one can design a fairly traditional cold trap. As a check on the design, and possibly an important iteration step in the design process, the expected capacity of the cold trap is compared with the capacity requirements of the system. Cold trapping experience[6,7] indicates that the capacity for oxide can be expected to be in the range of 20 to 35 wt %. Unfortunately, little, if any, data are available on the capacity of cold traps for hydrogen. We may assume that the same volume occupied by the oxide could be occupied by the hydride at the point of cold trap plugging. On the basis of volume, the capacity of a typical cold trap should be in the range of 10 to 20 vol %.

It should be pointed out that the density of NaH, normally reported as 0.92 g/cm^3 in most handbooks,[8] is probably incorrect. Two other sources, Zintl and Harder[9] and Kuznetsov and Shkrabkina,[10] report densities of 1.38 g/cm^3 at room temperature. The latter data appear to be more reliable than the data reported in the handbooks.

The approach described above is effective in producing cold traps of fairly conventional design; however, it does not provide the designer with the capability of examining different cold trap designs for maximizing the capacity or of optimizing the design in other ways. The effect of various design changes on the operating characteristics or capacity of the cold trap could only be determined by long and expensive tests and development programs. Although several such programs had been run in the past,[11,12] the results are applicable only to specific cases or to reaching broad conclusions. The purpose of this work was to develop a computer model that could be used in the design process to determine the effect of certain design options on the performance of the cold trap. In addition to developing the model, we checked its accuracy by comparing it with experimental results from the literature, as well as with our own experimental results. The final step in the development work was to perform a parametric study to determine which design variables are most important and how they affect cold trap capacity.

II. COMPUTER MODEL DESCRIPTION

A. Cold Trap Configuration

Traditional cold-trap designs have a configuration similar to that shown in Fig. 1. One of the first decisions in developing the Model for Analyzing Sodium Cold Traps (MASCOT) was to retain the general configuration of the traditional design unless a major result of the study suggested a different configuration. The design features that were retained include the following: (1) sodium inlet at the top, (2) downflow in an annulus with cooling on the outer surface of the annulus, (3) counter-current flow of the coolant upward on the outer surface of the cold trap, (4) a bottom region where the downward flow from the annulus turns around and flows upward into the center region, (5) a center, cylindrical section with upward sodium flow and sodium exit at the top, and (6) a flow divider between the center section and the annulus. Within this general structure, it is possible to simulate a large variety of dimensions and packing density arrangements.

Originally, the model was developed with the option of selecting a variety of coolants; however, that option was eliminated because of its complexity. The important consideration is the sodium temperature gradient; therefore, the method of cooling the sodium, regardless of coolant used, was not considered as part of the model. The objective of the model is to calculate impurity mass distributions, and the method of rejecting heat is considered a separate problem. For convenience, NaK alloy was selected as the coolant, and it is considered to flow in a coolant jacket surrounding the cold trap.

With this model, the divider wall can be made either conducting or insulating, depending on the case being run; furthermore, the wire mesh packing can be specified in terms of wire diameter, packing density, and

location. Three separate wire diameters and packing densities may be used in each simulation, and the position of each of these packing densities may be specified. The special case of no packing may be specified for either the annulus or the center section or both. A special case consisting of once-through flow (with no return flow up the center section) can be simulated by making the center section very small and the annulus section very large. The mass deposited in the center section can then be ignored, and the annulus section represents the once-through cold trap. Other special cold-trap configurations, such as radial flow with (1) sodium inlets on the O.D. or (2) holes in the divider wall to short-circuit some of the sodium flow, cannot be simulated with MASCOT.

B. Configuration of Cold Trap Simulation

The MASCOT is a two-dimensional simulation of the cold trap configuration. Cylindrical symmetry of the cold trap is assumed to allow a two-dimensional array to represent the three-dimensional cold trap. The MASCOT uses a 5° slice of the cold trap as shown in Fig. 2. The inlet pressure of the sodium is assumed to be uniform along the radial dimension of the annulus so that the sodium flow is uniformly distributed in the annulus at the beginning of the simulation. The 5° slice is divided into four regions: (1) the center section, (2) the annulus section, (3) the coolant channel, and (4) the bottom section. The entire slice is divided into an array which is 15 columns wide by 40 rows high. The coolant channel is really a one-dimensional column which comprises column 15 of the array. The remaining 14 columns are divided, as desired by the user, between the center section and the annulus. The bottom section is a one-dimensional row with elements directly corresponding to the 14 columns of the packed section above.

Where possible, matrix calculations are done over the entire 14 by 40 array; however, in most cases, such as pressure/flow calculations, each section is calculated separately, and the pressure drop through each section is adjusted until the desired flow is achieved. In the case of temperature calculations, heat is conducted across the divider wall and the outer wall (unless the wall is insulating); however, flow and mass transfer are, of course, prohibited across these boundaries.

The wire mesh packing is specified in terms of wire diameter, mesh packing density, and location. Any desired number of locations may be specified for any of three packing densities. The locations are specified in rectangular regions by node number, from left margin to right margin and from top to bottom. Rectangular areas are specified in any given pattern until the entire slice is filled with mesh. Regions of "no packing" are specified by using a very small number for the packing density; for example, a density of 0.001 times the normal density would be effectively "no packing." The MASCOT is limited to having "no packing" specified for an entire section only, i.e., the entire center section must be either packed or not, and the same for the annulus region. Packing is not permitted in either of the other two sections.

C. General Arrangement of Logic

The logic flow of the MASCOT is shown in Fig. 3. The computer code is arranged with dimension statements, data input, and preliminary geometric

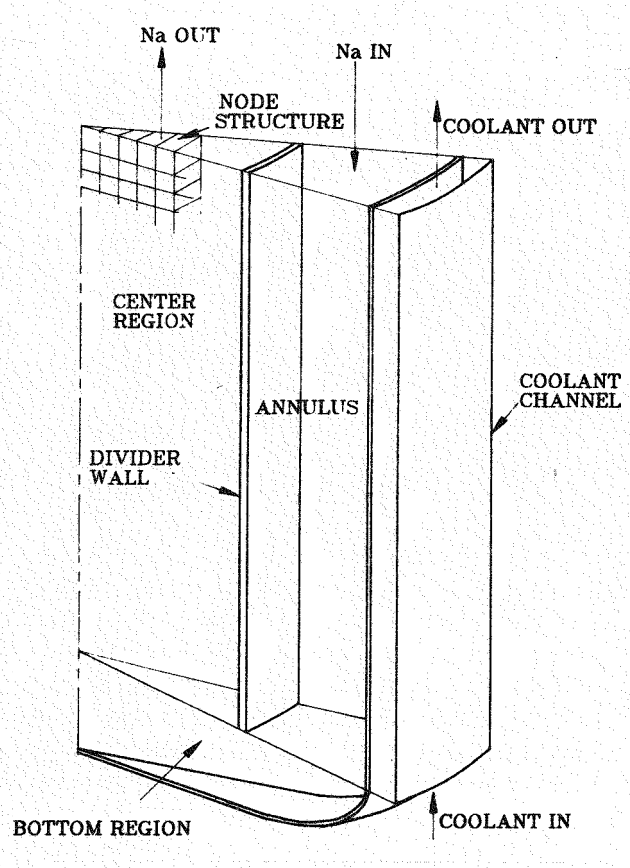

Fig. 2.

Five-Degree Slice of Cold Trap for Model Simulation

calculations at the beginning. The first major portion of the iteration section is the pressure/flow calculations. A uniform initial flow distribution is assumed, and the resulting pressure profile is calculated. The flow resulting from this pressure profile is then calculated, and this process is repeated until the pressures and flows in each node are unchanging. This brute-force method for calculating pressure and flow distributions in a packed bed is straightforward, but it is fairly inefficient in terms of computation time.

Once the flows are established, the next step is calculation of the temperatures. The same general approach is used in this calculation as in the pressure calculation. An initial temperature is set throughout the mesh region, and a heat balance is imposed. The temperatures are allowed to relax to their equilibrium values by repeated calculations through the nodes until each node temperature is unchanging. The overall heat balance is checked by calculating the heat removed by the coolant and comparing it with the heat lost by the sodium from inlet to outlet. At high sodium and NaK flows, the heat balance is very good; however, at very low flows in small cold traps the heat balance is poor. In the latter case, significant heat is lost to the incoming NaK, which is forced to remain at the inlet temperature. This heat imbalance for the small-cold-trap cases is not of serious concern since the main purpose of the model is to calculate impurity mass distribution rather than accurately represent heat transfer.

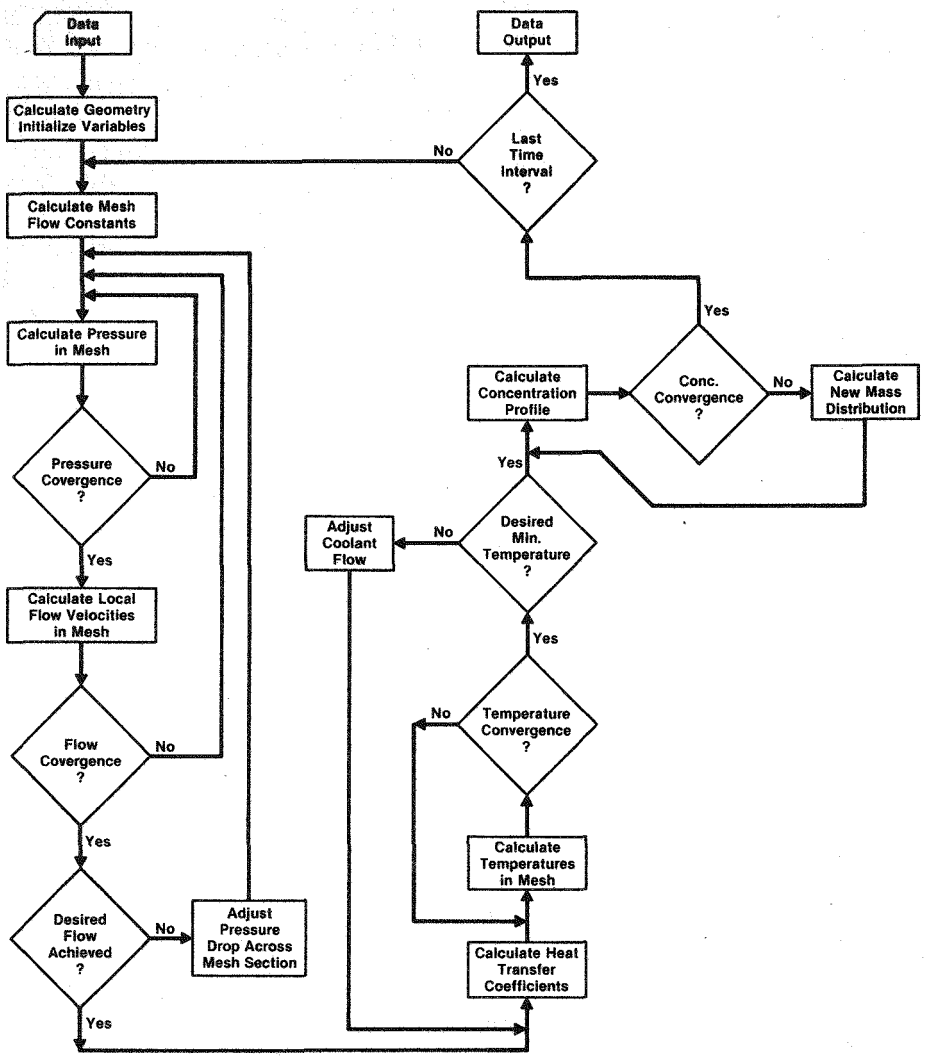

Fig. 3. The MASCOT Logic Flow Diagram

The next step in the calculation is the impurity concentration distribution. The same general method is used as before. Initial concentration values are set, and these values are allowed to relax to equilibrium values under forced mass balance. The situation is more complex in this case, however, because there are two ways mass can leave solution within each node: it can be carried out of the node with the flowing sodium, and it can precipitate on solid surfaces within the node. The concentration calculation continues in an iterative fashion until each node concentration is unchanging.

The final step is calculation of the impurity mass deposited in each node. This calculation is not of the iteration-type, but is done once for each node in the array. The rate of mass deposition in given by

$$\frac{dm}{dt} = kS(C-C_e) \qquad (1)$$

where m = the impurity mass, t = time, k = the mass transfer coefficient, S = the solid surface area, C = the impurity concentration in solution, and C_e = the equilibrium concentration at the node temperature. In the finite-difference calculation of this model, dt is a fairly large increment of time, and the incremental mass deposited, dm, is also fairly large. The assumption is that the other variables in the equation remain reasonably constant during the time step.

At the end of each time step, the computer code returns to the pressure/flow calculation. This process is repeated until either the maximum time specified by the user is reached or the pressure drop through the cold trap exceeds 48 kPa (1000 lb/ft^2).

D. Calculation Methods

1. Pressure Drop and Flow Correlation

Two pressure-drop correlations were considered for use in this model: the pressure drop through screens according to the work of Armour,[13] and the pressure drop through packed beds according to the work of Leva[14] presented in the Chemical Engineers' Handbook.[15] The latter correlation was chosen because of its more general applicability to a wide variety of packed-bed situations; its linear relationship with velocity was more easily handled in finite difference calculations. The pressure drop through a packed bed is given by

$$\Delta P = \frac{2 f_m G^2 L (1-\varepsilon)^{3-n}}{D_p g_c \rho \phi_s^{3-n} \varepsilon^3} \qquad (2)$$

where ΔP = the pressure drop through the bed, lb/ft^2; f_m = the friction factor = $100 \frac{\mu}{D_p G}$ for the cold trap flow regime; G = superficial mass velocity based on the cross-sectional area of the empty chamber, lb/s·ft^2; L = the bed depth, ft; ε = the void fraction; n = 1 for Reynolds Numbers less than 10, which is acceptable for the cold trap case; D_p = diameter of a sphere having the same volume as the bed particle, ft; g_c = the gravitational constant; ρ = fluid density, lb/ft^3; and ϕ_s = shape factor, which has been found to be 0.2 for Arnould's wire spirals (the closest to wire mesh that could be found). The wire mesh was assumed to be represented by wire "particles" that are 1-cm long and have the actual wire diameter. This assumption allowed us to define the "equivalent sphere" diameter, D_p, in terms of the wire "particle."

By combining constant terms and and converting mass velocity to actual fluid velocity, the pressure drop can be represented by the simpler equation

$$\Delta P = \frac{\alpha v A L^2}{V} \qquad (3)$$

where α is defined by the expression

$$\alpha = 155.42 \left(\frac{\mu(1-\epsilon)^2}{D_p^2 \epsilon^3} \right) \quad (4)$$

v = the actual fluid velocity, ft/s; A = the actual open cross-sectional area, ft^2; V = the open bed volume, ft^3; and μ = the fluid viscosity. The cold trap was divided into a 14 x 40 array of nodes, and each node was treated as a separate packed bed using the above relationships. The pressure drops between nodes were calculated both in the vertical and the radial directions.

2. Temperature

Two methods of heat transfer are assumed in this model: (1) simple conduction through barrier materials and sodium and (2) convection by the flowing sodium. The sodium flows calculated in the pressure/flow section are used to calculate the convective heat transfer rates. The conduction heat transfer is calculated as though the sodium were stagnant. The same node structure that was set up for the flow/pressure calculations is used in the heat transfer calculations and throughout the model. Film coefficients are used at the sodium/steel interfaces to account for the flow gradients in those regions.

Because the flow rates and Reynolds Numbers are so low in cold traps, the Nusselt Number was assumed to be constant. According to the Sodium-NaK Engineering Handbook,[16] the recommended value for the Nusselt Number is ~5.0, and this value was used for all film coefficients.

The relaxation technique was used to calculate the temperatures of the nodes, i.e., initial temperatures were assigned to the center, annulus, bottom, and coolant sections, and iterative calculations were used to relax these temperatures to their equilibrium values.

3. Impurity Concentration

Based on the temperature at each node, the equilibrium impurity concentration is calculated from published solubility relationships. The Smith[17] correlation was used for oxygen solubility, and the Vissers[1] correlation was used for hydrogen solubility. A mass balance was performed at each node to establish the correct impurity concentration at that node. Locations having temperatures above the impurity saturation temperature were assumed to have no impurity precipitation. The mass balance in those cases consisted of setting the concentration-times-mass-flow into the node equal to the concentration-times-mass-flow out of the node.

Locations having either temperatures below the impurity saturation temperature or some impurity mass already precipitated involved a more complicated mass balance. The product of concentration-times-mass-flow into the node was set equal to the sum of the rate of impurity mass precipitation and the concentration-times-mass-flow out of the node. The rate of impurity mass precipitation is given by Eq. 1 above.

At the beginning of the calculation, the surface area for mass deposition is taken simply as the solid steel surface in the node volume (including wall surfaces in nodes adjacent to walls). As the impurity accumulates, the surface area for precipitation increases. Several different models for describing this increase in surface area were examined, and the simplest model was selected. The impurities are assumed to precipitate as a continuous, solid mass on the wire or wall surfaces. The surface area increases linearly with the quantity of material deposited until ∿15% of the node volume is filled. The surface area is then held constant through the remainder of the calculation. The reasoning is that after the growing impurity crystals touch, the surface area no longer increases.

The same relaxation technique is used to calculate the equilibrium impurity concentration in the cold trap as are used in other parts of the model. Initial concentrations are assigned to each node, then repeated mass-balance calculations are performed until the concentration values are unchanging. Once these concentrations are unchanging, they are assumed to be at equilibrium.

4. Impurity Mass Distribution

The calculation for impurity mass distribution does not involve the iterative relaxation method. It is a once-through calculation that determines the total impurity mass accumulated in each node during the current time segment. Equation 1 is modified to the finite-difference form for use in this calculation:

$$\Delta m = Sk(C-C_e)\Delta t \qquad (5)$$

The assumption is made that the variables in the equation are essentially constant during the time interval being calculated. The ideal method for calculating the mass deposition would be to make the time interval very small so that the equation would approach a true differential; however, the computer time required for using a small time interval is prohibitive. The calculation method used by MASCOT is to divide the total (input) time of the calculation into 10 time segments. The Δt in the above equation is this time segment.

When the impurity mass deposition has been calculated, MASCOT goes back to the beginning of the pressure-flow calculation. The effect of the impurity deposits on the pressure and flow distribution is determined, and the calculation routine proceeds through the various calculations as before. This iteration procedure continues until either of two criteria are met: (1) the pressure drop through the cold trap exceedes 48 kPa (1000 lb/ft^2), or (2) ten times segments (the total time specified) have been completed. When MASCOT has completed all calculations, it simply exits the program with the message, "END OF SIMULATION." The MASCOT listing is included as Appendix A of this report.

E. Data Presentation Method

The output of MASCOT (See Appendix) consists of printed two-dimensional arrays of data. The data include sodium velocities through the mesh regions,

temperatures throughout the mesh regions and the bottom region, impurity concentrations throughout these regions, impurity mass in each node, and the volume percent of each node occupied by the impurity mass (assuming theoretical density). These data are printed out at the end of each time segment calculation.

It is difficult to visualize the distribution of the impurities in the regions of the cold trap by looking at printed two-dimensional arrays of data, so it was decided to develop three-dimensional plots of the calculated mass distributions.

Figure 4 is a typical three-dimensional display of the mass distribution calculated by MASCOT. Careful orientation is required to assure that the reader is properly viewing the three-dimensional plot. The five-degree slice of the cold trap is positioned horizontally at the base of the plot, with the centerline along the back edge and the top of the cold trap at the front left edge. The quantity of impurity deposited in each node is plotted vertically as volume percent of the node utilized (labeled "UTILIZATION, percent"). The divider wall position is marked by the vertical plane cutting through the center of the plot, and the sodium flow direction is indicated by the arrows on the left edge of the plot. In this figure, it can be seen that most of the impurity is deposited in the annulus region, and that little, if any, impurity deposition occurred in the center section.

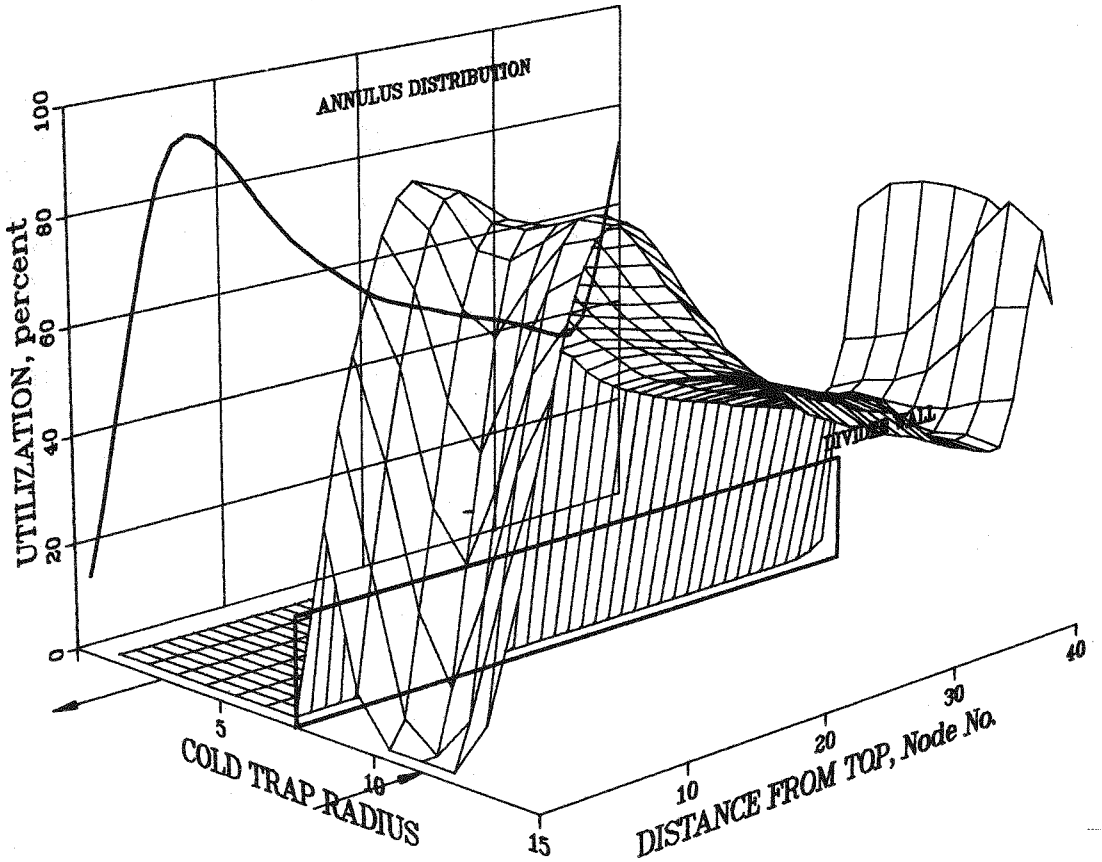

Fig. 4. Typical Three-Dimensional Plot of Mass Distribution

This method of presenting the MASCOT calculation data was chosen to allow easy visualization of the impurity distributions and the changes they undergo as the cold-trap design changes. In the following sections, this same type of data presentation is used. To avoid confusion, an attempt was made to keep the same orientation of the plot, axis labels, and numbering system. Note that the cold trap radius and the distance from the top are given as node numbers rather than unit dimensions. This method was used because the data are much easier to plot in this form; however, the true dimensions can be extracted from descriptions of the cold traps under study. The node spacings are always uniform, so they can be easily converted to actual dimensions.

III. COLD TRAP CASES FROM THE LITERATURE

Sodium cold traps have been in use since the 1950s in a wide variety of applications. During that time, several investigators have done thorough analyses to determine the distribution of impurities in specific cold traps after they had become plugged. The primary function of earlier cold traps was perceived to be removal of oxygen from sodium, so the studies were oriented toward the behavior of oxygen. The most important of these studies for our purposes were those of Billuris[18] and Rogers et al.[19] and the post-test examination of the Fermi cold trap.[20] In each of these studies, sufficient cold-trap design information is reported to allow simulation with MASCOT, and post-test analyses were done to determine the distribution of the impurities in the plugged cold trap.

A. Billuris Cold Trap Tests

In the late 1950s, Billuris[18] conducted a series of basic cold-trap experiments to determine which packing materials would be best for cold trap use. The cold trap that Billuris used in these tests was a simple once-through design with no heat regeneration, as shown in Fig. 5. Sodium entered the top of the cold trap, flowed downward through the packing as oil flowed upward through the coolant channel to remove heat, and the cool, purified sodium exited the cold trap at the bottom. The top of the cold trap was removable so that the internal packing could be removed for analysis after each test. Several types of packing were tested including Raschig rings, wire screen, and (of most interest to us) wire mesh; no packing was also tested. The design characteristics of the cold trap are listed in Table 1. The cold trap was loaded up with Na_2O by flowing sodium containing a high concentration of oxygen through the cold trap. This flow was continued until the cold trap became filled and the pressure drop increased to a high enough level to stop the sodium flow.

It was a challenge to make the MASCOT simulate the Billuris cold trap because MASCOT assumes the cold trap has a central tube with sodium flow upward, and the Billuris cold trap had no central tube. This problem was overcome in MASCOT by setting the size of the center tube very small, making the divider wall nonconducting, and placing no packing in the center tube. In this configuration, essentially all of the cold trap volume is in the large annulus. The center tube, although very small, was not allowed to plug because no surface area was present in those nodes on which impurities could deposit.

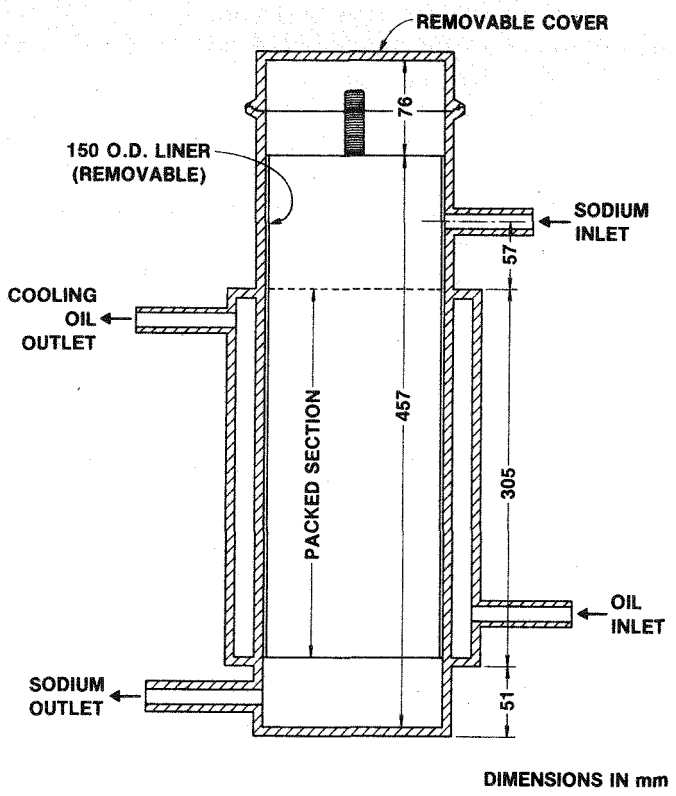

Fig. 5. Billuris Cold Trap for Testing Packing Materials

Table 1. Characteristics of the Billuris Cold Trap

Parameter	Value
Packing Type and Size	0.0152-cm-dia wire mesh
Mesh Density	0.0416 g/cm^3
Void Fraction	0.993
Sodium Flow	0.624 g/s
System Temperature	891 K (618°C)
Inlet Temperature	450 K (177°C)
Sodium Residence Time	470 s
Cold Trap Volume	5380 cm^3
Na_2O Capacity	20.3 vol %

The Billuris experiments were simulated with MASCOT by reading in the cold trap design parameters and the presumed operating conditions. (Unfortunately, the exact oxygen concentrations were not available.) Although we are more interested in the behavior of hydrogen in the cold trap, these experiments with oxygen are valuable for the purpose of testing the accuracy of the model for calculating impurity mass distributions. The MASCOT was run for these conditions until the pressure-drop limit was exceeded.

The assumption was made that the quantity of Na_2O in the inner annulus nodes adjacent to the small center tube would have prevailed in the center tube nodes as well. Therefore, the volume percent Na_2O calculated for the annulus nodes near the center tube were assigned to the nodes in the center tube as well, to simulate the Billuris cold trap design. The results were then plotted as described above and are shown in Fig. 6. The experimental results obtained by Billuris are plotted on the back plane of Fig. 6, along with the radial average of the calculated vol % utilizations. While the average curve does not pass directly through the experimental points, it is clear that the general pattern of impurity deposition is in good agreement between the experimental and calculated cases.

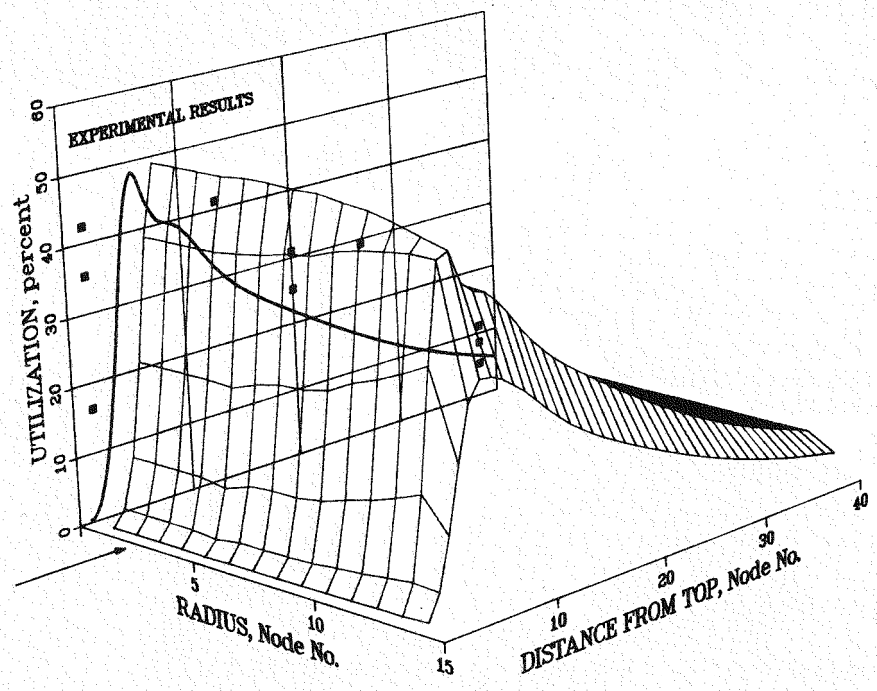

Fig. 6. Impurity Mass Distribution Calculated for the Billuris Cold Trap Compared with Experimental Results

An interesting point, illustrated in Fig. 6, is the decrease in mass deposition at the outer edge of the mesh (far right side of Fig. 6). Intuitively, one would expect an increase in mass deposition at this location

because it is cooler than the bulk sodium. However, another factor affecting mass deposition is the sodium flow rate through the region. This sodium flow is necessary to supply impurity mass to the region, and, near the outer wall, the flow is low due to frictional drag. The net effect is that less material is deposited near the wall than in the bulk mesh--a surprising result.

B. MSA Sodium Cold Trap Tests

During the 1960s, Mine Safety Appliances Research Corp. (MSA) conducted a series of tests to determine cold trap behavior in trapping oxygen and carbon. This work was done by Rogers et al.,[19] using an experimental sodium system with cold traps as shown in Fig. 7. The cold trap was of a very simple design that had sodium flow downward through an unpacked, narrow annulus, flow reversal at the bottom, and upward flow through a relatively large packed section in the center. The characteristics of the cold trap are listed in Table 2. The cold traps used in these experiments were not intentionally loaded with Na_2O, but became loaded in the course of other system operations. After the trap was removed from the system, samples were taken for analysis of the Na_2O distribution. These samples were taken by first drilling through

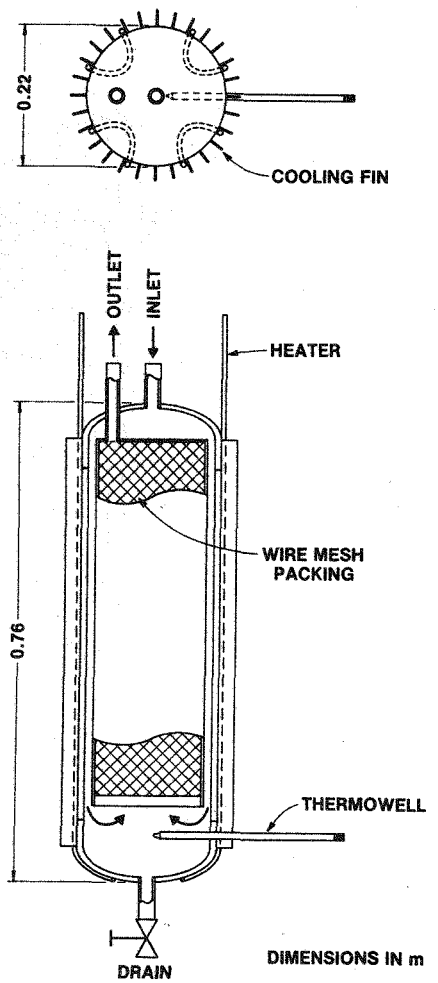

Fig. 7.

Cold Trap Used in the MSA Experiments

Table 2. Characteristics of the MSA Cold Trap

Parameter	Value
Packing Type and Size	0.028-cm-dia wire mesh
Mesh Density	0.192 g/cm^3
Sodium Flow	Not reported
System Temperature	700 K (427°C)
Inlet Temperature	700 K (427°C)
Cold Trap Volume	24730 cm^3

the outer wall and divider wall of the trap, then driving sharpened tubes into the center packed region. The samples were withdrawn and analyzed for Na_2O content.

The MASCOT was run using the design parameters and operating conditions of the MSA experiments, and the results of this run are shown in Fig. 8. It was not possible to run this case to plugging (large increase in pressure drop) because of the unusual behavior of Na_2O deposits in the annulus; therefore, the volume utilization reached a maximum of only ∿35% at the bottom of the packed section. As in the Billuris case, the calculated Na_2O distribution curve does not pass directly through the experimental points; however, the agreement between the experimental and calculated distributions is good. The Na_2O deposit is concentrated at the bottom of the mesh section in both cases. The reason for this concentration at the bottom of the mesh seems to be that the sodium is cooled far below the saturation temperature in the annulus, where little solid surface area is available for precipitation. The solution becomes supersaturated, and, when it enters the mesh, a large surface area is suddenly available and profuse precipitation occurs quickly.

An interesting feature of Fig. 8 is the large peaks of mass deposition in the annulus region. Where a decrease in mass deposition occurred near the wall in the Billuris cold trap, we find a large mass deposition on the wall in this case. The annulus is not packed in this case; thus, the only surface available for precipitation is the wall surface. The distribution of mass in the annulus is, therefore, determined by the availability of surface area rather than by the quantity of sodium flow. In the actual cold trap, the Na_2O that deposited on the walls of the annulus probably accumulated to a critical size, then broke off the wall and fell to the bottom of the cold trap. Unsupported Na_2O crystals probably would not have sufficient strength to withstand the hydraulic forces of the sodium flow.

C. Fermi Reactor Cold Trap Analysis

The most extensively analyzed cold trap in this study was the one removed from the primary sodium coolant system of the Fermi reactor[20] in February 1963. The Fermi cold trap was operated intermittently during the period from January

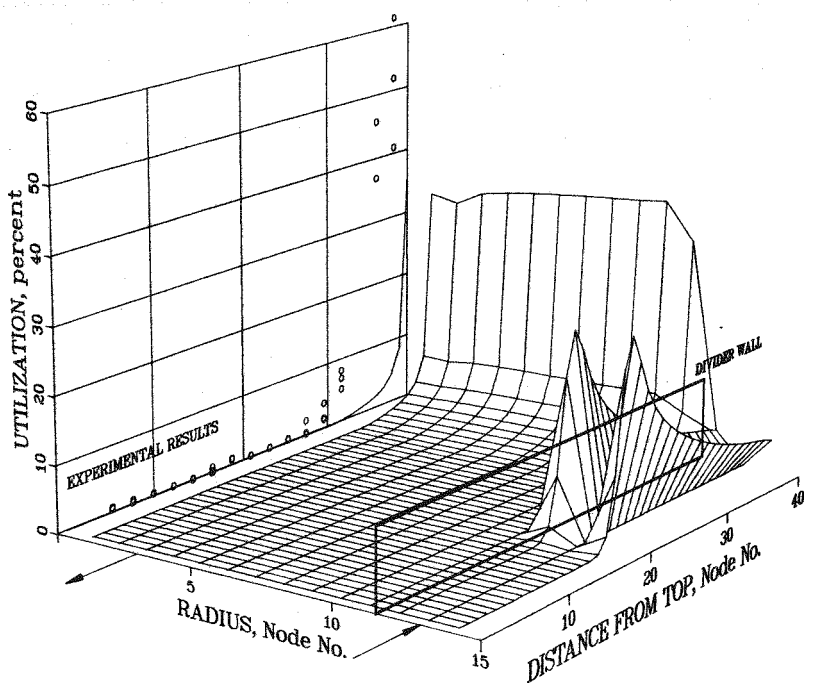

Fig. 8. Impurity Mass Distribution Calculated for the MSA Cold Trap Compared with the Experimental Results

1960 until its removal. The design configuration, shown in Fig. 9, was similar to that of the MSA experimental cold trap. Sodium flowed downward through a very narrow annulus that contained no packing material. A counterflow of cool NaK flowed in the outer jacket to cool the incoming sodium. The sodium flow direction reversed at the bottom of the trap and continued upward through a very large center section packed with wire mesh. The design features of the Fermi cold trap are listed in Table 3.

After the cold trap on the Fermi system had become plugged, it was removed, and samples were taken for analysis of impurity distributions. These samples were taken by first removing the coolant jacket, then drilling holes through the cold trap outer wall and the divider wall. Sharpened tubes were driven deeply into the center section to sample the sodium and impurity deposits. These tubes were long enough to allow several samples from the same axial position to be analyzed. Unfortunately, the annulus section was not sampled at all, since the experimenters did not expect to find any impurity deposits in that region. The samples were analyzed for Na_2O content as well as for a variety of other impurities.

The design features and operating conditions of the Fermi cold trap were read into the MASCOT, and the case was run. It was not possible to run the case all the way to plugging because of the large buildup of Na_2O deposits in the thin annulus. These large deposits caused calculational instabilities in the program before the mesh-section calculation could be completed. In the

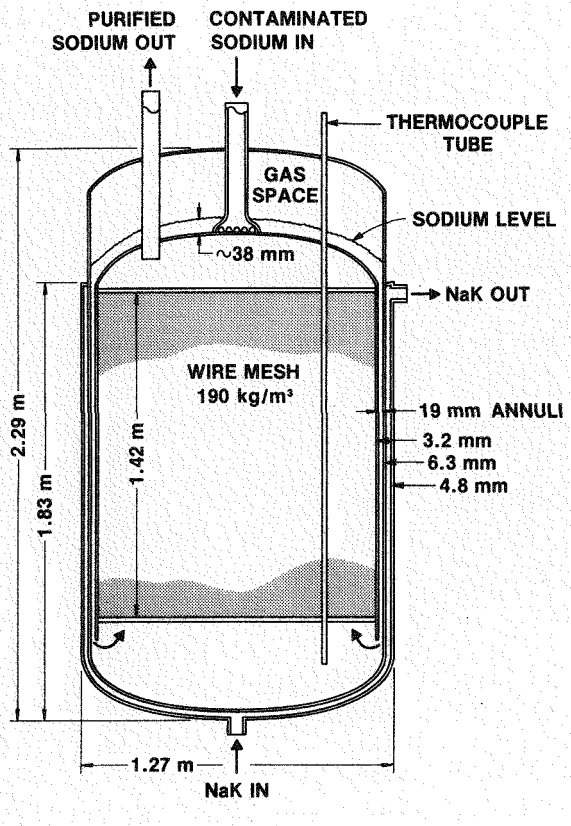

Fig. 9.

Design of the Fermi Primary System Cold Trap

Table 3. Characteristics of the Fermi Cold Trap

Parameter	Value
Packing Type and Size	0.028-cm-dia wire mesh
Mesh Density	0.192 g/cm^3
Sodium Flow	2850 g/s
System Temperature	813 K (540°C)
Inlet Temperature	393 to 753 K (120 to 480°C)
Sodium Residence Time	600 s
Cold Trap Volume	1.89 m^3
Capacity	2.0 vol %

actual cold trap, these deposits would likely have broken off the annulus walls and dropped to the bottom; however, the MASCOT has no mechanism for handling this sequence of events. Enough information was obtained in the calculation to allow comparison of the MASCOT results with the experimental measurements.

The Na_2O deposit distribution calculated for the Fermi case is shown in Fig. 10. The first feature that receives our attention, in Fig. 10, is the large deposits in the annulus region. As discussed above, these deposits would probably have spalled off the walls of the actual cold trap, so their significance should be minimized in this calculation. For our purposes, the most important feature of Fig. 10 is the Na_2O distribution in the mesh section. Note that the mass deposition is concentrated in the lower part of the central mesh section and that this location matches, very well, the location in which the Na_2O was found in the actual cold trap. Although the large mass desposits in the annulus prevented running the Fermi case to plugging, the trend of impurity mass deposition in the lower part of the center mesh section is in good agreement with the actual case. The shaded region represents the range of results from analyses of several samples from each axial location.

Operation of the Fermi cold trap resulted in an early increase in its pressure drop. The cold trap continued in operation, and after the pressure drop reached approximately 207 kPa (30 psi), the ΔP decreased to its normal

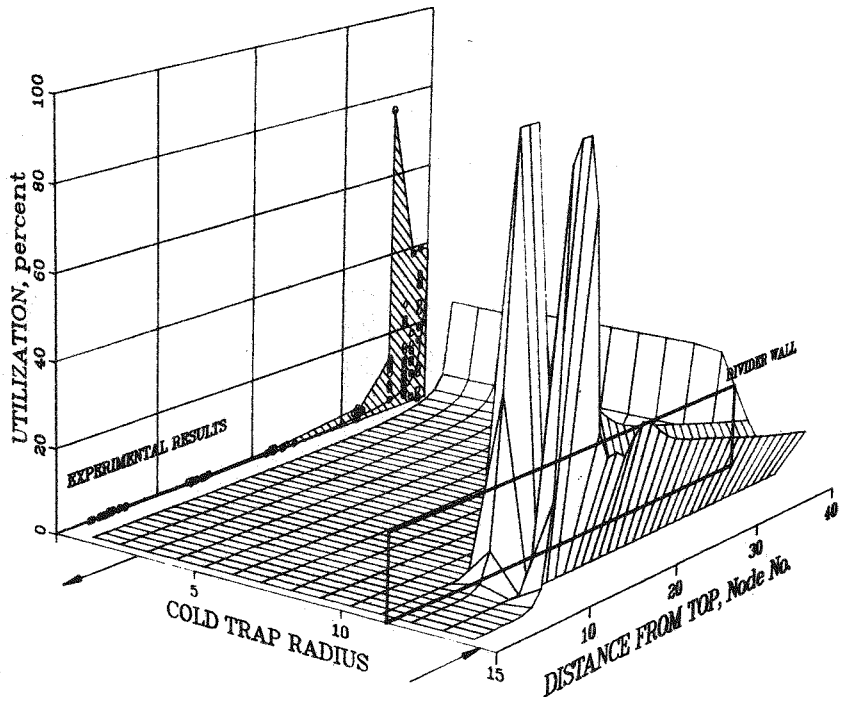

Fig. 10. Impurity Mass Distribution Calculated for the Fermi Primary System Cold Trap Compared with the Experimental Results

level of 69 kPa (10 psi). Post-test examination of the trap revealed that the large pressure drop had caused two effects: (1) the divider wall had collapsed slightly, and (2) the mesh had been pushed upward about four inches. These two deformations probably relieved some of the pressure by allowing some of the sodium flow to bypass the blockages in the lower mesh section and in the annulus.

The MASCOT simulation did not, of course, simulate the deformation effects which occurred in the Fermi cold trap; however, the calculation did reveal some of the possible causes of the deformations. The peak impurity concentration in the mesh determined by chemical analyses occurred a few inches above the bottom of the mesh (Fig. 10), rather than at the bottom edge as predicted by the model. This location for the peak was probably due to the mesh being pushed upward during operation. The observed impurity peak location corresponds with the post-test position of the bottom edge of the mesh.

IV. COLD TRAP EXPERIMENTS IN THIS STUDY

Essentially all of the cold-trap analysis data in the literature are concerned with the distribution of Na_2O in cold traps. While these data are important in confirming the accuracy of the computer model and in understanding the mechanisms of cold-trap operation, they are not directly applicable to the problem of NaH deposition in cold traps. There are two reasons why NaH is expected to behave differently from Na_2O: (1) the diffusivity of hydrogen in sodium is much greater than that of oxygen, and (2) the NaH mass per unit mass of hydrogen (24/1) is much greater than the Na_2O mass per unit mass of oxygen (62/16). The diffusivity difference has the effect of increasing the mass transfer coefficient, and, thus, the rate of mass deposition in a given location. The mass density difference has the effect of making the cold trap have less capacity for retaining hydrogen than for retaining oxygen.

To examine the effect of hydrogen on cold trap performance, it was necessary to test cold trap designs for hydrogen removal from sodium and to build into the MASCOT the capacity for handling hydrogen. The MASCOT is provided with the option of selecting either hydrogen or oxygen as part of the input data. When hydrogen is selected, the hydrogen diffusivity in sodium is used in the calculation of the mass transfer coefficient, and the hydrogen density in NaH is used for calculation of impurity density. In the same way, the oxygen data are used when oxygen is selected. An important point is that the diffusivity of hydrogen in sodium has not been reported in the literature. The diffusivity of oxygen in sodium was reported by Siegel and Epstein[21] and confirmed by Billuris[18] to be $\sim 5.6 \times 10^{-5}$ cm^2/s (extrapolated to cold trap temperatures). The hydrogen diffusivity was estimated to be approximately twice that value, or $\sim 1.1 \times 10^{-4}$ cm^2/s, as a first guess since no literature data are available.

Two tests were done in our study to determine the accuracy of the MASCOT model. The first test was done with a cold trap similar to the MSA and Fermi designs, and the trap was loaded to plugging with Na_2O. The second cold trap was similar to the typical cold trap configurations used in most sodium systems today; it was loaded to plugging with hydrogen. Both cold traps were small and were tested on the Apparatus for Monitoring and Purifying

Sodium (AMPS) located at ANL.[23] The AMPS is a forced-convection sodium system that contains ∿320 kg (700 lb) of sodium. The main sodium circuit has a sodium flow of 1 kg/s (20 gal/min); the experimental circuit has means for controlling the sodium flow in the range of 0 to 54 g/s (0 to 1 gal/min). The main system is designed for operation at temperatures up to 925 K (650°C) and pressures up to 450 kPa (50 psig). The experimental circuit has capabilities for measuring oxygen and hydrogen concentrations both on the inlet and the outlet of the experimental section where the cold trap tests were done.

A. Cold Trap ECT1

Experimental Cold Trap Number One (ECT1) was originally designed to test a vacuum evaporation process for removal of sodium from a loaded cold trap. The ECT1 had a long, thin configuration, as shown in Fig. 11. Sodium entered the top of the annulus and flowed downward through the narrow annulus to the bottom. Flow then reversed, and the sodium entered the bottom of the packed center section and flowed up and out of the trap. The bottom of the trap was attached with a Conoseal flange so that it could be removed after the test for inspection and analysis.

Oxygen was added to the AMPS sodium by means of a bed of Na_2O granules that were suspended in a flowing sodium stream in a system side leg. The temperature of the side leg was controlled so that the rate of oxygen

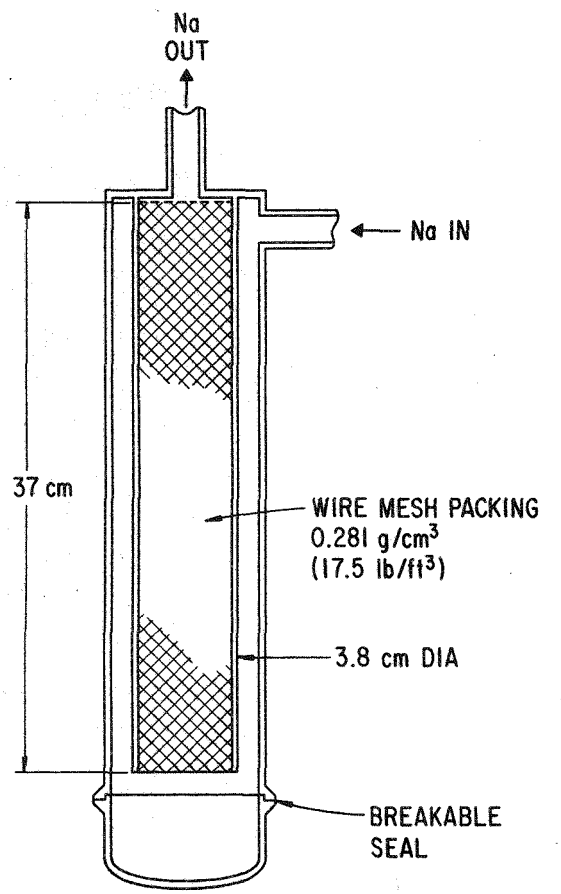

Fig. 11.

Design Configuration of ECT1

dissolution could be controlled to give the desired oxygen concentration in sodium entering the cold trap. Westinghouse-type electrochemical oxygen meters[22] were located in the sodium stream at the inlet to the cold trap and at the exit. The operating conditions and design details of the cold trap are listed in Table 4. The AMPS was operated at these constant conditions until ECT1 became plugged with Na_2O deposits. The test was then stopped, and ECT1 was removed from the system.

Table 4. Characteristics of the ECT1

Parameter	Value
Packing Type and Size	0.152-mm-dia wire mesh
Mesh Density	190 kg/m^3
Sodium Flow	6.4 g/s
System Temperature	623 K (350°C)
Inlet Temperature	443 K (170°C)
Sodium Residence Time	133 s
Cold Trap Volume	956 cm^3
Capacity	∿2%

The plugged ECT1 was then inverted and connected to the top of a drain tank which was connected to a vacuum system. The vacuum system was provided with a sodium-vapor trap on top of the drain tank to prevent sodium vapors from entering the vacuum components. The vapor trap was a refluxing type, packed with wire mesh. Sodium vapor in the gas stream condensed on the wire strands and ran back down into the drain tank. The ECT1 was heated to ∿630 K (360°C) under vacuum and was maintained at that temperature for 100 h to assure that all the sodium had been evaporated. It was then cooled to room temperature and transferred to an inert-environment glove box for disassembly and examination. The Conoseal union was disconnected, and the bottom was removed. A very thin layer of Na_2O crystals was observed on the inner surfaces in the annulus and on the bottom cap. A very heavy deposit of Na_2O crystals was observed on the bottom edge of the wire mesh packing. These crystal layers are shown in Fig. 12, which is a photograph of ECT1 taken moments after it was opened. One important observation in this photograph is that little, if any, Na_2O settled to the bottom of the cold trap. Apparently all of the deposition occurred on solid surfaces; this observation supports one of the key assumptions of the MASCOT model, i.e., that all nucleation is heterogeneous in sodium cold traps.

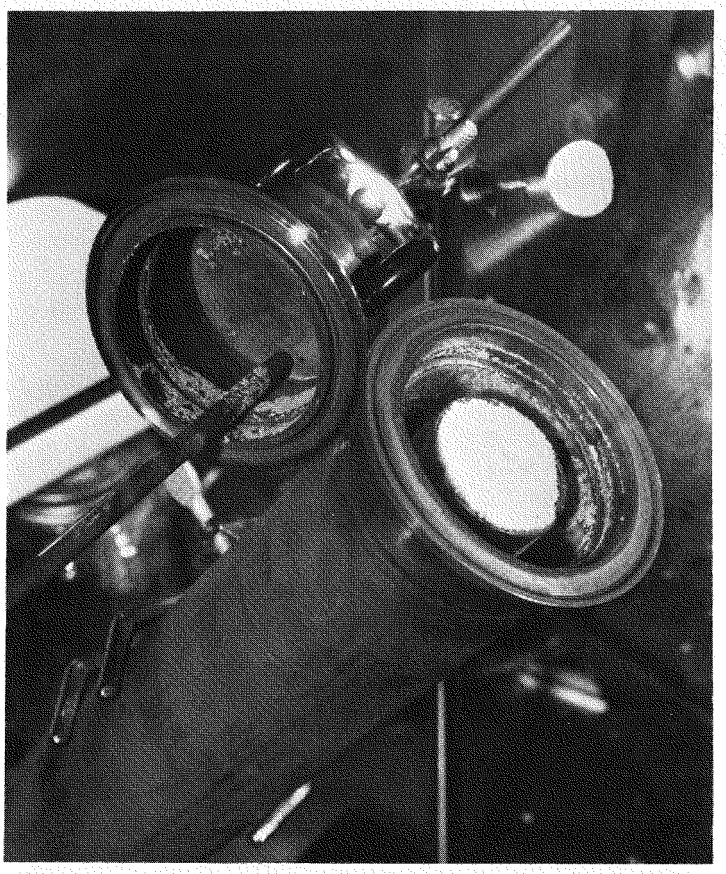

Fig. 12. Photograph of Bottom of ECT1 Mesh Section Moments after Removing Bottom Cap (ANL Neg. No. 308-80-445)

The center section of ECT1 was removed, cut into one-inch segments, and analyzed for both total sodium and elemental sodium. The total sodium less the elemental sodium was used to calculate the amount of Na_2O in each segment. The results of these analyses are presented in Table 5. Essentially all of the Na_2O was located in the bottom segment; incidentally, the evaporation method was found to be very effective, in this case, for removing sodium from cold-trap deposits. However, the deposit was not very thick, so this experiment was not a severe test of the evaporation method.

The operating conditions and geometric configuration of ECT1 were input to MASCOT, and the case was run. The results of the simulation were plotted in the same manner as were previous cases. The Na_2O distribution in ECT1 is shown in Fig. 13, where both the distribution calculated by MASCOT and the experimental results are shown. Note that very little Na_2O is deposited in the annulus in this case, in contrast to the large amounts observed in the MSA and Fermi cases. This effect is probably due to the very low oxgyen concentration in the inlet sodium in the ECT1 case as opposed to the relatively large concentrations in the MSA and Fermi cases. The low concentration provided a much smaller source of impurities for deposition on the ECT1 walls.

Table 5. Results of Analyses of ECT1 Segments

Sample Number	Distance from top, cm	Quantity, of Na_2O, g	Volume of Na_2O, vol %
1a[a]	0.32	4.09	29.5
1	1.27	4.09	5.9
2,3	5.08	0.10	0.09
4	8.89	0.0031	0.006
5,6	12.7	0.009	0.008
7,8	17.8	0.0093	0.008
9,10,11	24.1	0.0124	0.007
12	29.2	0.0496	0.089
13,14	33.0	1.64	1.48

[a]Sample 1 with all oxide assumed in first 0.64 cm of mesh.

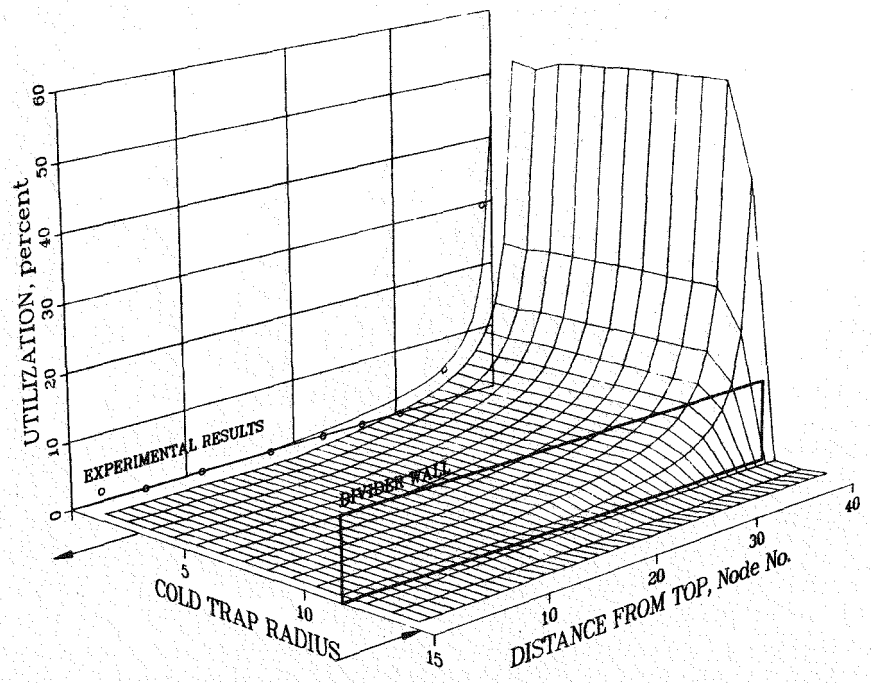

Fig. 13. Impurity Mass Distribution in the ECT1 Case

Although the annulus walls were not analyzed for quantity of Na_2O, the visual observation (Fig. 12) confirmed that little deposition occurred in that location. The agreement between the MASCOT calculation and the experimental measurements is excellent.

B. CRBR Model Cold Trap

The second cold trap tested in this program was originally designed as a scale model of the cold trap for Clinch River Breeder Reactor (CRBR) Intermediate Heat Transport System (IHTS). In later years, the design of the CRBR IHTS cold trap was changed several times; however, the designation, "CRBR model cold trap," was kept for the purposes of our program. Of course, the scale of the model is many times smaller (~1:7) than the real CRBR cold trap. The CRBR model cold trap is shown schematically in Fig. 14. This design is significantly different from the ECT1 design in several respects: (1) the cross-sectional areas of the annulus and the center section are approximately equal, (2) the mesh packing density is greater, (3) the overall size is greater, and (4) the sodium entrance is arranged to provide a tangential component to more uniformly distribute the flow in the annulus. The cold trap was air-cooled, and cooling fins were provided on the outside surface to enhance the heat transfer.

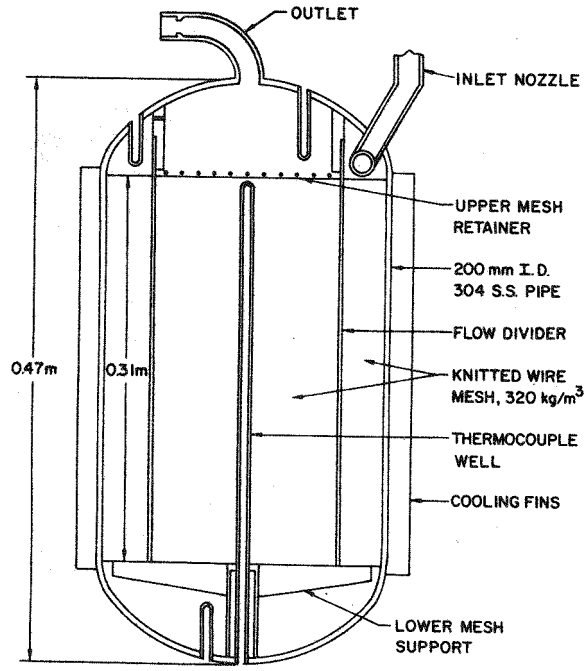

Fig. 14.

Configuration of the CRBR Model Cold Trap

The CRBR model cold trap was operated on the AMPS system for several years and was used to test an in situ method for cold trap regeneration.[4] During this service, it was loaded with hydrogen to plugging five times, and after each loading, it was regnerated by heating under vacuum. Under vacuum, NaH decomposes, and the rate of decomposition becomes practical at temperatures

above 573 K (300°C). After the fifth regeneration cycle, the cold trap was loaded under very carefully controlled conditions for the final time. Hydrogen was injected into the sodium by diffusion through nickel membranes. Pure hydrogen was introduced into a closed, thin-walled nickel tube at a pressure of ∿170 kPa (10 psig), and it diffused through the tube wall into the sodium. Hydrogen concentrations in the sodium entering and exiting the cold trap were measured with diffusion-type hydrogen meters.[1] The design details and operating conditions of the CRBR model cold trap are listed in Table 6.

Table 6. Characteristics of the CRBR Model Cold Trap

Parameter	Value
Packing Type and Size	0.0152-cm-dia wire mesh
Mesh Density	320 kg/m^3
Divider Radius	7.6 cm
Outer Radius	11 cm
Sodium Flow	4.6 g/s
Inlet H Concentration	1.2 ppm
System Temperature	623 K (350°C)
Inlet Temperature	483 K (210°C)
Minimum Temperature	413 K (140°C)
Sodium Residence Time	744 s
Cold Trap Volume	3800 cm^3
Capacity	18.3%

The CRBR model cold trap was the most carefully documented case in this study (in terms of operating parameters and hydrogen inlet concentration) because the experiment was performed specifically for the purpose of testing the MASCOT model. The operating conditions and geometry of the cold trap were input to the MASCOT with an accuracy limited only by the error of the experimental measurements. This accuracy is in contrast to most of the above experiments, where some of the values of parameters had to be guessed, based on our own experience and on general system operating procedures.

The CRBR case was run with MASCOT to calculate the expected hydrogen distribution. The results of this calculation are presented in the usual format in Fig. 15. The hydrogen distribution in this case was essentially

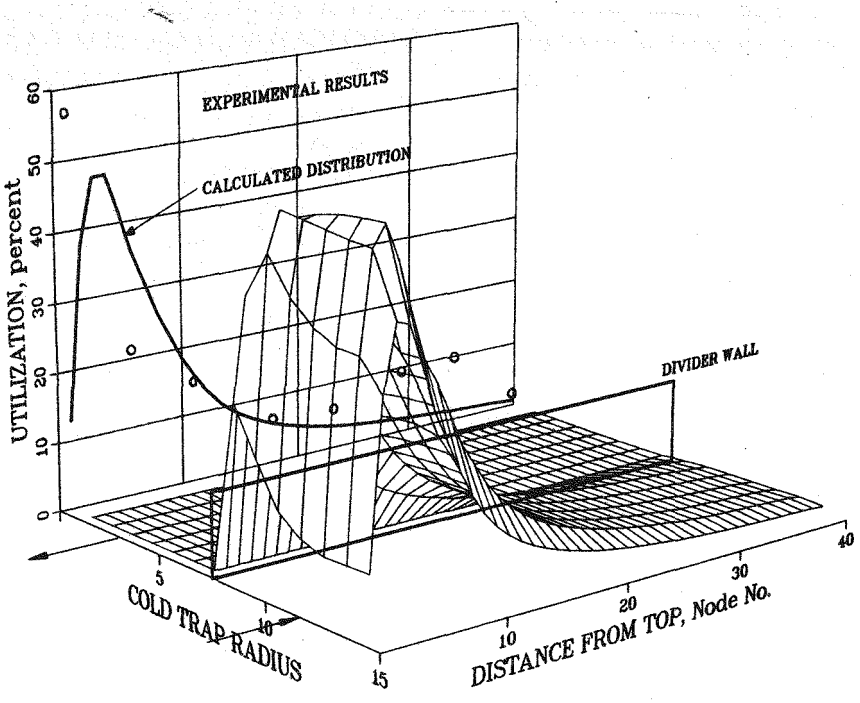

Fig. 15. Impurity Mass Distribution Calculated and Measured in CRBR Model Cold Trap Case

all concentrated in the upper part of the annulus region, and the agreement between the model calculation and the experimental results is good. The position of the NaH deposit is a direct result of the operating conditions, i.e., the hydrogen concentration at the inlet was high (1.2 ppm) and constant during the entire experiment. This condition results in precipitation near the inlet end of the annulus. If the hydrogen concentration had been reduced to a low level (say, 0.2 ppm) for a short time, the NaH deposit would have redissolved and reprecipitated near the bottom of the cold trap. This type of redistribution can be done during operation of the cold trap to extend its life, if the system operator has the flexibility to perform such an operation, i.e., no upset of the system to deal with.

It should be noted that the method used to cool the cold trap seems to have no significant effect on the impurity mass distribution. The MASCOT uses NaK coolant in all cases, while some of the cold trap cases that were calculated (including the CRBR model) were cooled by air.

C. Conclusions of Tests of Model Performance

The MASCOT has been shown to calculate accurately the distribution of impurity mass deposits in cold traps, both from data in the literature and from data generated in experiments in this work. Although the general pattern of mass distribution has been shown to be calculated accurately by MASCOT, the absolute values of the concentrations in different positions are not accurately calculated. Part of this failure to calculate accurate absolute concentrations

is due to lack of accurate historical data; however, much of the failure can be blamed on failure of the MASCOT. The method used to calculate pressures and flows in the mesh regions is limited in its ability to treat the case where the flow passages are almost blocked. When the flow passages are very open with greater than 90% void fraction, the pressures and flows are calculated very effectively; however, when the void fraction is reduced to less than 20%, the pressure calculation tends to "blow up," i.e., become unstable and create unusual and erratic mass distributions.* As a consequence of this unstable behavior, some cold trap cases cannot be completely evaluated beyond ∿80% plugging. It has been found, though, that the point at which the calculation procedure fails corresponds well to the point of cold trap plugging; thus, the point of failure of the calculation can be taken as a reasonable approximation of the point of plugging of the cold trap.

The conclusions of this study of the accuracy of the MASCOT model in simulating actual cold trap cases can be summarized as follows:

1. The pattern of impurity deposition in cold traps of a wide variety of designs and operating conditions was simulated very well by MASCOT.

2. The MASCOT simulation was equally good for both hydrogen and oxygen in sodium.

3. Although the pattern of mass distribution was good, the absolute values of mass deposition were sometimes different than the actual cases.

4. The MASCOT model should be suitable for use in studying various cold trap configurations and the effect of design variables on the capacity of the cold traps for retaining impurity deposits.

5. The MASCOT model should be useful in assisting cold trap designers to achieve designs optimized for specific applications.

6. The MASCOT model cannot simulate unusual cold-trap configurations, nor can it handle changes in configuration (such as movement of the mesh) during a run.

VI. PARAMETRIC STUDY OF COLD TRAP DESIGNS

One of the earliest and most important uses of the MASCOT model was to study the effect of many different design variables on the performance of cold traps. For the purposes of this study, the most important performance criterion was the capacity of the cold trap for retaining impurities. Efficiency was monitored for all cold trap cases studied, and it is part of the MASCOT output data; however, it was found not to vary significantly for any of the cases studied. Cost is an important design criterion; however, the kinds of design variations studied, i.e., length-to-diameter ratios, mesh densities, etc., have little effect on cold trap cost. Therefore, no attempt was made to optimize the cold trap design with respect to cost. Future

*This problem has recently been corrected, and the listing provided in the Appendix is the corrected version.

studies will, of course, refine the cold trap design in this respect, but such a refinement was not the purpose of this study. Other performance criteria such as pressure drop and heat transfer were considered not to have a significant impact on the large hydrogen burden of the LMFBR.

A. Objectives and Approach

The objectives of the parametric study were to determine which design variables are most important in maximizing cold trap capacity, which direction these parameters should be changed to result in maximum capacity, and whether or not optimum values exist. The most important design parameters were selected, based on past experience with cold traps and on experience to date with the MASCOT model. The parameters considered to be most important, in terms of their supposed effect on capacity, were (1) mesh packing density, (2) length-to-diameter ratio, (3) the ratio of the annulus to center section cross-sectional areas, and (4) mesh wire diameter. Several values of each of these variables were studied, and the parameter matrix is shown in Table 7.

Table 7. Parameter Matrix Used in This Study

ANN/CEN* Area Ratio	Mesh Density, kg/m^3	Length-to-Diameter Ratio	Wire Diameter, mm
0.35	130	1.5	0.23
0.35	190	1.5	0.23
0.35	290	1.5	0.23
0.35	400	1.5	0.23
1.00	130	1.5	0.23
1.00	190	1.5	0.23
1.00	290	1.5	0.23
1.00	400	1.5	0.23
78.0	130	1.5	0.38
78.0	190	1.5	0.23
78.0	290	1.5	0.23
78.0	400	1.5	0.23
78.0	130	1.0	0.23
78.0	130	1.75	0.23
78.0	130	2.0	0.23
78.0	130	2.5	0.23

*Annulus-to-center cross-sectional area ratio.

The CRBR IHTS cold trap was chosen as the reference design, and the parametric study was done by calculating the capacities of designs which were variations of that design. Mesh packing densities of 130, 190, 290, and 400 kg/m^3 (8, 12, 18, and 25 lb/ft^3) were studied using three different configurations: (1) the CRBR IHTS design, which has equal cross-sectional areas in the annulus and the center section and equal mesh densities in both

regions, (2) a variation with a large annulus region containing mesh and a small center section with no mesh, and (3) a variation with a large center section containing mesh and a narrow annulus containing no mesh. The effect of the length-to-diameter (L/D) ratio of the mesh region was studied using values of 1.0, 1.5, 1.75, 2.0, and 2.5 (the CRBR IHTS cold trap has an L/D of 1.5). In all of the parametric study cases, the other system variables were held constant. The sodium flow rate was 3.2 kg/s (∿60 gal/min), the inlet hydrogen concentration was 135 ppb, the inlet sodium temperature was 423 K (150°C), and the minimum cold trap temperature (average temperature in the bottom region) was 383 K (110°C).

Each of the sixteen cases shown in Table 7 was run with the MASCOT for the conditions described above. For each time increment of the simulation, the total pressure drop through the cold trap was recalculated. As more hydrogen accumulated in the trap, the pressure drop increased--gradually at first, then more rapidly. The end of the cold trap life was signaled by a very rapid increase in pressure drop. The pressure drop as a function of the quantity of hydrogen trapped in the CRBR model cold trap is shown in Fig. 16. The pressure drop is initially very low, and it builds slowly until the limit of the capacity is approached. At that point, the pressure drop rises very sharply, signaling that the trap is plugged. The run is terminated at a fairly low pressure because the MASCOT has some difficulty calculating the high-pressure-drop cases. For this reason, all of the cases were terminated at ∿6.9 kPa (144 lb/ft^2) pressure drop. Some additional capacity could be forced for each case; however, the pressure drop rises so sharply that the additional capacity would be very small. The quantity of hydrogen trapped at the point when the pressure drop rises above 6.9 kPa (144 lb/ft^2) was defined as the capacity of that case, and the capacity was expressed in terms of percent of the mesh volume occupied by the NaH at theoretical density.

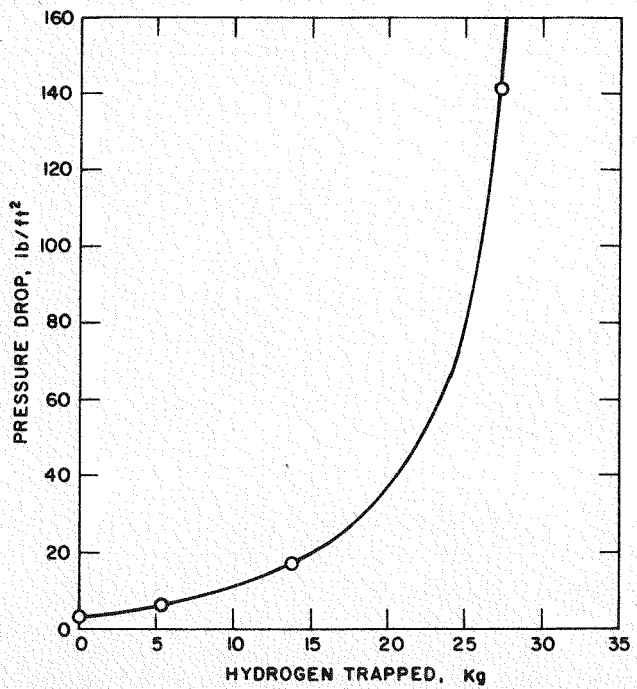

Fig. 16.

Pressure Drop across the CRBR Model Cold Trap as a Function of Quantity of Hydrogen Trapped

B. Results of Parametric Study

Variations on the CRBR IHTS design resulted in remarkable changes in the expected capacity. Figure 17 shows the results of the parametric study in terms of cold trap capacity as a function of the L/D ratio and as a function of the ratio of the annulus-to-center (ANN/CEN) cross-sectional areas. The different L/D ratios were calculated for the configuration having a large annulus region filled with mesh and a small, unpacked center section. The total mesh-region volume was kept constant while the L/D ratio was changed. The S-shaped L/D ratio curve (Fig. 17) should develop into a family of parallel curves at lower capacities as the ratio of ANN/CEN areas is decreased.

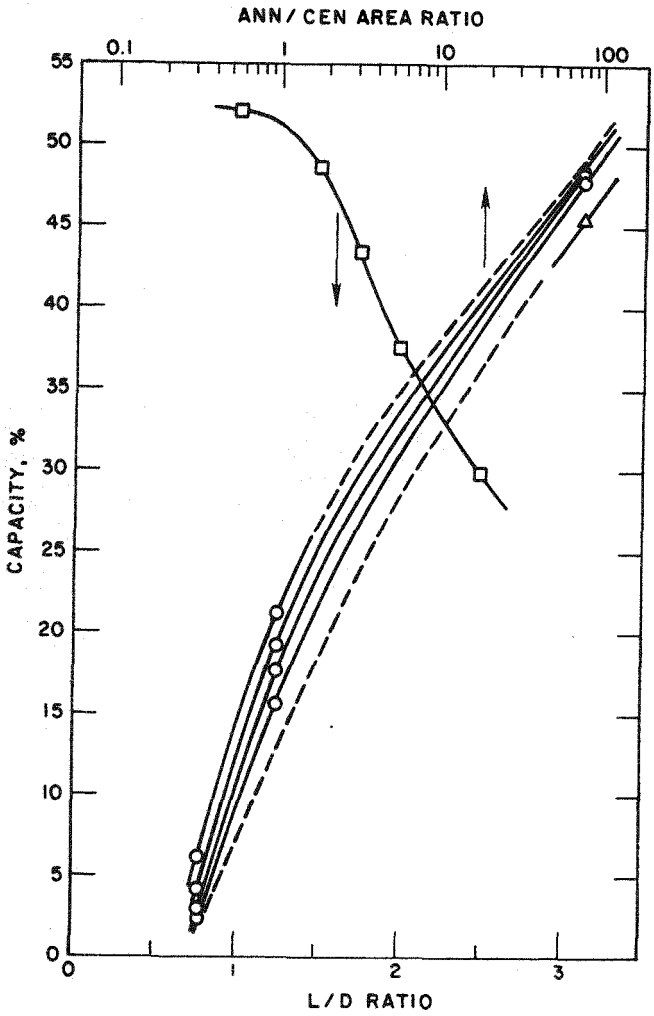

Fig. 17.

Cold Trap Capacity as a Function of Annulus/Center Area Ratio and of Length/Diameter Ratio

In Fig. 17, the circles are cases where the ANN/CEN ratios and the mesh densities are changed while the L/D ratio remains constant at 1.5. The upper curves (higher capacities) in that group have lower mesh densities. The triangle represents a case having low mesh density (130 kg/m^3) and a large mesh-wire diameter (0.38 mm). The dashed lines are extrapolations from cases that were studied to expected results of cases that were not studied. The squares represent cases where the L/D ratios were varied while mesh density remained constant at 130 kg/m^3 and the ANN/CEN ratio remained constant at 78.

Further, the most important parameter appears to be the ratio of ANN/CEN cross-sectional areas. The larger the annulus region, the greater the cold trap capacity. This conclusion is reasonable because the hydride precipitates rapidly in the region where it first becomes supersaturated. In the cold trap, this region is in the annulus where the incoming sodium is cooled. Thus, the larger the annulus cross-sectional area, the more sodium hydride can be accommodated before plugging.

A surprising result of this study is that the wire mesh packing density has a relatively small effect on capacity. These results indicate that, for the CRBR design, the capacity could be increased from 15.5% to 22.5% by reducing the packing density from 400 kg/m^3 (25 lb/ft^3) to 130 kg/m^3 (8 lb/ft^3). This improvement is small compared to the increase from 15.5% to 45.5% calculated for an increase in the ANN/CEN area ratio from 1.0 to 78. The relatively small effect of mesh density variations is probably due to the fact that the wire occupies a very small volume in all cases. Once the wire is coated with the impurity, its only impact on the capacity is its actual volume relative to the total cold trap volume. Since the wire volume is small in all cases, the variation in capacity is small.

The L/D ratio has a significant impact on the capacity, with lower L/D ratios having the greatest capacity. Long, thin cold traps (high L/D ratio) have significantly lower capacity than short, fat cold traps; however, little capacity can be gained by reducing the L/D ratio below ∿1.5.

The wire diameter also appears to have a small effect on the cold trap capacity. In all cases except one, a wire diameter of 0.23 mm (0.009 in) was used. In one case 0.38 mm (0.015 in) wire was used. This wire diameter change resulted in a decrease in capacity from an expected value of ∿48% to a calculated value of 46%. For a given mesh density, changes in wire diameter would not be expected to change the capacity because the total wire volume remains constant. However, the surface area per unit volume decreases with increasing wire diameter, and this decrease in area could cause an unfavorable distribution of impurity deposits that would decrease the capacity. More study is required before firm conclusions can be drawn on this wire-diameter effect.

Examination of Fig. 17 would lead the designer interested in maximizing cold trap capacity to design a cold trap having a very large annulus, a small center tube, a very short mesh region having a large diameter, and very low mesh density. In general, these are the directions to go for increasing cold trap capacity; however, care should be used in taking these guidelines to extremes. For example, the very short, fat cold trap design could lead to uneven distribution of sodium flow and, possibly, thermal convection that could result in upward flow near the center. The MASCOT was not designed to calculate effects, such as thermal convection, that might lead to uneven flow. Another example of an ill-advised change in design would be to reduce the mesh density to an extremely low level. Such a design could lead to the trap behaving like a packless trap, and the mesh might be incapable of supporting its own weight or the weight of the impurity deposits. Therefore, care should be taken in attempting to take the conclusions of this study to extremes.

Use of wire mesh of graded density has been suggested by some as a method for increasing cold trap capacities, and this approach has, in fact, been used in the United Kingdom. Graded mesh densities, while not studied specifically in this parametric study, were examined extensively in the course of development of the MASCOT model. It was found that some significant benefit could be derived from use of low mesh densities, as discussed above; however, no benefit could be found in increasing the mesh density downstream. That is, an overall decrease in mesh density seemed to do as well as grading the mesh density. The only reason for placing higher density mesh downstream from the point of heaviest precipitation would be to increase the cold trap efficiency, but efficiency was not found to be a critical issue in these studies. In general, high efficiencies were found in all cases where wire mesh was used in any density.

C. Conclusions of Parametric Study

The conclusions of the parametric study are as follows:

1. The CRBR IHTS cold trap should be capable of retaining ∿28 kg of hydrogen before plugging (∿15% of the mesh volume).

2. The most sensitive parameter for increasing capacity appears to be the ANN/CEN area ratio, with larger ratios giving greater capacities.

3. The L/D ratio is important, with a ratio of ∿1.5 giving optimum capacity.

4. The mesh density has a relatively small effect on cold trap capacity, but lower densities give greater capacities than higher densities.

5. Mesh wire diameter, surprisingly, seems to have an effect, with larger diameters resulting in lower capacities.

6. The MASCOT model can be very useful in developing cold trap designs. Information such as the parameters examined in this study will be helpful in selecting configurations for specific cold trap applications.

D. Use of MASCOT in Cold Trap Designs

The MASCOT was developed for the purpose of assisting the cold trap designer in determining the optimum cold trap design for his specific sodium system. The MASCOT is not a complete cold-trap design code; however, it will be useful in assisting the cold trap designer to determine the most important variables in meeting his system requirements. Many different cold trap configurations may be tested with the MASCOT to determine their relative performance in terms of capacity, efficiency, and mass transfer characteristics. The procedure that should be used in applying the MASCOT to cold trap design problems is as follows:

1. Establish the system purification requirements in terms of sodium inventory, impurity types and source rates, system purity requirements, available pressure drop for operation of the cold trap, and system temperature at the purification system attachment point.

2. Using conservative initial estimates of cold trap efficiency (perhaps ∿70% efficiency may be used for this purpose), calculate the sodium flow required to maintain the required system purity. Assume that the cold trap inlet impurity concentration is equal to the system purity specification. The outlet concentration is then given by

$$C_o = C-\varepsilon(C-C_e) \qquad (6)$$

where C_o = the outlet concentration, C = the inlet concentration, C_e = the equilibrium concentration based on the minimum cold trap temperature, and ε = the cold trap efficiency. The concentration difference, $C-C_o$, times the cold trap flow rate, should be equal to or greater than the impurity source rate. Otherwise, the flow rate is too small, and a higher flow rate must be specified.

3. Once the flow rate is determined, the volume of the cold trap may be determined by two methods: (a) the volume and configuration necessary to transfer the required heat load for cooling the sodium to the minimum cold trap temperature, and (b) the volume required to retain the impurity burden over the required cold trap lifetime. The traditional "rule of thumb" method for sizing a cold trap was to allow a five-minute residence time within the mesh region. This method is sufficient for the initial guess at the cold trap size. The MASCOT may then be used to refine the volume estimate on the basis described above.

4. The configuration of the cold trap may be studied in as much detail as allowed by the design effort. Many different configurations, sizes, and operating conditions should be studied to allow the designer to acquire adequate knowledge of the cold trap behavior and capabilities over a wide range of design parameters and operating conditions.

5. The final cold trap configuration should be thoroughly tested with MASCOT under a wide variety of conditions to determine the adequacy of the design.

6. The heat transfer system must be designed by conventional methods. MASCOT uses a NaK heat transfer medium to cool the sodium; however, the designer may wish to use air or nitrogen, etc.

7. The cold trap configuration must be translated into a code design as determined by the system code requirements.

ACKNOWLEDGMENTS

The authors wish to express thanks to several people involved in helping put this study together. In particular, thanks to Dr. F. A. Cafasso, Manager of the Sodium Technology Program in which this work was done, for invaluable overall direction of the effort. Special thanks to R. Land and S. Gabelnick who continually assisted in keeping the computer effort on track and helped us work out endless computational problems, and R. Kumar for helping to develop the three-dimensional plotting routines. We thank R. Wolson and V. Kolba, who are continuing this work, for providing valuable assistance in reviewing this work and checking over the computer model. We also wish to thank M. Homa, F. Williams, and K. Jensen of the Analytical Chemistry Laboratory for analyzing the cold trap residues and other cold trap samples, and D. Hamrin for valuable assistance in editing the report.

REFERENCES

1. D. R. Vissers, J. T. Holmes, L. G. Bartholme, and P. A. Nelson, A Hydrogen-Activity Meter for Liquid Sodium and Its Application to Hydrogen Solubility Measurements, Nucl. Technol. 21, 235, March 1974.

2. J. M. McKee, Water-to-Sodium Leak Detector: Development and Testing, Proc. Int. Conf. Liquid Metals Technol. in Energy Production, Champion, Pa, CONF-760503-P2, p. 500, May 1976.

3. D. N. Rogers et al., Sodium Concentration and Departure from Nucleate Boiling in the Clinch River Breeder Reactor Plant, AIChE 17th National Heat Transfer Conf., Salt Lake City, UT, August 1977.

4. S. B. Skladzien, D. J. Raue, and C. C. McPheeters, Method for Regenerating Sodium Cold Traps, Argonne National Laboratory Report ANL-81-52, October 1981.

5. I. L. Gray, R. L. Neal, and B. G. Voorhees, Control of Oxygen in Sodium Heat Transfer Systems, Liquid Metal Technology, Part I. Vol. 53, 1957.

6. W. H. Bruggeman, Purity Control in Sodium Cooled Reactor Systems, AIChE J. 2, 153, 1956.

7. R. Cygan, HNPF Cold Trap Evaluation, Atomics International, Canoga Park, CA, Report NAA-SR-4382, December 1959.

8. Handbook of Chemistry and Physics, 52nd Edition, The Chemical Rubber Company, 1971-1972.

9. Zintl and Harder, Z. Physik. Chem. Leipzig. B14, 265, 1931.

10. Kuznetsov and Shkrabkina, Zh. Strukt. Khim. 3, 553, 1962.

11. R. B. Hinze, Control of Oxygen Concentration in a Large Sodium System, Atomics International, Canoga Park, CA, Report NAA-SR-3638, August 1959.

12. L. G. Volchkov, M. K. Gorchakov, F. A. Kozlov, V. V. Matyukhin, Yu. P. Nalimov, and B. I. Tonov, Operation of a Cold Trap for Sodium Impurities, Sov. At. Energy 35, 1094, 1973.

13. J. C. Armour and J. N. Cannon, Fluid Flow through Woven Screens, AIChE J. 14, 415, 1968.

14. Leva, Chem. Eng. 56(5), 115-117, 1949.

15. R. H. Perry and C. H. Chilton, Chemical Engineers' Handbook, Fifth Edition, McGraw-Hill Book Company, 1973.

16. O. J. Foust, Ed., Sodium-NaK Engineering Handbook. Volume II: Sodium Flow, Heat Transfer, Intermediate Heat Exchangers, and Steam Generators, Gordon and Breach, Science Publishers, Inc., NY, 1972.

17. D. L. Smith, Monitoring and Measurement of Oxygen Concentrations in Liquid Sodium, Int. Conf. Liquid Metals Technol. in Energy Production, Champion, Pa., CONF-760503-P2, May 1976.

18. G. Billuris, Experimental Investigations of the Removal of Sodium Oxide from Liquid Sodium, General Electric Company, San Jose, CA, Report GEAP-3328, January 1960.

19. S. J. Rogers, C. A. Palladino, and T. J. Wildeman, Topical Report No. 9--Analysis of High Oxygen and High Carbon Cold Traps, MSA Research Corporation, Evans City, PA, Report MSAR 67-203, December 1967.

20. J. Herb et al., Examination of the Enrico Fermi Sodium Cold Trap, Westinghouse Electric Corporation, Pittsburgh, PA, Report WCAP-4321, November 1965.

21. S. Siegel and L. F. Epstein, Diffusion of Na_2O in Sodium in the Range of 900 to 1000°F, General Electric Company, San Jose, CA, Report GEAP-3357, December 1959.

22. J. M. McKee, D. R. Vissers, and P. A. Nelson of Argonne National Laboratory and B. R. Grundy, E. Berkey, and G. R. Taylor of Westinghouse Electric Corp., Calibration Stability of Oxygen Meters for LMFBR Sodium Systems, Nucl. Technol. 21, 217, March 1974.

23. V. A. Maroni et al., Liquid Metal Chemistry and Tritium Control Technology Annual Report. July 1974-June 1975, Argonne National Laboratory Report ANL-75-50, September 1975.

APPENDIX

MASCOT LISTING AND SAMPLE OUTPUT

(see p. 56 for sample output)

```
      DIMENSION WRHO(3),WDIA(3),NMESH(3),SWPUV(3),VWPUV(3),ANODE(15,50)
      DIMENSION VNODE(15,50),TITLE(20),VWIRE(14,40),OPENV(15,50)
      DIMENSION WSURFA(14,40),T(15,40),OR(15),OPENA(15,40),TOLD(15,40)
      DIMENSION HMASS(14,40),SORHO(14,40),P(14,40),POLD(14,40),VZ(15,50)
      DIMENSION VR(14,40),GAMAZ(14,40),ARO(14,40),TBOT(14),GAMAR(14,40)
      DIMENSION VZOLD(15,40),VROLD(14,40),VZOUT(12),VZIN(15),HMID(50)
      DIMENSION AZ(15,40),ALPHA(14,40),HMOD(50),HMW(50)
      DIMENSION HTZ(15,40),HTR(15,40),HDIV(50),HWALL(50),HTOP(15)
      DIMENSION CH(14,40),CE(14,40),SMFZ(14,40),SMFR(14,40),CBOT(15)
      DIMENSION CEBOT(15),SBOT(15),HMTC(14,40),COLD(14,40),HMBOT(15)
      DIMENSION UTILB(14),UTIL(14,40),VFRACT(15,40),S(15,40)
      DIMENSION DMASS(14,40),DMID(40),DMOD(40),DMW(40),DMBOT(14)
      DIMENSION DMOLD(14,40)
      READ 106,TITLE
      READ 100,WRHO(1),WRHO(2),WRHO(3)
      READ 100,WDIA(1),WDIA(2),WDIA(3)
      READ 101,NMESH(1),NMESH(2),NMESH(3)
      READ 102,TOTAL
      READ 102,SFLOW,CFLOW
      READ 102,CCP,CRHO
      READ 100,STEMP,CTEMP,TMIN
      READ 103,R1,R2,R3,R4,R5
      READ 104,HEIGHT
      READ 101,NCI,NAI,NJ
      READ 104,CIN
      READ 107,IMPUR
      READ 107,IHDIV
      READ 107,IAPACK
      READ 107,ICPACK
      IF(IHDIV)1,2,2
    1 READ 104,HDIVH
    2 CONTINUE
C
C     END OF CONSTANT INPUT
C
C     NOW DEFINE THE FORMATS
C
  100 FORMAT(3E10.0)
  101 FORMAT(3I5)
  102 FORMAT(2E10.0)
  103 FORMAT(5E10.0)
  104 FORMAT(E10.0)
  105 FORMAT(4I5)
  106 FORMAT(20A4)
  107 FORMAT(I5)
  550 FORMAT (1HO,'FOLLOWING IS THE INPUT DATA')
  551 FORMAT(1HO,'MESH DENSITIES FOR REGIONS 1, 2, AND 3 WERE ',F9.5,
     1',  ',F9.5,', AND',F9.5,'  G/CM**3')
  552 FORMAT(1HO,'WIRE DIAMETERS FOR REGIONS 1, 2, AND 3 WERE',F9.5,
     1',  ',F9.5,', AND',F9.5,'  CM')
  553 FORMAT(1HO,'THE NUMBER OF RECTANGLES REQUIRED TO DEFINE THE MESH
     1 REGIONS 1, 2, AND 3 WERE',I5,',  ',I5,', AND',I5)
  554 FORMAT(1HO,'THE TOTAL CALCULATION TIME WAS',E12.4,' SEC.')
  555 FORMAT(1HO,'THE SODIUM FLOW WAS',F8.4,'  CM**3/SEC '
     1/1HO,'THE COOLANT (NAK) FLOW WAS',F8.4,'  CM**3/SEC.')
  556 FORMAT(1HO,'THE COOLANT HEAT CAPACITY WAS',F9.5,'  CAL/G-DEG.'
     1/1HO,'THE COOLANT DENSITY WAS',F9.5,'  G/CM**3')
  557 FORMAT(1HO,'TEMPERATURES:  SODIUM INLET =',F8.2,'    MINIMUM COLD
     1TRAP TEMPERATURE  =',F8.2,'   NAK INLET =',F8.2,'  C.')
  558 FORMAT(1HO,'RADII:  R1=',F6.2,' R2=',F6.2,' R3=',F6.2,' R4 ='
     1,F6.2,' R5=',F6.2,'  CM.')
  559 FORMAT(1HO,'NUMBER OF NODES:  CENTER =',I5,'  ANNULUS =',I5,'
     1  AXIAL NODES =',I5)
```

```
  560 FORMAT(1HO,'INLET IMPURITY CONCENTRATION =',F6.2,'  PPM, AND THE
     1IMPURITY IS',I3,',    (1 = H, AND 0 = O)')
  561 FORMAT(1HO,'INDICATORS OF VARIOUS OPTIONS:  IHDIV =',I3,'  (-1 =
     1INPUT VALUE, 0 = ZERO, AND 1 = CALCULATED VALUE OF DIVIDER'
     2/1HO,'WALL HEAT TRANSFER COEFF.)'
     3/1HO,'IAPACK = ',I3,'  (1 = PACKING IN ANNULUS, 0 = NO PACKING IN
     4ANNULUS)'
     5/1HO,'ICPACK = ',I3,'  (1 = PACKING IN CENTER, 0 = NO PACKING IN
     6CENTER)')
C
C   PRINT OUT THE INPUT DATA.
C
      PRINT 600, TITLE
      PRINT 550
      PRINT 551, WRHO(1), WRHO(2), WRHO(3)
      PRINT 552, WDIA(1), WDIA(2), WDIA(3)
      PRINT 553, NMESH(1), NMESH(2), NMESH(3)
      PRINT 554, TOTAL
      PRINT 555, SFLOW, CFLOW
      PRINT 556, CCP, CRHO
      PRINT 557, STEMP, TMIN, CTEMP
      PRINT 558, R1,R2,R3,R4,R5
      PRINT 559, NCI, NAI, NJ
      PRINT 560, CIN, IMPUR
      PRINT 561, IHDIV, IAPACK, ICPACK
C
C    DO PRELIMINARY CALCULATIONS
C
      DO 5N=1,3
      SWPUV(N) = WRHO(N)*4./(WDIA(N)*8.028)
    5 VWPUV(N) = WRHO(N)/8.028
      PI = 3.141592654
      ANJ = NJ
      HNODE=HEIGHT/ANJ
      ANCI = NCI
      DELRC=R1/ANCI
      ANAI = NAI
      DELRA=(R3-R2)/ANAI
      DO6I=1,NCI
      RI = I
      OR(I)=DELRC*RI
    6 CONTINUE
      DO7I=1,NAI
      K=I+NCI
      RI = I
      OR(K)=R2+DELRA*RI
    7 CONTINUE
      NI=NCI+NAI+1
      N=NCI+NAI
      NAI1=NCI+1
      DO8J=1,NJ
      ANODE(NAI1,J) = 0.0138889*PI*(OR(NAI1)**2-R2**2)
      ANODE(1,J) = 0.0138889*PI*OR(1)**2
      WSURFA(NI,J) = 0.0
    8 ANODE(NI,J) = 0.0138889*PI*(R5**2-R4**2)
      DO9I=2,NCI
      K=I-1
      AZNODE = 0.0138889*PI*(OR(I)**2-OR(K)**2)
      DO9J=1,NJ
      ANODE(I,J)=AZNODE
    9 CONTINUE
      NAI2=NCI+2
      DO10I=NAI2,N
```

```
      K=I-1
      AZNODE = 0.0138889*PI*(OR(I)**2-OR(K)**2)
      DO10J=1,NJ
      ANODE(I,J)=AZNODE
   10 CONTINUE
      DO11I=1,NI
      DO11J=1,NJ
      VNODE(I,J)=ANODE(I,J)*HNODE
   11 CONTINUE
C
C     NOW READ IN THE LIMITS OF THE MESH REGIONS
C     ANC DO THE NODE CALCULATIONS.
C
C
      DO12N=1,3
      NREG=NMESH(N)
      DO12M=1,NREG
      READ 105,ILL,IUL,JLL,JUL
      DO12I=ILL,IUL
      DO12J=JLL,JUL
      VWIRE(I,J)=VWPUV(N)*VNODE(I,J)
      OPENV(I,J)=VNODE(I,J)-VWIRE(I,J)
      OPENA(I,J)=OPENV(I,J)/HNODE
      WSURFA(I,J)=SWPUV(N)*VNODE(I,J)
   12 CONTINUE
      N=NCI+1
      M=NCI+NAI
       DO14J=1,NJ
      AJ = J
      T(NI,J) = TMIN+50.-AJ*(TMIN+50.-CTEMP)/ANJ
      TOLD(NI,J) = T(NI,J)
       DO13I=N,M
      T(I,J)=STEMP-AJ*(STEMP-TMIN)/ANJ
      TOLD(I,J)=T(I,J)
      HMBOT(I) = 0.0
   13 CONTINUE
       DO14I=1,NCI
      T(I,J)=TMIN
      TOLD(I,J) = TMIN
      HMBOT(I) = 0.0
   14 CONTINUE
      AM = M
      DO15J=1,NJ
      HMW(J) = 0.0
      HMID(J) = 0.0
      HMOD(J) = 0.0
      DO15I=1,M
      IF(I.EQ.NCI)GO TO 317
      IF(I.EQ.N)GO TO 318
      IF(I.EQ.M)GO TO 317
      GO TO 321
  317 WSURFA(I,J) = WSURFA(I,J)+.0872665*OR(I)*HNODE
      GO TO 321
  318 WSURFA(I,J) = WSURFA(I,J) + PI*2.*R2*HNODE*5./360.
  321 CONTINUE
      SORHO(I,J)=(.9501-2.2976D-04*T(I,J)-1.46D-08*T(I,J)**2+5.638D-12
     1*T(I,J)**3)
   15 HMASS(I,J) = 0.0
      VFRC = SFLOW/72.
      VFRA = SFLOW/72.
      IF(IMPUR)16,16,17
   16 RHO = 2.27*16./62.
      GO TO 18
```

```
 17 RHO = 1.38/24.
 18 CONTINUE
    FLOAA = 0.0
    FLOAC = 0.0
    DO 19 I=1,NCI
    TBOT(I) = TMIN
 19 FLOAC = FLOAC + OPENA(I,1)
    DO 20 I=N,M
    TBOT(I) = TMIN
 20 FLOAA = FLOAA + OPENA(I,1)
    VISC=8.298E-05*SORHO(3,20)**.3333*EXP(697.*SORHO(3,20)/
   1(273.15 + T(3,20)))
    VFRACT(3,20)= (VNODE(3,20) - VWIRE(3,20))/VNODE(3,20)
    VFRACT(13,20)=(VNODE(13,20)-VWIRE(13,20))/VNODE(13,20)
    SODENS = SORHO(3,20)*62.428
    VTOT=4.*PI*(VWIRE(3,20)/WSURFA(3,20))**2.
    DPART = (6.*VTOT/PI)**.33333/30.48
    ALPHA(3,20) = 155.42*VISC*(1.-VFRACT(3,20))**2/DPART**2/
   1VFRACT(3,20)**3
    VZ(13,20) = SFLOW*5./360./FLOAA/30.48
    VZ(3,20) = SFLOW*5./360./FLOAC/30.48
    DPCEN = ALPHA(3,20)*VZ(3,20)*HEIGHT/30.48*VFRACT(3,20)
    VTOT = 4.*PI*(VWIRE(13,20)/WSURFA(13,20))**2
    DPART=(6.*VTOT/PI)**.33333/30.48
    ALPHA(13,20)=155.42*VISC*(1.-VFRACT(13,20))**2/DPART
   1**2/VFRACT(13,20)**3
    DPANN = ALPHA(13,20)*VZ(13,20)*HEIGHT/30.48*VFRACT(13,20)
    PINLET = DPANN + DPCEN + .001
    TIME = 0.0
    PRINT 600,TITLE
600 FORMAT(1H1,20A4)
    PRINT 602
602 FORMAT(1HO,'*********************************************
   1INITIAL CONDITIONS AND INPUT DATA.  TIME = 0.0 SEC.******')
    PRINT 605,NCI,NAI,NJ,SFLOW,CFLOW,TMIN,R1,R2,R3,R4,R5,HEIGHT
605 FORMAT(1HO,'CENTER SECTION DIVIDED INTO',I3,'  NODES HORIZONTALLY
   1ON THE RADIUS'/1HO,'ANNULAR SECTION DIVIDED INTO',I3,'  NODES HORI
   2ZONTALLY ON THE RADIUS'/1HO,'ENTIRE TRAP DIVIDED INTO',I3,' NODES
   3VERTICALLY'/1HO,'THE SODIUM FLOW WAS',1PE12.4,'  CM**3/S'/1HO,'THE
   4 COOLANT FLOW WAS',E12.4,'  CM**3/S'/1HO,'THE MINIMUM COLD TRAP TE
   5MPERATURE WAS',0PF7.1,'  DEG. C'/1HO,'THE CENTER TUBE INSIDE RADIU
   6S WAS',F7.2,'  CM'/1HO,'THE CENTER TUBE OUTSIDE RADIUS WAS',F7.2,'
   7  CM'/1HO,'THE ANNULAR OUTSIDE RADIUS WAS',F7.2,'  CM'/1HO,'THE CO
   8OLING JACKET INSIDE RADIUS (COLD TRAP OUTSIDE RADIUS) WAS',F7.2,'
   9 CM'/1HO,'THE COOLING JACKET OUTER RADIUS WAS',F7.2,'  CM'/
   A1HO,'THE MESH SECTION HEIGHT WAS',F7.2,'  CM')
    PRINT 606,PINLET
606 FORMAT(1HO,'INLET PRESSURE WAS',E12.4,'  LB/FT**2')
    PRINT 607,STEMP,CIN,TOTAL
607 FORMAT(1HO,'THE SODIUM INLET TEMPERATURE =',F8.2,'  DEG C'/
   11HO,'THE INLET IMPURITY CONCENTRATION =',F8.4,'  PPM'/
   31HO,'THE TOTAL TIME OF THE CALCULATION IS',E12.4,'  SEC')
612 FORMAT(1HO,'NODE',14I8)
620 FORMAT(I3,5X,14F8.2)
    PRINT 621,FLOAA,FLOAC
621 FORMAT(1HO,'THE OPEN FLOW AREA IN THE TOP OF THE ANNULUS IS',E12.4
   1,'  CM**2'/1HO,'THE OPEN FLOW AREA IN THE TOP OF THE CENTER SECTIO
   2N IS',E12.4,'  CM**2')
627 FORMAT(I3,5X,14F8.1)
636 FORMAT(1HO,'NODE',15I8)
637 FORMAT(I3,5X,15F8.1)
    POUT = .001
    BOTP = PINLET - DPANN
```

```
      DO 22 J=1,NJ
      DO 21 I=N,M
      VZ(I,J) = SFLOW*5./360./FLOAA/30.48
      VZIN(I) = VZ(I,J)
      VR(I,J) = 0.00001*VZ(I,J)
      VZOLD(I,J) = VZ(I,J)
   21 VROLD(I,J) = VR(I,J)
      DO 22 I=1,NCI
      VZ(I,J) = -SFLOW*5./360./FLOAC/30.48
      VZOUT(I) = VZ(I,J)
      VR(I,J) = 0.00001*VZ(I,J)
      VZOLD(I,J) = VZ(I,J)
   22 VROLD(I,J) = VR(I,J)
      DO 26 J=1,NJ
      AJ = J
      DO 25 I=1,NCI
      P(I,J) = POUT + AJ*(BOTP-POUT)/ANJ
   25 POLD(I,J) = 100.
      DO 26 I=N,M
      P(I,J) = PINLET - AJ*(PINLET-BOTP)/ANJ
   26 POLD(I,J) = 100.
      TINLET = STEMP
      TCOUT = TMIN + 50.
      HZ = .20125/HNODE
      HRA = .20125/DELRA
      HRC = .20125/DELRC
      CPNA = .325
      HANN = 1.006/DELRA
      HCEN = 1.006/DELRC
      HSS = .0422/(R2-R1)
      HSSCO = .0422/(R4-R3)
      HZC = .04980/HNODE
      ITEMP = 0
C
C     NOW CALCULATE PRESSURE AND VELOCITY THROUGH EACH NODE.
C
C
      TSEG  = TOTAL/40.
  745 CONTINUE
      INNERP = 0
      NPIT = 0
      LOOPS = 9000
      NLOOPS = 20
      CONV = .001
      FLCONV = .01
      PFCONV = .001
      DO 23 J=1,NJ
      DO 23 I=1,M
      VTOT=4.*PI*(VWIRE(I,J)/WSURFA(I,J))**2*(1.+HMASS(I,J)/
     1RHO/VWIRE(I,J))
      DPART = (6.*VTOT/PI)**.33333/30.48
      SODENS = SORHO(I,J)*62.428
      VISC =8.298D-05*SORHO(I,J)**.33333*EXP(697.*SORHO(I,J)/(273.15
     1 + T(I,J)))
      VFRACT(I,J)=(VNODE(I,J)-VWIRE(I,J)-HMASS(I,J)/RHO)/VNODE(I,J)
      IF(VFRACT(I,J).LT.1.E-03)VFRACT(I,J) = 1.E-03
      ARO(I,J) = (.0872665*OR(I)*HNODE)/929.0304*VFRACT(I,J)
      IF(I.EQ.NCI)ARO(I,J) = ARO(I,J)/VFRACT(I,J)
      IF(I.EQ.M)ARO(I,J) = ARO(I,J)/VFRACT(I,J)
      AZ(I,J) =VNODE(I,J)/HNODE*VFRACT(I,J)/929.0304
      ALPHA(I,J)=155.42*(VISC*(1.-VFRACT(I,J))**2/DPART**2/
     1VFRACT(I,J)**3)
      GAMAZ(I,J) = VNODE(I,J)/(ALPHA(I,J)*HNODE**2*30.48)
```

```
      IF(I.LT.N)GO TO 29
      IF(I.GT.NCI)GO TO 30
   29 GAMAR(I,J)=VNODE(I,J)/(ALPHA(I,J)*DELRC**2*30.48)
      GO TO 31
   30 GAMAR(I,J)=VNODE(I,J)/(ALPHA(I,J)*DELRA**2*30.48)
   31 CONTINUE
   23 CONTINUE
   24 CONTINUE
      NPIT = NPIT + 1
      LFLOW = 0
   27 CONTINUE
      LFLAG = 0
   32 CONTINUE
      NIT = 0
   34 CONTINUE
      INNERP = INNERP + 1
C
C    ANNULUS SECTION PRESSURE CALCULATION.
C
      IF(IAPACK.EQ.0) GO TO 510
      DO 45 J=1,NJ
      DO 45 I=N,M
      IF(J.EQ.1)GO TO 36
      TNUM = GAMAZ(I,J)*P(I,J-1)
      GO TO 37
   36 TNUM = GAMAZ(I,J)*PINLET
   37 DENOM = GAMAZ(I,J)
      IF(I.EQ.M)GO TO 39
      IF(VR(I,J).LT.0.0)GO TO 38
      TNUM = TNUM + GAMAR(I+1,J)*P(I+1,J)
      DENOM = DENOM + GAMAR(I+1,J)
      GO TO 39
   38 TNUM = TNUM + GAMAR(I,J)*P(I+1,J)
      DENOM = DENOM + GAMAR(I,J)
   39 IF(J.EQ.NJ)GO TO 40
      TNUM = TNUM + GAMAZ(I,J+1)*P(I,J+1)
      DENOM = DENOM + GAMAZ(I,J+1)
      GO TO 41
   40 TNUM = TNUM + GAMAZ(I,J)*BOTP
      DENOM = DENOM + GAMAZ(I,J)
   41 IF(I.EQ.N)GO TO 43
      IF(VR(I-1,J).LT.0.0)GO TO 42
      TNUM = TNUM + GAMAR(I,J)*P(I-1,J)
      DENOM = DENOM + GAMAR(I,J)
      GO TO 43
   42 TNUM = TNUM + GAMAR(I-1,J)*P(I-1,J)
      DENOM = DENOM + GAMAR(I-1,J)
   43 P(I,J) = TNUM/DENOM
   45 CONTINUE
  510 CONTINUE
C
C    CENTER SECTION PRESSURE CALCULATION.
C
      IF(ICPACK.EQ.0) GO TO 520
      DO 60 J=1,NJ
      DO 60 I=1,NCI
      IF(J.EQ.1)GO TO 46
      TNUM = GAMAZ(I,J-1)*P(I,J-1)
      DENOM = GAMAZ(I,J-1)
      GO TO 47
   46 TNUM = GAMAZ(I,J)*POUT
      DENOM = GAMAZ(I,J)
   47 IF(I.EQ.NCI)GO TO 49
```

```
      IF(VR(I,J).LT.0.0)GO TO 48
      TNUM = TNUM + GAMAR(I+1,J)*P(I+1,J)
      DENOM = DENOM + GAMAR(I+1,J)
      GO TO 49
   48 TNUM = TNUM + GAMAR(I,J)*P(I+1,J)
      DENOM = DENOM + GAMAR(I,J)
   49 IF(J.EQ.NJ)GO TO 50
      TNUM = TNUM + GAMAZ(I,J)*P(I,J+1)
      DENOM = DENOM + GAMAZ(I,J)
      GO TO 51
   50 TNUM = TNUM + GAMAZ(I,J)*BOTP
      DENOM = DENOM + GAMAZ(I,J)
   51 IF(I.EQ.1)GO TO 55
      IF(VR(I-1,J).LT.0.0)GO TO 54
      TNUM = TNUM + GAMAR(I,J)*P(I-1,J)
      DENOM = DENOM + GAMAR(I,J)
      GO TO 55
   54 TNUM = TNUM + GAMAR(I-1,J)*P(I-1,J)
      DENOM = DENOM + GAMAR(I-1,J)
   55 P(I,J) = TNUM/DENOM
   60 CONTINUE
  520 CONTINUE
C
C    THE CONVERGENCE CRITERIA.
C
      LFLAG = LFLAG + 1
      NIT = NIT + 1
      IF(NIT.GT.49)GO TO 65
      GO TO 34
   65 CONTINUE
      ERR = 0.0
      DO 66J=1,NJ
      DO 66 I=1,M
      FRERR = (P(I,J) - POLD(I,J))/P(I,J)
      ERR = ERR + ABS(FRERR)
   66 POLD(I,J) = P(I,J)
C
C   TEST FOR CONVERGENCE.
C
      IF(CONV.GT.ERR)GO TO 67
      IF(LFLAG.GT.LOOPS)GO TO 67
      GO TO 32
   67 CONTINUE
C
C    NEW SODIUM VELOCITIES .
C
      IF(IAPACK.EQ.0) GO TO 530
      DO 75 I=N,M
      VZIN(I) = GAMAZ(I,1)/AZ(I,1)*(PINLET-P(I,1))
      DO 75 J=1,NJ
      IF(J.EQ.NJ)GO TO 68
      VZ(I,J)=GAMAZ(I,J+1)/AZ(I,J+1)*(P(I,J)-P(I,J+1))
      GO TO 69
   68 VZ(I,J)=GAMAZ(I,J)/AZ(I,J)*(P(I,J)-BOTP)
   69 IF(I.EQ.M)GO TO 73
      IF(P(I+1,J).GT.P(I,J)) GO TO 71
      VR(I,J)=GAMAR(I+1,J)/ARO(I,J)*(P(I,J)-P(I+1,J))
      GO TO 74
   71 VR(I,J)=GAMAR(I,J)/ARO(I,J)*(P(I,J)-P(I+1,J))
      GO TO 74
   73 VR(I,J) = 0.0
   74 CONTINUE
   75 CONTINUE
```

```
C
C  END OF ANNULUS VELOCITY CALCULATIONS.
C  CALCULATE CENTER SECTION VELOCITIES.
C
  530 CONTINUE
      IF(ICPACK.EQ.0) GO TO 540
      DO 85 I=1,NCI
      VZOUT(I)=GAMAZ(I,1)/AZ(I,1)*(POUT - P(I,1))
      DO 85 J=1,NJ
      IF(J.EQ.NJ)GO TO 76
      VZ(I,J)=GAMAZ(I,J)/AZ(I,J)*(P(I,J) - P(I,J+1))
      GO TO 77
   76 VZ(I,J)=GAMAZ(I,J)/AZ(I,J)*(P(I,J) - BOTP)
   77 IF(I.EQ.NCI)GO TO 83
      IF(P(I+1,J).GT.P(I,J)) GO TO 78
      VR(I,J)=GAMAR(I+1,J)/ARO(I,J)*(P(I,J)-P(I+1,J))
      GO TO 84
   78 VR(I,J) = GAMAR(I,J)/ARO(I,J)*(P(I,J) - P(I+1,J))
      GO TO 84
   83 VR(I,J) = 0.0
   84 CONTINUE
   85 CONTINUE
  540 CONTINUE
C
C   TEST FOR FLOW CONVERGENCE
C
      LFLOW = LFLOW + 1
      FLERR = 0.
      DO 91 J=1,NJ
      DO 91 I=1,M
      DFLOW = (VZ(I,J)-VZOLD(I,J))+(VR(I,J) - VROLD(I,J))
      FLERR = FLERR + ABS(DFLOW)
      VZOLD(I,J) = VZ(I,J)
   91 VROLD(I,J) = VR(I,J)
      IF(FLCONV.GT.FLERR)GO TO 92
      IF(LFLOW.GT.NLOOPS)GO TO 92
      GO TO 27
   92 CONTINUE
      DPANN = PINLET - BOTP
      IF(IAPACK.EQ.0) DPANN = 0.0
      IF(ICPACK.EQ.0) BOTP = POUT
      IF(ICPACK.EQ.0) GO TO 96
      VFRC = 0.
      DO 93 I=1,NCI
   93 VFRC=VFRC+ABS(VZ(I,1))*VNODE(I,1)/HNODE*VFRACT(I,1)*30.48
   96 IF(IAPACK.EQ.0) GO TO 97
      VFRA = 0.0
      DO 94 I=N,M
   94 VFRA=VFRA+ABS(VZ(I,1))*VNODE(I,1)/HNODE*VFRACT(I,1)*30.48
   97 CFLERR = ABS(SFLOW*5./360.-VFRC)/(SFLOW*5./360.)
      AFLERR = ABS(SFLOW*5./360.-VFRA)/(SFLOW*5./360.)
      Y = 0.4
      X = 0.4
      IF(CFLERR.GT..16) Y = 0.9
      IF(AFLERR.GT..16) X = 0.9
      IF(NPIT.GT.20)GO TO 98
      IF(CFLERR.GT.PFCONV)GO TO 95
      IF(AFLERR.LT.PFCONV)GO TO 99
   95 BOTP = POUT + (BOTP-POUT)*(SFLOW*5./360.)**Y/VFRC**Y
      PINLET = BOTP + DPANN*(SFLOW*5./360.)**X/VFRA**X
      PRINT 807,BOTP,PINLET,DPANN,VFRA,VFRC
  807 FORMAT(1HO,'BOTP =',E12.5,'    PINLET =',E12.5,'  DPANN =',E12.5,
     1'   VFRA =',E12.5,'  VFRC =',E12.5)
```

```
      GO TO 24
   98 PRINT 805
  805 FORMAT(1H1,'PRESSURE/FLOW CONVERGENCE TOO DIFFICULT!  I QUIT!')
      GO TO 750
   99 CONTINUE
      TVFRA = VFRA*72.
      TVFRC = VFRC*72.
      DPANN = PINLET -BOTP
      DPCEN = BOTP - POUT
      DPTOT = PINLET - POUT
  650 FORMAT(1HO,'NODE',14I9)
  655 FORMAT(I3,2X,1PE9.2,13E9.2)
  652 FORMAT(1HO,'NODE',11I11)
  656 FORMAT(I4,1X,1PE11.4,10(E11.4))
      PRINT 674,ERR,LFLAG
  674 FORMAT(1HO,'PRESSURE CONVERGENCE ERROR WAS',E12.4,' , DIMENSIONLES
     1S'/1HO,'NUMBER OF ITERATIONS DURING LAST CONVERGENCE WAS',I5)
      PRINT 660,DPANN,DPCEN,DPTOT
  660 FORMAT(1HO,'ANNULUS PRESSURE DROP WAS',1PE12.4,'  LB/FT**2'/1HO,'C
     1ENTER SECTION PRESSURE DROP WAS',E12.4,'  LB/FT**2'/1HO,'TOTAL COL
     2D TRAP PRESSURE DROP WAS',E12.4,'  LB/FT**2')
      PRINT 661,NPIT
  661 FORMAT(1HO,'THE NUMBER OF PRESSURE/FLOW CYCLES WAS',I5)
      PRINT 662,INNERP
  662 FORMAT(1HO,'TOTAL NUMBER OF CYCLES THROUGH INNER PRESSURE LOOP WAS
     1',I8)
      PRINT 665
  665 FORMAT(1H1,'FOLLOWING ARE THE AXIAL SODIUM VELOCITIES IN THE COLD
     1TRAP, UNITS OF FT/S.    * ')
      PRINT 650,(I,I=1,M)
      DO 666 J=1,NJ
  666 PRINT 655,J,(VZ(I,J),I=1,M)
      PRINT 663,TVFRA
  663 FORMAT(1HO,'SODIUM FLOW RATE CALCULATED FOR ANNULUS SECTION IS',E1
     12.4,'  CM**3/S.')
      PRINT 664,TVFRC
  664 FORMAT(1HO,'SODIUM FLOW RATE CALCULATED FOR CENTER SECTION IS',E12
     1.4,'  CM**3/S.')
      PRINT 673
  673 FORMAT(1HO,'*  ALL VELOCITIES ARE POSITIVE IN THE DOWNWARD AND THE
     1 RIGHTWARD DIRECTIONS.')
      PRINT 675,FLERR,LFLOW
  675 FORMAT(1HO,'THE FLOW CONVERGENCE ERROR WAS',E12.4,', DIMENSIONLESS
     1'/1HO,'THE NUMBER OF ITERATIONS DURING LAST FLOW/PRESSURE CYCLE WA
     2S',I5)
      A = TOTAL - 100.
      IF(TIME.GT.A)GO TO 750
      IF(DPTOT.GT.4000.)GO TO 750
      IF(ITEMP.GT.0) GO TO 299
C
C   TEMPERATURE CALCULATION SECTION.
C
      DO 154 J=1,NJ
      DO 152 I=1,M
  152 HTZ(I,J)=(CPNA*SORHO(I,J)*ABS(VZ(I,J))*30.48+HZ)*AZ(I,J)*929.03
     104
      DO 153 I=1,NCI
  153 HTR(I,J)=(CPNA*SORHO(I,J)*ABS(VR(I,J))*30.48+HRC)*ARO(I,J)*
     1929.0304
      DO 154 I=N,M
  154 HTR(I,J)=(CPNA*SORHO(I,J)*ABS(VR(I,J))*30.48+HRA)*ARO(I,J)*
     1929.0304
      IF(IHDIV)155,156,157
```

```
  155 DO 148 J=1,NJ
  148 HDIV(J) = HDIVH
      GO TO 161
  156 DO 149 J=1,NJ
  149 HDIV(J) = .0000001
      GO TO 161
  157 DO 160 J=1,NJ
      HM = HMOD(J) + HMID(J)
      IF(HM.LT.1.0E-10)GO TO 158
      HNAH = .0022*RHO*ARO(NCI,J)*929.0304/HM
      HDIV(J)=1./(1./HANN+1./HCEN+1./HSS+1./HNAH)
      GO TO 159
  158 HDIV(J)=1./(1./HANN + 1./HCEN + 1./HSS)
  159 CONTINUE
  160 CONTINUE
  161 CONTINUE
      NCTIT = 0
      NTOT = 0
      DO 167 I=1,NCI
  167 HTOP(I)=(SORHO(I,1)*CPNA*ABS(VZOUT(I)*30.48)+HZ)*AZ(I,1)*
     1929.0304
      DO 168 I=N,M
  168 HTOP(I)=(SORHO(I,1)*CPNA*ABS(VZIN(I)*30.48)+HZ)*AZ(I,1)*
     1929.0304
  162 CONTINUE
      PE=(R5-R4)*2.*CCP*(CFLOW*CRHO/(PI*(R5**2-R4**2)))/.055
      HNAK = (7.+.025*PE**.8)*.055/(R5-R4)/2.
      HTZC = CRHO*CCP*CFLOW*5./360.+HZC*(R5**2-R4**2)*PI*5./
     1360.
      DO 165 J=1,NJ
      IF(HMW(J).LT.1.0E-10)GO TO 163
      HNAH = .0022*RHO*ARO(M,J)*929.0304/HMW(J)
      HWALL(J)=1./(1./HNAK + 1./HNAH + 1./HSSCO + 1./HANN)
      GO TO 164
  163 HWALL(J)=1./(1./HNAK + 1./HSSCO + 1./HANN)
  164 CONTINUE
  165 CONTINUE
      DO 166 J=1,NJ
      HTR(M,J)=HWALL(J)*ARO(M,J)*929.0304
      HTR(NCI,J)=HDIV(J)*ARO(NCI,J)*929.0304
  166 HTZ(NI,J)=HTZC
      NTIT = 0
  169 CONTINUE
      NTIT = NTIT + 1
      NTOT = NTOT + 1
      SUMT = 0.
      SUM = 0.
      DO 170 I=1,NCI
      SUMT = SUMT + HTOP(I)*T(I,1)
  170 SUM = SUM + HTOP(I)
      TOUT = SUMT/SUM
      AZC = PI*5./360.*(R5**2-R4**2)
C   TEMPERATURE CALCULATION IN COOLANT CHANNEL.
C
      DO 175 K=1,NJ
      J= 1+ NJ -K
      IF(J.EQ.NJ)GO TO 171
      TNUM = HTZ(NI,J)*T(NI,J+1)
      GO TO 172
  171 TNUM = HTZ(NI,J)*CTEMP
  172 DENOM = HZC*AZC
      TNUM = TNUM + HTR(M,J)*T(M,J)
      DENOM = DENOM + HTR(M,J)
```

```
      IF(J.EQ.1)GO TO 173
      TNUM = TNUM + HZC*AZC*T(NI,J-1)
      DENOM = DENOM + HTZ(NI,J-1)
      GO TO 175
  173 TNUM = TNUM + HZC*AZC*TCOUT
      DENOM = DENOM + HTZ(NI,J)
  175 T(NI,J) = TNUM/DENOM
      TCOUT = T(NI,1) + (T(NI,1) - T(NI,2))/2.
C
C   TEMPERATURE CALCULATION IN THE ANNULUS REGION.
C
      DO 190 J=1,NJ
      DO 190 I=N,M
      IF(J.EQ.1)GO TO 176
      TNUM = HTZ(I,J-1)*T(I,J-1)
      DENOM = HZ*AZ(I,J-1)*929.0304
      GO TO 177
  176 TNUM = HTOP(I)*TINLET
      DENOM = HZ*AZ(I,J)*929.0304
  177 IF(I.EQ.M)GO TO 180
      IF(VR(I,J))179,181,178
  178 TNUM = TNUM + HRA*ARO(I,J)*T(I+1,J)*929.0304
      DENOM = DENOM + HTR(I,J)
      GO TO 182
  179 TNUM = TNUM + HTR(I,J)*T(I+1,J)
      DENOM = DENOM + HRA*ARO(I,J)*929.0304
      GO TO 182
  180 TNUM = TNUM + HTR(I,J)*T(I+1,J)
      DENOM = DENOM + HTR(I,J)
      GO TO 182
  181 TNUM = TNUM + HRA*ARO(I,J)*T(I+1,J)*929.0304
      DENOM = DENOM + HRA*ARO(I,J)*929.0304
  182 IF(J.EQ.NJ)GO TO 183
      TNUM = TNUM + HZ*AZ(I,J)*T(I,J+1)*929.0304
      GO TO 184
  183 TNUM = TNUM + HZ*AZ(I,J)*TBOT(I)*929.0304
  184 DENOM = DENOM + HTZ(I,J)
      IF(I.EQ.N)GO TO 187
      IF(VR(I-1,J))186,189,185
  185 TNUM = TNUM + HTR(I-1,J)*T(I-1,J)
      DENOM = DENOM + HRA*ARO(I-1,J)*929.0304
      GO TO 188
  186 TNUM = TNUM + HRA*ARO(I-1,J)*T(I-1,J)*929.0304
      DENOM = DENOM + HTR(I-1,J)
      GO TO 188
  187 TNUM = TNUM + HTR(I-1,J)*T(I-1,J)
      DENOM = DENOM + HTR(I-1,J)
      GO TO 188
  189 TNUM = TNUM + HRA*ARO(I-1,J)*T(I-1,J)*929.0304
      DENOM = DENOM + HRA*ARO(I-1,J)*929.0304
  188 T(I,J) = TNUM/DENOM
  190 CONTINUE
C
C   TEMPERATURE CALCULATION IN THE CENTER SECTION.
C
      DO 210 K=1,NJ
      DO 210 I=1,NCI
      J = 1+NJ-K
      IF(J.EQ.1)GO TO 196
      TNUM = HZ*AZ(I,J-1)*T(I,J-1)*929.0304
      DENOM = HTZ(I,J-1)
      GO TO 197
  196 TNUM = HZ*AZ(I,J)*TOUT*929.0304
```

```
      DENOM = HTOP(I)
  197 IF(I.EQ.NCI)GO TO 200
      IF(VR(I,J))199,201,198
  198 TNUM = TNUM + HRC*ARO(I,J)*T(I+1,J)*929.0304
      DENOM = DENOM + HTR(I,J)
      GO TO 202
  199 TNUM = TNUM + HTR(I,J)*T(I+1,J)
      DENOM = DENOM + HRC*ARO(I,J)*929.0304
      GO TO 202
  200 TNUM = TNUM + HTR(I,J)*T(I+1,J)
      DENOM = DENOM + HTR(I,J)
      GO TO 202
  201 TNUM = TNUM + HRC*ARO(I,J)*T(I+1,J)*929.0304
      DENOM = DENOM + HRC*ARO(I,J)*929.0304
  202 IF(J.EQ.NJ)GO TO 203
      TNUM = TNUM + HTZ(I,J)*T(I,J+1)
      DENOM = DENOM + HZ*AZ(I,J)*929.0304
      GO TO 204
  203 TNUM = TNUM + HTZ(I,J)*TBOT(I)
      DENOM = DENOM + HZ*AZ(I,J)*929.0304
  204 IF(I.EQ.1)GO TO 207
      IF(VR(I-1,J))206,208,205
  205 TNUM = TNUM + HTR(I-1,J)*T(I-1,J)
      DENOM = DENOM + HRC*ARO(I-1,J)*929.0304
      GO TO 207
  206 TNUM = TNUM + HRC*ARO(I-1,J)*T(I-1,J)*929.0304
      DENOM = DENOM + HTR(I-1,J)
      GO TO 207
  208 TNUM = TNUM + HRC*ARO(I-1,J)*T(I-1,J)*929.0304
      DENOM = DENOM + HRC*ARO(I-1,J)*929.0304
  207 T(I,J) = TNUM/DENOM
  210 CONTINUE
C
C   TEMPERATURE CALCULATION IN THE BOTTOM REGION.
C
      VRBOT = 0.0
      DO 225 K=1,M
      I = 1+M-K
      IF(I.LT.N)GO TO 211
      TNUM = HTZ(I,NJ)*T(I,NJ)
      DENOM = HZ*AZ(I,NJ)*929.0304
      GO TO 212
  211 TNUM = HZ*AZ(I,NJ)*T(I,NJ)*929.0304
      DENOM = HTZ(I,NJ)
  212 IF(I.EQ.M)GO TO 215
      IF(I.LT.N)GO TO 213
      TNUM=TNUM+(SORHO(I,NJ)*CPNA*VRBOT+HRA*OR(I)*HNODE*.34907)*
     1TBOT(I+1)
      DENOM = DENOM + HRA*OR(I)*HNODE*.34907
      GO TO 215
  213 IF(I.EQ.1)VRBOT = -AZ(I,NJ)*VZ(I,NJ)*28316.8
      TNUM=TNUM+(SORHO(I,NJ)*CPNA*VRBOT+HRC*OR(I)*HNODE*.34907)*
     1TBOT(I+1)
      DENOM = DENOM + HRC*OR(I)*HNODE*.34907
  215 VRBOT = VRBOT + AZ(I,NJ)*VZ(I,NJ)*28316.8
      IF(I.EQ.1)GO TO 214
      IF(I.LT.N)GO TO 220
      TNUM = TNUM + HRA*OR(I-1)*HNODE*.34907*TBOT(I-1)
      DENOM = DENOM+(SORHO(I,NJ)*CPNA*VRBOT+HRA*OR(I-1)*HNODE*.34907)
      GO TO 214
  220 TNUM = TNUM + HRC*OR(I-1)*HNODE*.34907*TBOT(I-1)
      DENOM=DENOM+(SORHO(I,NJ)*CPNA*VRBOT+HRC*OR(I-1)*HNODE*.34907)
  214 TBOT(I) = TNUM/DENOM
```

```
225 CONTINUE
    IF(NTIT.LT.100)GO TO 169
    TBOTAV = 0.0
    DO 216 I=1,M
216 TBOTAV = TBOTAV + TBOT(I)
    AM = M
    TBOTAV = TBOTAV/AM
    NTIT = 0
    SUMT = 0.
    DO 217 J=1,NJ
    DO 217 I=1,NI
    TERR = ABS(T(I,J) - TOLD(I,J))
    SUMT = SUMT + TERR
217 TOLD(I,J) = T(I,J)
    TERR = ABS(TBOTAV-TMIN)
    IF(NTOT.GT.40000)GO TO 219
    IF(SUMT.GT.0.01)GO TO 169
    IF(TERR.GT.2.)GO TO 218
    GO TO 221
218 IF(NCTIT.GT.8)GO TO 250
    CTEMP = CTEMP + 0.8*(TMIN - TBOTAV)
    PRINT 801,NCTIT,NTOT,TBOTAV
801 FORMAT(1HO,'NCTIT =',I5,'  NTOT =',I5,'  AVE. BOT. TEMP=',F8.2)
    PRINT 802,CTEMP
802 FORMAT(1HO,'CTEMP WAS CHANGED TO',F8.2)
    NCTIT = NCTIT + 1
    GO TO 169
250 CFLOW=CFLOW*((TINLET-TMIN)**2/(TINLET-TBOTAV)**2)
    PRINT 803,CFLOW
803 FORMAT(1HO,'CFLOW WAS CHANGED TO',1PE12.4,' CM**3/S')
    NCTIT = 0
    GO TO 162
219 PRINT 806
806 FORMAT(1H1,'TEMPERATURE CALCULATION MUCHO DIFFICULTO! VAMINOS!')
    GO TO 750
221 CONTINUE
    SHEAT = (TINLET-TOUT)*CPNA*SFLOW*SORHO(11,20)
    CHEAT = (TCOUT-CTEMP)*CCP*CFLOW*CRHO
    PRINT 682,TINLET,TBOTAV,TOUT,CTEMP,TCOUT,CFLOW
682 FORMAT(1H1,'THE COLD TRAP INLET TEMPERATURE WAS',F10.2,'  DEG. C'/
   11HO,'THE BOTTOM (MIN) TEMPERATURE WAS',F10.2,'  DEG. C'/1HO,'THE O
   2UTLET TEMPERATURE WAS',F10.2,'  DEG. C'/1HO,'THE COOLANT INLET TEM
   3PERATURE WAS',F10.2,'  DEG. C'/1HO,'THE COOLANT OUTLET TEMPERATURE
   4WAS',F10.2,'  DEG. C'/1HO,'THE FINAL COOLANT FLOW WAS',E12.4,'   C
   5M**3/S')
    PRINT 683
683 FORMAT(1HO,'FOLLOWING ARE THE CALCULATED TEMPERATURES IN ALL NODES
   1, DEG. C')
    PRINT 636,(I,I=1,NI)
    DO 684 J=1,NJ
684 PRINT 637,J,(T(I,J),I=1,NI)
    PRINT 693,(TBOT(I),I=1,M)
693 FORMAT(1HO,'TBOT',3X,15F8.1)
    PRINT 690,NTOT,NCTIT
690 FORMAT(1HO,'THE TOTAL NUMBER OF TEMPERATURE ITERATIONS WAS',I7,/1H
   1O,'THE NUMBER OF COOLANT TEMP. ADJUSTMENTS WAS',I4)
    PRINT 691,SUMT,TERR
691 FORMAT(1H1,'THE SUM OF TEMPERATURE CHANGES DURING THE LAST ITERATI
   1ON WAS',1PE12.4,'  DEG. C'/1HO,'THE DIFFERENCE BETWEEN THE CALCULA
   2TED BOTTOM TEMPERATURE AND THE INPUT VALUE WAS',E12.4,'  DEG. C')
    PRINT 692,SHEAT,CHEAT
692 FORMAT(1HO,'THE HEAT LOST BY THE SODIUM WAS',1PE12.4,'  CAL/S'/1HO
   1,'THE HEAT GAINED BY THE NAK COOLANT WAS',E12.4,'  CAL/S')
```

```
C
C    TEMPERATURE CONVERGENCE ACHIEVED. MASS TRANSFER SECTION IS NEXT.
C
C     BEGINNING OF THE CONCENTRATION SECTION.
C     CALCULATE INITIAL CONDITIONS.
C
      DO 251 J=1,NJ
      DO 251 I=1,M
      CH(I,J) = CIN
      COLD(I,J) = CIN
      IF(IMPUR)314,314,315
  314 A = 7.0058-2820.1/(T(I,J)+273.15)
      CE(I,J) = 10.**A
      GO TO 316
  315 A = 6.067-2880./(T(I,J)+273.15)
      CE(I,J) = 10.**A
  316 CONTINUE
  251 CONTINUE
      DO 305 I=1,NCI
      RI = I
      RI = RI*DELRC
      SBOT(I)=PI*(RI**2 - (RI-DELRC)**2)*5./360.
      CBOT(I) = CIN
      IF(IMPUR)300,300,301
  300 A = 7.0058-2820.1/(TBOT(I)+273.15)
      CEBOT(I) = 10.**A
      GO TO 302
  301 A = 6.067 - 2880./(TBOT(I)+273.15)
      CEBOT(I) = 10.**A
  302 CONTINUE
  305 CONTINUE
      DO 310 I=N,M
      RI = I-NCI
      RI = R2 + RI*DELRA
      SBOT(I)=PI*(RI**2-(RI-DELRA)**2)*5./360.
      CBOT(I) = CIN
      IF(IMPUR)306,306,307
  306 A = 7.0058 - 2820.1/(TBOT(I)+273.15)
      CEBOT(I) = 10.**A
      GO TO 308
  307 A = 6.067-2880./(TBOT(I)+273.15)
      CEBOT(I) = 10.**A
  308 CONTINUE
  310 CONTINUE
      IF(IMPUR)311,311,312
  311 DIFF = 5.6E-05
      GO TO 313
  312 DIFF = 1.0E-04
  313 CONTINUE
  299 CONTINUE
      DO 322 J=1,NJ
      DO 322 I=1,M
      IF(I.LT.N) GO TO 367
      IF(J.EQ.NJ) GO TO 367
      SMFZ(I,J)=SORHO(I,J)*VZ(I,J)*AZ(I,J+1)*.0283168
      GO TO 319
  367 SMFZ(I,J)=SORHO(I,J)*VZ(I,J)*AZ(I,J)*.0283168
  319 SMFR(I,J)=SORHO(I,J)*VR(I,J)*ARO(I,J)*.0283168
      F = HMASS(I,J)/RHO/VNODE(I,J)
      IF(F.GT..15) GO TO 320
      S(I,J) = (WSURFA(I,J)**2+4.*HMASS(I,J)*WSURFA(I,J)/
     1WDIA(3)/RHO)**.5
  320 IF(ITEMP.GT.0.)GO TO 322
```

```
      VISC=.001235*SORHO(I,J)**.3333*EXP(697.*SORHO(I,J)/(273.15
     1+T(I,J)))
      HMTC(I,J)=(ABS(VZ(I,J))*30.48/VFRACT(I,J)/(VISC/SORHO(I,J)/
     1DIFF)**.66667)/(WDIA(2)*ABS(VZ(I,J))*30.48*SORHO(I,J)/
     2((1.-VFRACT(I,J))*VISC))**.5
      HMTC(I,J) = HMTC(I,J)*SORHO(I,J)*1.E-06
  322 CONTINUE
C
C MASS TRANSFER COEFFICIENT IN GM/CM**2-S-PPM.
C
C BEGIN CONCENTRATION ITERATON LOOP, ANNULUS SECTION.
C
      LOOPC = 0
  323 NCIT = 0
  324 CONTINUE
      DO 340 J=1,NJ
      DO 340 I=N,M
      IF(CE(I,J).LT.CIN)GO TO 325
      IF(HMASS(I,J).GT.0.0)GO TO 325
      GO TO 328
  325 IF(J.EQ.1)GO TO 326
      TNUM = HMTC(I,J)*S(I,J)*CE(I,J)+SMFZ(I,J-1)*CH(I,J-1)
      GO TO 327
  326 TNUM = HMTC(I,J)*S(I,J)*CE(I,J)+SORHO(I,J)*VZIN(I)*
     1AZ(I,J)*CIN*.0283168
  327 DENOM = HMTC(I,J)*S(I,J)
      GO TO 330
  328 IF(J.EQ.1)GO TO 329
      TNUM = SMFZ(I,J-1)*CH(I,J-1)
      DENOM = 0.0
      GO TO 330
  329 TNUM = SORHO(I,J)*VZIN(I)*AZ(I,J)*CIN*.0283168
      DENOM = 0.0
  330 IF(I.EQ.M)GO TO 333
      IF(VR(I,J).GT.0.0)GO TO 331
      TNUM = TNUM - SMFR(I,J)*CH(I+1,J)
      GO TO 333
  331 DENOM = DENOM + SMFR(I,J)
  333 DENOM = DENOM + SMFZ(I,J)
      IF(I.EQ.N)GO TO 336
      IF(VR(I-1,J).GT.0.0)GO TO 335
      DENOM = DENOM - SMFR(I-1,J)
      GO TO 336
  335 TNUM = TNUM+SMFR(I-1,J)*CH(I-1,J)
  336 CH(I,J) = TNUM/DENOM
  340 CONTINUE
C
C  NOW THE BOTTOM SECTION.
C
      VRBOT = 0.0
      A = 0.0
      DO 345 K=1,M
      I = 1+M-K
      IF(CEBOT(I).LT.CBOT(I))GO TO 341
      TNUM = 0.0
      DENOM = 0.0
      GO TO 342
  341 TNUM = HMTC(I,NJ)*SBOT(I)*CEBOT(I)
      DENOM = HMTC(I,NJ)*SBOT(I)
  342 IF(I.GT.NCI)GO TO 343
      DENOM = DENOM - SMFZ(I,NJ)
      GO TO 344
  343 TNUM = TNUM + SMFZ(I,NJ)*CH(I,NJ)
```

```
  344 IF(I.EQ.M)GO TO 348
      TNUM = TNUM + VRBOT*CBOT(I+1)
  348 VRBOT = VRBOT + SMFZ(I,NJ)
      DENOM = DENOM + VRBOT
      CBOT(I) = TNUM/DENOM
  345 CONTINUE
C
C  NOW THE CENTER SECTION.
C
      DO 360 K=1,NJ
      J = 1+NJ-K
      DO 360 I=1,NCI
      IF(CE(I,J).LT.CH(I,J))GO TO 346
      IF(HMASS(I,J).GT.0.0)GO TO 346
      TNUM = 0.0
      DENOM = 0.0
      GO TO 347
  346 TNUM = HMTC(I,J)*S(I,J)*CE(I,J)
      DENOM = HMTC(I,J)*S(I,J)
  347 IF(J.EQ.1)GO TO 350
      DENOM = DENOM - SMFZ(I,J-1)
      GO TO 351
  350 DENOM = DENOM - SORHO(I,J)*AZ(I,J)*VZOUT(I)*.0283168
  351 IF(I.EQ.NCI)GO TO 355
      IF(VR(I,J).GT.0.0)GO TO 352
      TNUM = TNUM - SMFR(I,J)*CH(I+1,J)
      GO TO 355
  352 DENOM = DENOM + SMFR(I,J)
  355 IF(J.EQ.NJ)GO TO 356
      TNUM = TNUM - SMFZ(I,J)*CH(I,J+1)
      GO TO 357
  356 TNUM = TNUM - SMFZ(I,J)*CBOT(I)
  357 IF(I.EQ.1)GO TO 359
      IF(VR(I-1,J).GT.0.0)GO TO 358
      DENOM = DENOM - SMFR(I-1,J)
      GO TO 359
  358 TNUM = TNUM + SMFR(I-1,J)*CH(I-1,J)
  359 CH(I,J) = TNUM/DENOM
  360 CONTINUE
C
C   TEST FOR CONVERGENCE OF THE CONCENTRATIONS.
C
      LOOPC = LOOPC + 1
      NCIT = NCIT + 1
      IF(NCIT.GT.19)GO TO 361
      GO TO 324
  361 CERR = 0.0
      DO 370 J=1,NJ
      DO 370 I=1,M
      CERR = CERR + ABS(COLD(I,J)-CH(I,J))
  370 COLD(I,J) = CH(I,J)
      IF(CERR.GT.0.001)GO TO 323
C
C   CONCENTRATION CONVERGENCE IS COMPLETE.
C

  368 CONTINUE
      DO 385 I=1,M
      IF(CEBOT(I).LT.CBOT(I))GO TO 372
      DMBOT(I) = 0.0
      GO TO 373
  372 DMBOT(I)=HMTC(I,NJ)*SBOT(I)*(CBOT(I)-CEBOT(I))*TSEG
  373 CONTINUE
```

```
      IF(DMBOT(I).LT.0.0)DMBOT(I) = 0.0
      DO 385 J=1,NJ
      IF(CE(I,J).LT.CH(I,J))GO TO 376
      DMASS(I,J) = 0.0
      GO TO 384
  376 IF(I.EQ.NCI)GO TO 377
      IF(I.EQ.N)GO TO 378
      IF(I.EQ.M)GO TO 379
      GO TO 380
  377 DMID(J) = HMTC(I,J)*ARO(I,J)*929.0304*(CH(I,J)-CE(I,J))
     1 * TSEG
      IF(DMID(J).LT.0.0)DMID(J) = 0.0
      GO TO 380
  378 DMOD(J)=HMTC(I,J)*ARO(I-1,J)*929.0304*(CH(I,J)-CE(I,J))
     1 *TSEG
      IF(DMOD(J).LT.0.0)DMOD(J) = 0.0
      GO TO 380
  379 DMW(J)=HMTC(I,J)*ARO(I,J)*929.0304*(CH(I,J)-CE(I,J))*
     1TSEG
      IF(DMW(J).LT.0.0)DMW(J) = 0.0
  380 DMASS(I,J)=HMTC(I,J)*S(I,J)*(CH(I,J)-CE(I,J))
     1*TSEG
      IF(DMASS(I,J).LT.0.0)DMASS(I,J) = 0.0
  384 CONTINUE
  385 CONTINUE
C
C     MASS/CONC CONVERGENCE
C
C
      SERR=0
      DO 410 I=1,14
      DO 410 J=1,40
         IF(DMASS(I,J).LE.0.) GO TO 405
         ERR=ABS((DMASS(I,J)-DMOLD(I,J))/DMASS(I,J))
         SERR=SERR+ERR
  405    DMOLD(I,J)=DMASS(I,J)
  410 DMASS(I,J)=HMASS(I,J)+DMASS(I,J)
      IF (SERR.LT..01)GO TO 420
      IF (LOOPC.GT.5000) GO TO 418
      CALL NEWAREA (WSURFA,DMASS,WDIA,RHO,S,F)
      GO TO 323
  418 PRINT 741
  741 FORMAT(1H1,'KICKED OUT ON TOO MANY CONC./MASS ITERATIONS')
  420 DO 425 J=1,40
      DO 425 I=1,14
         HMID(J)=HMID(J)+DMID(J)
         HMOD(J)=HMOD(J)+DMOD(J)
         HMW(J)=HMW(J)+DMW(J)
  425 HMASS(I,J)=DMASS(I,J)
      SUM = 0.0
      COUT = 0.0
      AMASS = 0.0
      BMASS = 0.0
      CMASS = 0.0
      TIME = TIME + TSEG
      DO 390 I=1,NCI
      COUT = COUT - CH(I,1)*SMFZ(I,1)
  390 SUM = SUM - SMFZ(I,1)
      COUT = COUT/SUM
      CALMAS = (CIN-COUT)*SFLOW*SORHO(N,1)*5.E-06/360.*TIME
      DO 392 J=1,NJ
      DO 392 I=N,M
  392 AMASS = AMASS + HMASS(I,J)
```

```
      DO 394 I=1,M
  394 BMASS = BMASS + HMBOT(I)
      DO 396 J=1,NJ
      DO 396 I=1,NCI
  396 CMASS = CMASS + HMASS(I,J)
      TMASS = AMASS + BMASS + CMASS
      EFF = (CIN-COUT)/(CIN-CEBOT(M))*100.
      DO 398 I=1,M
      UTILB(I) = HMBOT(I)/RHO/(VNODE(I,NJ)*4.)*100.
      DO 398 J=1,NJ
      UTIL(I,J)=HMASS(I,J)/RHO/(VNODE(I,J)-VWIRE(I,J))*100.
  398 CONTINUE
C
C   MASS DEPOSIT CALCULATION COMPLETE.
C
      PRINT 705
  705 FORMAT(1H1,'ALL IMPURITY CONCENTRATIONS, PPM.')
      IF(IMPUR)706,706,707
  706 PRINT 708
      GO TO 710
  707 PRINT 709
  708 FORMAT(1HO,'IMPURITY IS OXYGEN.')
  709 FORMAT(1HO,'IMPURITY IS HYDROGEN.')
  710 PRINT 636,(I,I=1,M)
      DO 712 J=1,NJ
  712 PRINT 715,J,(CH(I,J),I=1,M)
  715 FORMAT(I3,5X,15F8.4)
      PRINT 716,(CBOT(I),I=1,M)
  716 FORMAT(1HO,'CBOT',3X,15F8.4)
      PRINT 717,COUT,LOOPC,CERR,EFF,CIN
  717 FORMAT(1HO,'THE OUTLET CONCENTRATION WAS',F8.4,'  PPM.'/
     11HO,'THE NUMBER OF CONCENTRATION ITERATIONS:',I8,/
     21HO,'THE SUM OF CONCENTRATION ERRORS =',E12.4,'  PPM'/
     31HO,'THE COLD TRAP EFFICIENCY =',F8.2,'  %'/
     41HO,'THE INLET CONCENTRATION =',F8.4,'  PPM.')
      PRINT 726,TIME,ITEMP
  726 FORMAT(1H1,'************************************************
     1MASS DEPOSITED AT END OF',1PE12.4,'  SEC.*****************'/
     21HO,'*******************************************************
     3*****   ITERATION NUMBER',I3,'************************')
      PRINT 720
  720 FORMAT(1HO,'IMPURITY MASS DEPOSITED IN THE ANNULUS, G.')
      PRINT 652,(I,I=N,M)
      DO 721 J=1,NJ
  721 PRINT 656,J,(HMASS(I,J),I=N,M)
      PRINT 718
  718 FORMAT(1HO,'IMPURITY MASS DEPOSITED IN BOTTOM, G.')
      PRINT 636,(I,I=1,M)
      PRINT 719,(HMBOT(I),I=1,M)
  719 FORMAT(1HO,'HMBOT',2X,15F8.4)
      PRINT 722
  722 FORMAT(1H1,'IMPURITY MASS DEPOSITED IN THE CENTER, G.')
      PRINT 652,(I,I=1,NCI)
      DO 723 J=1,NJ
  723 PRINT 656,J,(HMASS(I,J),I=1,NCI)
      PRINT 725,AMASS,CMASS,BMASS,TMASS,CALMAS
  725 FORMAT(1HO,'TOTAL MASS IN THE ANNULUS = ',1PE12.4,'  G.'/
     11HO,'TOTAL MASS IN THE CENTER SECTION = ',E12.4,'  G.'/
     21HO,'TOTAL MASS IN THE BOTTOM SECTION = ',E12.4,'  G.'/
     31HO,'TOTAL MASS IN THE WHOLE TRAP = ',E12.4,'  G.'/
     41HO,'MASS CALCULATED, FLOW X DELTA-C =',E12.4,'  G.')
      PRINT 730
  730 FORMAT(1H1,'FOLLOWING IS THE PERCENT OF NODE VOLUME USED.')
```

```
      PRINT 636,(I,I=1,M)
      DO 732 J=1,NJ
  732 PRINT 637,J,(UTIL(I,J),I=1,M)
      PRINT 733,(UTILB(I),I=1,M)
  733 FORMAT(1HO,'BOTTOM',15F8.1)
      PRINT 740,TIME,ITEMP
  740 FORMAT(1H1,'**************************************************
     1PRESSURES AND FLOWS AFTER',1PE12.4,'  SEC, BELOW.******'/
     21HO,'**************************************************
     3**********  ITERATION NUMBER',I3,'***************')
      WRITE(8) UTIL,HMASS,UTILB,TIME
      REWIND 8
      ITEMP = ITEMP + 1
      GO TO 745
  750 PRINT 1000
 1000 FORMAT(1HO,'END OF SIMULATION')
      STOP
      END
      SUBROUTINE NEWAREA(WSURFA,DMASS,WDIA,RHO,S,F)
      DIMENSION WSURFA(14,40),DMASS(14,40),WDIA(3),S(15,40)
      DO 20 I=1,14
      DO 20 J=1,40
         IF(F.GT..15)GO TO 20
         S(I,J)=(WSURFA(I,J)**2+4.*DMASS(I,J)*WSURFA(I,J)/
     1   WDIA(3)/RHO)**.5
   20 CONTINUE
      RETURN
      END
```

SAMPLE OUTPUT FROM MASCOT

```
LARGE-SCALE BREEDER REACTOR IHTS - CASE 47a  5/18/83
FOLLOWING IS THE INPUT DATA
MESH DENSITIES FOR REGIONS 1, 2, AND 3 WERE   0.40045,    0.40045, AND  0.40045  G/CM**3
WIRE DIAMETERS FOR REGIONS 1, 2, AND 3 WERE  0.02790,    0.02790, AND  0.02790  CM
THE NUMBER OF RECTANGLES REQUIRED TO DEFINE THE MESH REGIONS 1, 2, AND 3 WERE    1,      1, AND    1
THE TOTAL CALCULATION TIME WAS  0.2880E+09 SEC.
THE SODIUM FLOW WAS********  CM**3/SEC
THE COOLANT (NAK) FLOW WAS********  CM**3/SEC.
THE COOLANT HEAT CAPACITY WAS  0.22500  CAL/G-DEG.
THE COOLANT DENSITY WAS  0.84000  G/CM**3
TEMPERATURES:  SODIUM INLET =  152.50    MINIMUM COLDTRAP TEMPERATURE  =  117.50   NAK INLET =  100.00  C.
RADII:  R1= 26.58 R2= 27.46 R3= 81.07 R4 = 82.34 R5= 89.96  CM.
NUMBER OF NODES:  CENTER =    7  ANNULUS =    7  AXIAL NODES =   40
INLET IMPURITY CONCENTRATION =  0.20  PPM, AND THEIMPURITY IS  1,   (1 = H, AND 0 = O)
INDICATORS OF VARIOUS OPTIONS:  IHDIV =  1  (-1 =INPUT VALUE, 0 = ZERO, AND 1 = CALCULATED VALUE OF DIVIDER
WALL HEAT TRANSFER COEFF.)
IAPACK =   1  (1 = PACKING IN ANNULUS, 0 = NO PACKING INANNULUS)
ICPACK =   1  (1 = PACKING IN CENTER, 0 = NO PACKING INCENTER)
```

```
LARGE-SCALE BREEDER REACTOR IHTS - CASE 47a  5/18/83
**********************************************INITIAL CONDITIONS AND INPUT DATA.  TIME = 0.0 SEC.******
CENTER SECTION DIVIDED INTO  7  NODES HORIZONTALLYON THE RADIUS
ANNULAR SECTION DIVIDED INTO  7  NODES HORIZONTALLY ON THE RADIUS
ENTIRE TRAP DIVIDED INTO 40 NODESVERTICALLY
THE SODIUM FLOW WAS  4.5000E+03  CM**3/S
THE COOLANT FLOW WAS  4.0000E+03  CM**3/S
THE MINIMUM COLD TRAP TEMPERATURE WAS  117.5  DEG. C
THE CENTER TUBE INSIDE RADIUS WAS  26.58  CM
THE CENTER TUBE OUTSIDE RADIUS WAS  27.46  CM
THE ANNULAR OUTSIDE RADIUS WAS  81.07  CM
THE COOLING JACKET INSIDE RADIUS (COLD TRAP OUTSIDE RADIUS) WAS  82.34 CM
THE COOLING JACKET OUTER RADIUS WAS  89.96  CM
THE MESH SECTION HEIGHT WAS 162.14  CM
INLET PRESSURE WAS  0.6286E+01  LB/FT**2
THE SODIUM INLET TEMPERATURE =  152.50  DEG C
THE INLET IMPURITY CONCENTRATION =  0.2000  PPM
THE TOTAL TIME OF THE CALCULATION IS  0.2880E+09  SEC
```

THE OPEN FLOW AREA IN THE TOP OF THE ANNULUS IS 0.2412E+03 CM**2

THE OPEN FLOW AREA IN THE TOP OF THE CENTER SECTION IS 0.2929E+02 CM**2

BOTP = 0.56913E+01 PINLET = 0.63605E+01 DPANN = 0.68049E+00 VFRA = 0.65185E+02 VFRC = 0.60160E+02

BOTP = 0.57438E+01 PINLET = 0.64062E+01 DPANN = 0.66914E+00 VFRA = 0.64098E+02 VFRC = 0.61082E+02

BOTP = 0.57755E+01 PINLET = 0.64339E+01 DPANN = 0.66242E+00 VFRA = 0.63455E+02 VFRC = 0.61645E+02

BOTP = 0.57947E+01 PINLET = 0.64507E+01 DPANN = 0.65841E+00 VFRA = 0.63067E+02 VFRC = 0.61986E+02

BOTP = 0.58062E+01 PINLET = 0.64608E+01 DPANN = 0.65603E+00 VFRA = 0.62839E+02 VFRC = 0.62190E+02

BOTP = 0.58131E+01 PINLET = 0.64668E+01 DPANN = 0.65462E+00 VFRA = 0.62706E+02 VFRC = 0.62314E+02

BOTP = 0.58172E+01 PINLET = 0.64705E+01 DPANN = 0.65376E+00 VFRA = 0.62627E+02 VFRC = 0.62388E+02

BOTP = 0.58197E+01 PINLET = 0.64727E+01 DPANN = 0.65322E+00 VFRA = 0.62573E+02 VFRC = 0.62433E+02

PRESSURE CONVERGENCE ERROR WAS 0.9452E-03 , DIMENSIONLESS

NUMBER OF ITERATIONS DURING LAST CONVERGENCE WAS 1050

ANNULUS PRESSURE DROP WAS 6.5292E-01 LB/FT**2

CENTER SECTION PRESSURE DROP WAS 5.8187E+00 LB/FT**2

TOTAL COLD TRAP PRESSURE DROP WAS 6.4717E+00 LB/FT**2

THE NUMBER OF PRESSURE/FLOW CYCLES WAS 9

TOTAL NUMBER OF CYCLES THROUGH INNER PRESSURE LOOP WAS 15950

FOLLOWING ARE THE AXIAL SODIUM VELOCITIES IN THE COLDTRAP, UNITS OF FT/S. *

NODE	1	2	3	4	5	6	7	8	9	10	11	12	13	14
1	-7.09E-02	-7.09E-02	-7.09E-02	-7.09E-02	-7.09E-02	-7.09E-02	-6.73E-02	8.39E-03	8.57E-03	8.57E-03	8.57E-03	8.57E-03	8.56E-03	8.35E-03
2	-7.09E-02	-7.09E-02	-7.09E-02	-7.09E-02	-7.09E-02	-7.09E-02	-6.73E-02	8.39E-03	8.56E-03	8.57E-03	8.57E-03	8.57E-03	8.56E-03	8.35E-03
3	-7.09E-02	-7.09E-02	-7.09E-02	-7.09E-02	-7.09E-02	-7.09E-02	-6.73E-02	8.39E-03	8.57E-03	8.57E-03	8.57E-03	8.57E-03	8.57E-03	8.35E-03
4	-7.09E-02	-7.09E-02	-7.09E-02	-7.09E-02	-7.09E-02	-7.09E-02	-6.73E-02	8.39E-03	8.57E-03	8.57E-03	8.56E-03	8.56E-03	8.57E-03	8.35E-03
5	-7.09E-02	-7.09E-02	-7.09E-02	-7.09E-02	-7.09E-02	-7.09E-02	-6.73E-02	8.39E-03	8.57E-03	8.57E-03	8.56E-03	8.56E-03	8.56E-03	8.35E-03
6	-7.09E-02	-7.09E-02	-7.09E-02	-7.09E-02	-7.09E-02	-7.09E-02	-6.73E-02	8.38E-03	8.56E-03	8.56E-03	8.56E-03	8.56E-03	8.56E-03	8.35E-03
7	-7.09E-02	-7.09E-02	-7.09E-02	-7.09E-02	-7.09E-02	-7.09E-02	-6.73E-02	8.38E-03	8.56E-03	8.56E-03	8.56E-03	8.56E-03	8.56E-03	8.35E-03
8	-7.09E-02	-7.09E-02	-7.09E-02	-7.09E-02	-7.09E-02	-7.09E-02	-6.73E-02	8.38E-03	8.56E-03	8.56E-03	8.56E-03	8.56E-03	8.56E-03	8.35E-03
9	-7.09E-02	-7.09E-02	-7.09E-02	-7.09E-02	-7.09E-02	-7.09E-02	-6.73E-02	8.38E-03	8.56E-03	8.56E-03	8.56E-03	8.56E-03	8.56E-03	8.35E-03
10	-7.09E-02	-7.09E-02	-7.09E-02	-7.09E-02	-7.09E-02	-7.09E-02	-6.73E-02	8.38E-03	8.56E-03	8.56E-03	8.56E-03	8.56E-03	8.56E-03	8.35E-03
11	-7.09E-02	-7.09E-02	-7.09E-02	-7.09E-02	-7.09E-02	-7.09E-02	-6.73E-02	8.38E-03	8.56E-03	8.56E-03	8.56E-03	8.56E-03	8.56E-03	8.35E-03
12	-7.09E-02	-7.09E-02	-7.09E-02	-7.09E-02	-7.09E-02	-7.09E-02	-6.73E-02	8.38E-03	8.56E-03	8.56E-03	8.56E-03	8.56E-03	8.56E-03	8.35E-03
13	-7.09E-02	-7.09E-02	-7.09E-02	-7.09E-02	-7.09E-02	-7.09E-02	-6.73E-02	8.38E-03	8.56E-03	8.56E-03	8.56E-03	8.56E-03	8.56E-03	8.35E-03
14	-7.09E-02	-7.09E-02	-7.09E-02	-7.09E-02	-7.09E-02	-7.09E-02	-6.73E-02	8.38E-03	8.56E-03	8.56E-03	8.56E-03	8.56E-03	8.56E-03	8.35E-03
15	-7.09E-02	-7.09E-02	-7.09E-02	-7.09E-02	-7.09E-02	-7.09E-02	-6.73E-02	8.38E-03	8.56E-03	8.56E-03	8.56E-03	8.56E-03	8.56E-03	8.35E-03
16	-7.09E-02	-7.09E-02	-7.09E-02	-7.09E-02	-7.09E-02	-7.09E-02	-6.73E-02	8.38E-03	8.56E-03	8.56E-03	8.56E-03	8.56E-03	8.56E-03	8.35E-03
17	-7.09E-02	-7.09E-02	-7.09E-02	-7.09E-02	-7.09E-02	-7.09E-02	-6.73E-02	8.38E-03	8.56E-03	8.56E-03	8.56E-03	8.56E-03	8.56E-03	8.35E-03
18	-7.09E-02	-7.09E-02	-7.09E-02	-7.09E-02	-7.09E-02	-7.09E-02	-6.73E-02	8.38E-03	8.56E-03	8.56E-03	8.56E-03	8.56E-03	8.56E-03	8.35E-03
19	-7.09E-02	-7.09E-02	-7.09E-02	-7.09E-02	-7.09E-02	-7.09E-02	-6.73E-02	8.38E-03	8.56E-03	8.56E-03	8.56E-03	8.56E-03	8.56E-03	8.35E-03
20	-7.09E-02	-7.09E-02	-7.09E-02	-7.09E-02	-7.09E-02	-7.09E-02	-6.73E-02	8.38E-03	8.56E-03	8.56E-03	8.56E-03	8.56E-03	8.56E-03	8.35E-03
21	-7.09E-02	-7.09E-02	-7.09E-02	-7.09E-02	-7.09E-02	-7.09E-02	-6.73E-02	8.38E-03	8.56E-03	8.56E-03	8.56E-03	8.56E-03	8.56E-03	8.35E-03
22	-7.09E-02	-7.09E-02	-7.09E-02	-7.09E-02	-7.09E-02	-7.09E-02	-6.73E-02	8.38E-03	8.56E-03	8.56E-03	8.56E-03	8.56E-03	8.56E-03	8.35E-03
23	-7.09E-02	-7.09E-02	-7.09E-02	-7.09E-02	-7.09E-02	-7.09E-02	-6.73E-02	8.38E-03	8.56E-03	8.56E-03	8.56E-03	8.56E-03	8.56E-03	8.35E-03
24	-7.09E-02	-7.09E-02	-7.09E-02	-7.09E-02	-7.09E-02	-7.09E-02	-6.73E-02	8.38E-03	8.56E-03	8.56E-03	8.56E-03	8.56E-03	8.56E-03	8.35E-03
25	-7.09E-02	-7.09E-02	-7.09E-02	-7.09E-02	-7.09E-02	-7.09E-02	-6.73E-02	8.38E-03	8.56E-03	8.56E-03	8.56E-03	8.56E-03	8.56E-03	8.35E-03
26	-7.09E-02	-7.09E-02	-7.09E-02	-7.09E-02	-7.09E-02	-7.09E-02	-6.73E-02	8.38E-03	8.56E-03	8.56E-03	8.56E-03	8.56E-03	8.56E-03	8.35E-03
27	-7.09E-02	-7.09E-02	-7.09E-02	-7.09E-02	-7.09E-02	-7.09E-02	-6.73E-02	8.38E-03	8.56E-03	8.56E-03	8.56E-03	8.56E-03	8.56E-03	8.35E-03
28	-7.09E-02	-7.09E-02	-7.09E-02	-7.09E-02	-7.09E-02	-7.09E-02	-6.73E-02	8.38E-03	8.56E-03	8.56E-03	8.56E-03	8.56E-03	8.56E-03	8.35E-03
29	-7.09E-02	-7.09E-02	-7.09E-02	-7.09E-02	-7.09E-02	-7.09E-02	-6.73E-02	8.38E-03	8.56E-03	8.56E-03	8.56E-03	8.56E-03	8.56E-03	8.35E-03
30	-7.09E-02	-7.09E-02	-7.09E-02	-7.09E-02	-7.09E-02	-7.09E-02	-6.73E-02	8.38E-03	8.56E-03	8.56E-03	8.56E-03	8.56E-03	8.56E-03	8.35E-03
31	-7.09E-02	-7.09E-02	-7.09E-02	-7.09E-02	-7.09E-02	-7.09E-02	-6.73E-02	8.38E-03	8.56E-03	8.56E-03	8.56E-03	8.56E-03	8.56E-03	8.35E-03
32	-7.09E-02	-7.09E-02	-7.09E-02	-7.09E-02	-7.09E-02	-7.09E-02	-6.73E-02	8.38E-03	8.56E-03	8.56E-03	8.56E-03	8.56E-03	8.56E-03	8.35E-03
33	-7.09E-02	-7.09E-02	-7.09E-02	-7.09E-02	-7.09E-02	-7.09E-02	-6.73E-02	8.38E-03	8.56E-03	8.56E-03	8.56E-03	8.56E-03	8.56E-03	8.35E-03
34	-7.09E-02	-7.09E-02	-7.09E-02	-7.09E-02	-7.09E-02	-7.09E-02	-6.73E-02	8.38E-03	8.56E-03	8.56E-03	8.56E-03	8.56E-03	8.56E-03	8.35E-03
35	-7.09E-02	-7.09E-02	-7.09E-02	-7.09E-02	-7.09E-02	-7.09E-02	-6.73E-02	8.38E-03	8.56E-03	8.56E-03	8.56E-03	8.56E-03	8.56E-03	8.35E-03
36	-7.09E-02	-7.09E-02	-7.09E-02	-7.09E-02	-7.09E-02	-7.09E-02	-6.73E-02	8.38E-03	8.56E-03	8.56E-03	8.56E-03	8.56E-03	8.56E-03	8.35E-03
37	-7.09E-02	-7.09E-02	-7.09E-02	-7.09E-02	-7.09E-02	-7.09E-02	-6.73E-02	8.38E-03	8.56E-03	8.56E-03	8.56E-03	8.56E-03	8.56E-03	8.35E-03
38	-7.09E-02	-7.09E-02	-7.09E-02	-7.09E-02	-7.09E-02	-7.09E-02	-6.73E-02	8.38E-03	8.56E-03	8.56E-03	8.56E-03	8.56E-03	8.56E-03	8.35E-03
39	-7.09E-02	-7.09E-02	-7.09E-02	-7.09E-02	-7.09E-02	-7.09E-02	-6.73E-02	8.38E-03	8.56E-03	8.56E-03	8.56E-03	8.56E-03	8.56E-03	8.35E-03
40	-7.09E-02	-7.09E-02	-7.09E-02	-7.09E-02	-7.09E-02	-7.09E-02	-6.73E-02	8.38E-03	8.56E-03	8.56E-03	8.56E-03	8.56E-03	8.56E-03	8.35E-03

SODIUM FLOW RATE CALCULATED FOR ANNULUS SECTION IS 0.4503E+04 CM**3/S.

SODIUM FLOW RATE CALCULATED FOR CENTER SECTION IS 0.4497E+04 CM**3/S.

* ALL VELOCITIES ARE POSITIVE IN THE DOWNWARD AND THE RIGHTWARD DIRECTIONS.

THE FLOW CONVERGENCE ERROR WAS 0.9570E-02, DIMENSIONLESS

THE NUMBER OF ITERATIONS DURING LAST FLOW/PRESSURE CYCLE WAS 1

```
NCTIT =    0  NTOT =  300  AVE. BOT. TEMP=  130.57
CTEMP WAS CHANGED TO   89.54
NCTIT =    1  NTOT =  600  AVE. BOT. TEMP=  126.41
CTEMP WAS CHANGED TO   82.41
NCTIT =    2  NTOT =  900  AVE. BOT. TEMP=  123.57


 CTEMP WAS CHANGED TO   77.55

 NCTIT =    3  NTOT = 1200  AVE. BOT. TEMP=  121.64
 CTEMP WAS CHANGED TO   74.24
 NCTIT =    4  NTOT = 1500  AVE. BOT. TEMP=  120.32
 CTEMP WAS CHANGED TO   71.98


THE COLD TRAP INLET TEMPERATURE WAS    152.50  DEG. C
THE BOTTOM (MIN) TEMPERATURE WAS    119.42  DEG. C
THE OUTLET TEMPERATURE WAS    127.76  DEG. C
THE COOLANT INLET TEMPERATURE WAS     71.98  DEG. C
THE COOLANT OUTLET TEMPERATUREWAS    115.71  DEG. C
THE FINAL COOLANT FLOW WAS  0.4000E+04   CM**3/S
```

FOLLOWING ARE THE CALCULATED TEMPERATURES IN ALL NODES, DEG. C

NODE	1	2	3	4	5	6	7	8	9	10	11	12	13	14	15
1	123.0	123.2	123.6	124.4	125.9	128.6	133.5	150.1	152.1	152.4	152.4	152.4	152.0	149.6	115.1
2	122.7	122.8	123.2	124.0	125.6	128.4	133.4	148.1	151.6	152.3	152.3	152.2	151.2	147.0	113.9
3	122.6	122.8	123.2	123.9	125.4	128.2	132.9	146.6	151.0	152.1	152.2	151.8	150.3	144.8	112.6
4	122.6	122.7	123.1	123.8	125.3	127.9	132.5	145.3	150.4	151.8	152.0	151.5	149.4	142.8	111.5
5	122.6	122.7	123.0	123.8	125.1	127.7	132.1	144.2	149.8	151.5	151.8	151.0	148.4	141.0	110.3
6	122.6	122.7	123.0	123.7	125.0	127.5	131.7	143.2	149.2	151.2	151.5	150.5	147.3	139.3	109.2
7	122.5	122.6	122.9	123.6	124.9	127.3	131.4	142.4	148.6	150.9	151.1	150.0	146.3	137.7	108.1
8	122.5	122.6	122.9	123.5	124.7	127.0	131.1	141.7	148.1	150.5	150.8	149.4	145.3	136.3	107.0
9	122.5	122.6	122.8	123.4	124.6	126.8	130.8	141.0	147.5	150.1	150.4	148.7	144.3	134.9	105.9
10	122.5	122.6	122.8	123.4	124.5	126.7	130.5	140.5	147.0	149.6	149.9	148.1	143.2	133.6	104.8
11	122.5	122.5	122.8	123.3	124.4	126.5	130.2	139.9	146.4	149.2	149.4	147.4	142.2	132.4	103.8
12	122.4	122.5	122.7	123.2	124.2	126.3	129.9	139.4	145.9	148.7	148.9	146.7	141.2	131.2	102.7
13	122.4	122.5	122.7	123.1	124.1	126.1	129.6	138.9	145.4	148.3	148.4	146.0	140.2	130.0	101.7
14	122.4	122.5	122.7	123.1	124.0	125.9	129.4	138.5	144.9	147.8	147.8	145.2	139.3	128.9	100.6
15	122.4	122.5	122.6	123.0	123.9	125.7	129.1	138.0	144.4	147.3	147.3	144.5	138.3	127.8	99.6
16	122.4	122.4	122.6	123.0	123.8	125.5	128.8	137.6	143.9	146.8	146.7	143.7	137.4	126.7	98.6
17	122.4	122.4	122.6	122.9	123.7	125.4	128.6	137.2	143.4	146.2	146.1	143.0	136.4	125.6	97.5
18	122.4	122.4	122.5	122.8	123.6	125.2	128.3	136.8	143.0	145.7	145.5	142.2	135.5	124.6	96.5
19	122.4	122.4	122.5	122.8	123.5	125.0	128.1	136.4	142.5	145.2	144.8	141.4	134.6	123.6	95.5
20	122.4	122.4	122.5	122.7	123.4	124.9	127.8	136.0	142.0	144.6	144.2	140.7	133.6	122.6	94.4
21	122.4	122.4	122.5	122.7	123.3	124.7	127.6	135.7	141.5	144.1	143.6	139.9	132.7	121.6	93.4
22	122.4	122.4	122.4	122.7	123.2	124.5	127.3	135.3	141.1	143.5	142.9	139.1	131.8	120.6	92.3
23	122.4	122.4	122.4	122.6	123.1	124.4	127.1	134.9	140.6	143.0	142.2	138.3	130.9	119.6	91.3
24	122.4	122.4	122.4	122.6	123.0	124.2	126.8	134.5	140.1	142.4	141.6	137.6	130.0	118.6	90.3
25	122.3	122.4	122.4	122.5	123.0	124.1	126.6	134.2	139.6	141.8	140.9	136.8	129.1	117.6	89.2
26	122.3	122.4	122.4	122.5	122.9	123.9	126.3	133.8	139.2	141.3	140.2	136.0	128.2	116.7	88.2
27	122.3	122.4	122.4	122.5	122.8	123.8	126.1	133.4	138.7	140.7	139.6	135.2	127.3	115.7	87.1
28	122.3	122.4	122.4	122.5	122.7	123.6	125.8	133.1	138.2	140.1	138.9	134.4	126.5	114.8	86.1
29	122.3	122.3	122.4	122.4	122.7	123.5	125.6	132.7	137.7	139.5	138.2	133.6	125.6	113.8	85.0
30	122.3	122.3	122.4	122.4	122.6	123.3	125.3	132.3	137.2	139.0	137.5	132.9	124.7	112.9	84.0
31	122.3	122.3	122.3	122.4	122.6	123.2	125.1	132.0	136.7	138.4	136.8	132.1	123.8	111.9	82.9
32	122.3	122.3	122.3	122.4	122.5	123.1	124.8	131.6	136.3	137.8	136.1	131.3	122.9	111.0	81.8
33	122.3	122.3	122.3	122.4	122.5	122.9	124.5	131.2	135.8	137.2	135.4	130.5	122.1	110.0	80.8
34	122.3	122.3	122.3	122.4	122.4	122.8	124.3	130.8	135.3	136.6	134.8	129.7	121.2	109.0	79.7
35	122.3	122.3	122.3	122.3	122.4	122.7	124.0	130.4	134.8	136.0	134.0	128.9	120.3	108.1	78.6
36	122.3	122.3	122.3	122.3	122.4	122.6	123.7	130.0	134.2	135.3	133.3	128.1	119.4	107.2	77.5
37	122.3	122.3	122.3	122.3	122.4	122.5	123.4	129.6	133.6	134.6	132.5	127.2	118.5	106.2	76.4
38	122.3	122.3	122.3	122.3	122.4	122.5	123.1	129.0	132.8	133.6	131.4	126.1	117.5	105.3	75.3
39	122.3	122.3	122.3	122.3	122.3	122.4	122.8	128.1	131.4	131.9	129.7	124.5	116.3	104.6	74.2
40	122.3	122.3	122.3	122.3	122.3	122.4	122.6	126.3	128.5	128.5	126.3	121.6	114.5	104.5	73.1
TBOT	122.3	122.3	122.3	122.3	122.3	122.3	122.3	122.3	121.8	120.5	118.3	115.1	111.1	106.5	

THE TOTAL NUMBER OF TEMPERATURE ITERATIONS WAS 1800

THE NUMBER OF COOLANT TEMP. ADJUSTMENTS WAS 5

THE SUM OF TEMPERATURE CHANGES DURING THE LAST ITERATION WAS 0.0000E+00 DEG. C

THE DIFFERENCE BETWEEN THE CALCULATED BOTTOM TEMPERATURE AND THE INPUT VALUE WAS 1.9233E+00 DEG. C

THE HEAT LOST BY THE SODIUM WAS 3.3246E+04 CAL/S

THE HEAT GAINED BY THE NAK COOLANT WAS 3.3056E+04 CAL/S

ALL IMPURITY CONCENTRATIONS, PPM.

IMPURITY IS HYDROGEN.

NODE	1	2	3	4	5	6	7	8	9	10	11	12	13	14
1	0.0609	0.0609	0.0609	0.0607	0.0604	0.0596	0.0584	0.1861	0.1989	0.1998	0.1999	0.1997	0.1980	0.1828
2	0.0609	0.0609	0.0609	0.0607	0.0604	0.0596	0.0584	0.1737	0.1963	0.1995	0.1996	0.1990	0.1937	0.1668
3	0.0609	0.0609	0.0609	0.0607	0.0604	0.0596	0.0584	0.1643	0.1929	0.1988	0.1992	0.1977	0.1882	0.1538
4	0.0609	0.0609	0.0609	0.0607	0.0604	0.0596	0.0584	0.1569	0.1892	0.1977	0.1985	0.1957	0.1822	0.1431
5	0.0609	0.0609	0.0609	0.0607	0.0604	0.0596	0.0584	0.1510	0.1854	0.1963	0.1975	0.1931	0.1760	0.1340
6	0.0609	0.0609	0.0609	0.0607	0.0604	0.0596	0.0584	0.1461	0.1817	0.1946	0.1961	0.1901	0.1699	0.1262
7	0.0609	0.0609	0.0609	0.0607	0.0604	0.0596	0.0584	0.1419	0.1781	0.1925	0.1943	0.1866	0.1638	0.1192
8	0.0609	0.0609	0.0609	0.0607	0.0604	0.0596	0.0584	0.1383	0.1746	0.1901	0.1920	0.1829	0.1578	0.1130
9	0.0609	0.0609	0.0609	0.0607	0.0604	0.0596	0.0584	0.1350	0.1711	0.1874	0.1894	0.1789	0.1521	0.1073
10	0.0609	0.0609	0.0609	0.0607	0.0604	0.0596	0.0584	0.1320	0.1678	0.1846	0.1865	0.1747	0.1465	0.1021
11	0.0609	0.0609	0.0609	0.0607	0.0604	0.0596	0.0584	0.1293	0.1645	0.1816	0.1833	0.1704	0.1411	0.0973
12	0.0609	0.0609	0.0609	0.0607	0.0604	0.0596	0.0584	0.1268	0.1613	0.1786	0.1799	0.1660	0.1359	0.0928
13	0.0609	0.0609	0.0609	0.0607	0.0604	0.0596	0.0584	0.1244	0.1582	0.1754	0.1764	0.1616	0.1309	0.0887
14	0.0609	0.0609	0.0609	0.0607	0.0604	0.0596	0.0584	0.1222	0.1552	0.1722	0.1728	0.1572	0.1261	0.0847
15	0.0609	0.0609	0.0609	0.0607	0.0604	0.0596	0.0584	0.1201	0.1523	0.1690	0.1691	0.1529	0.1215	0.0811
16	0.0609	0.0609	0.0609	0.0607	0.0604	0.0596	0.0584	0.1180	0.1495	0.1658	0.1654	0.1486	0.1171	0.0776
17	0.0609	0.0609	0.0609	0.0607	0.0604	0.0596	0.0584	0.1161	0.1467	0.1626	0.1617	0.1444	0.1129	0.0743
18	0.0608	0.0609	0.0609	0.0607	0.0604	0.0596	0.0584	0.1142	0.1440	0.1594	0.1580	0.1402	0.1089	0.0712
19	0.0608	0.0609	0.0609	0.0607	0.0604	0.0596	0.0584	0.1124	0.1413	0.1561	0.1542	0.1361	0.1049	0.0683
20	0.0608	0.0608	0.0609	0.0607	0.0604	0.0596	0.0584	0.1107	0.1387	0.1529	0.1506	0.1321	0.1012	0.0654
21	0.0607	0.0608	0.0609	0.0607	0.0604	0.0596	0.0584	0.1090	0.1361	0.1497	0.1470	0.1282	0.0976	0.0628
22	0.0607	0.0607	0.0608	0.0607	0.0604	0.0596	0.0584	0.1073	0.1336	0.1466	0.1434	0.1244	0.0941	0.0602
23	0.0607	0.0607	0.0608	0.0607	0.0604	0.0596	0.0584	0.1056	0.1312	0.1435	0.1398	0.1207	0.0908	0.0578
24	0.0606	0.0606	0.0607	0.0608	0.0604	0.0596	0.0584	0.1040	0.1288	0.1405	0.1362	0.1171	0.0876	0.0554
25	0.0606	0.0606	0.0606	0.0608	0.0604	0.0597	0.0584	0.1023	0.1264	0.1374	0.1328	0.1136	0.0845	0.0532
26	0.0605	0.0605	0.0605	0.0607	0.0604	0.0597	0.0584	0.1008	0.1240	0.1345	0.1294	0.1101	0.0815	0.0511
27	0.0604	0.0604	0.0605	0.0606	0.0604	0.0597	0.0584	0.0993	0.1217	0.1315	0.1261	0.1068	0.0786	0.0490
28	0.0603	0.0603	0.0604	0.0604	0.0605	0.0597	0.0584	0.0978	0.1194	0.1287	0.1229	0.1036	0.0758	0.0470
29	0.0602	0.0602	0.0603	0.0603	0.0605	0.0597	0.0584	0.0963	0.1172	0.1258	0.1196	0.1004	0.0732	0.0452
30	0.0601	0.0601	0.0601	0.0602	0.0603	0.0597	0.0584	0.0949	0.1150	0.1229	0.1165	0.0974	0.0706	0.0434
31	0.0600	0.0600	0.0600	0.0600	0.0601	0.0597	0.0584	0.0935	0.1127	0.1202	0.1135	0.0944	0.0682	0.0417
32	0.0598	0.0598	0.0598	0.0598	0.0599	0.0598	0.0584	0.0921	0.1106	0.1174	0.1105	0.0915	0.0658	0.0401
33	0.0596	0.0596	0.0596	0.0596	0.0597	0.0598	0.0584	0.0907	0.1085	0.1147	0.1075	0.0888	0.0636	0.0387
34	0.0593	0.0593	0.0593	0.0594	0.0594	0.0595	0.0584	0.0893	0.1063	0.1121	0.1047	0.0862	0.0616	0.0373
35	0.0590	0.0590	0.0591	0.0591	0.0591	0.0591	0.0584	0.0879	0.1042	0.1094	0.1019	0.0837	0.0597	0.0362
36	0.0587	0.0587	0.0587	0.0587	0.0587	0.0587	0.0584	0.0865	0.1021	0.1067	0.0992	0.0813	0.0580	0.0351
37	0.0582	0.0582	0.0583	0.0583	0.0583	0.0583	0.0584	0.0850	0.0998	0.1037	0.0962	0.0789	0.0564	0.0342
38	0.0577	0.0577	0.0577	0.0577	0.0577	0.0577	0.0577	0.0835	0.0970	0.1001	0.0926	0.0761	0.0546	0.0333
39	0.0571	0.0571	0.0571	0.0571	0.0571	0.0570	0.0570	0.0814	0.0927	0.0946	0.0872	0.0720	0.0523	0.0325
40	0.0563	0.0563	0.0563	0.0563	0.0563	0.0563	0.0562	0.0774	0.0845	0.0843	0.0773	0.0644	0.0484	0.0315
CBOT	0.0553	0.0553	0.0553	0.0553	0.0553	0.0553	0.0553	0.0553	0.0525	0.0493	0.0457	0.0415	0.0368	0.0315

THE OUTLET CONCENTRATION WAS 0.0598 PPM.

THE NUMBER OF CONCENTRATION ITERATIONS: 120

THE SUM OF CONCENTRATION ERRORS = 0.5968E-05 PPM

THE COLD TRAP EFFICIENCY = 82.57 %

THE INLET CONCENTRATION = 0.2000 PPM.

**********MASS DEPOSITED AT END OF 5.0400E+07 SEC.**********

********** ITERATION NUMBER 6**********

IMPURITY MASS DEPOSITED IN THE ANNULUS, G.

NODE	8	9	10	11	12	13	14
1	1.0158E+00	2.7230E-01	7.7165E-02	6.8264E-02	1.4882E-01	6.5108E-01	2.6473E+00
2	1.2708E+00	5.7782E-01	1.9849E-01	1.6105E-01	3.8754E-01	1.3627E+00	3.3970E+00
3	1.3169E+00	8.4027E-01	3.5154E-01	2.8812E-01	6.9906E-01	1.9302E+00	3.5788E+00
4	1.3291E+00	1.0298E+00	5.3163E-01	4.6199E-01	1.0247E+00	2.3295E+00	3.6528E+00
5	1.3277E+00	1.1705E+00	7.1731E-01	6.7547E-01	1.3364E+00	2.6208E+00	3.6766E+00
6	1.3181E+00	1.2624E+00	8.8251E-01	8.9412E-01	1.6106E+00	2.8339E+00	3.6650E+00
7	1.2997E+00	1.3310E+00	1.0472E+00	1.1104E+00	1.8399E+00	2.9785E+00	3.6087E+00
8	1.2650E+00	1.3703E+00	1.1729E+00	1.2977E+00	2.0077E+00	3.0484E+00	3.5222E+00
9	1.2225E+00	1.3844E+00	1.2522E+00	1.4391E+00	2.1247E+00	3.0758E+00	3.4106E+00
10	1.1723E+00	1.3699E+00	1.3220E+00	1.5532E+00	2.2058E+00	3.0452E+00	3.2775E+00
11	1.1157E+00	1.3397E+00	1.3608E+00	1.6383E+00	2.2252E+00	2.9966E+00	3.1349E+00
12	1.0540E+00	1.3097E+00	1.3665E+00	1.6667E+00	2.2241E+00	2.9111E+00	2.9744E+00
13	9.9266E-01	1.2573E+00	1.3653E+00	1.6712E+00	2.2016E+00	2.8138E+00	2.8151E+00
14	9.3306E-01	1.2057E+00	1.3469E+00	1.6650E+00	2.1633E+00	2.7056E+00	2.6590E+00
15	8.7634E-01	1.1587E+00	1.3266E+00	1.6392E+00	2.1081E+00	2.5901E+00	2.5063E+00
16	8.2332E-01	1.1017E+00	1.3001E+00	1.6096E+00	2.0527E+00	2.4726E+00	2.3682E+00
17	7.7253E-01	1.0557E+00	1.2685E+00	1.5833E+00	1.9950E+00	2.3642E+00	2.2451E+00
18	7.2657E-01	1.0100E+00	1.2435E+00	1.5527E+00	1.9381E+00	2.2660E+00	2.1221E+00
19	6.8584E-01	9.6149E-01	1.2211E+00	1.5156E+00	1.8807E+00	2.1638E+00	2.0079E+00
20	6.4852E-01	9.2700E-01	1.1872E+00	1.4731E+00	1.8179E+00	2.0679E+00	1.9053E+00
21	6.1359E-01	8.9387E-01	1.1573E+00	1.4329E+00	1.7631E+00	1.9822E+00	1.8126E+00
22	5.7946E-01	8.5547E-01	1.1258E+00	1.4050E+00	1.7104E+00	1.9020E+00	1.7271E+00
23	5.4740E-01	8.2446E-01	1.1018E+00	1.3789E+00	1.6658E+00	1.8254E+00	1.6479E+00
24	5.1919E-01	7.9444E-01	1.0734E+00	1.3485E+00	1.6161E+00	1.7565E+00	1.5759E+00
25	4.9542E-01	7.6711E-01	1.0436E+00	1.3091E+00	1.5671E+00	1.6926E+00	1.5110E+00
26	4.7804E-01	7.3780E-01	1.0124E+00	1.2838E+00	1.5273E+00	1.6346E+00	1.4490E+00
27	4.6528E-01	7.1644E-01	9.8784E-01	1.2537E+00	1.4924E+00	1.5800E+00	1.3917E+00
28	4.5264E-01	6.9978E-01	9.6717E-01	1.2319E+00	1.4554E+00	1.5262E+00	1.3422E+00
29	4.4199E-01	6.7885E-01	9.4974E-01	1.2099E+00	1.4191E+00	1.4843E+00	1.2994E+00
30	4.3291E-01	6.6072E-01	9.2642E-01	1.1865E+00	1.3901E+00	1.4487E+00	1.2653E+00
31	4.2203E-01	6.4352E-01	9.0526E-01	1.1655E+00	1.3667E+00	1.4278E+00	1.2437E+00
32	4.1403E-01	6.2475E-01	8.8010E-01	1.1466E+00	1.3591E+00	1.4226E+00	1.2351E+00
33	4.0601E-01	6.1178E-01	8.5851E-01	1.1382E+00	1.3598E+00	1.4357E+00	1.2438E+00
34	3.9905E-01	6.0144E-01	8.3861E-01	1.1312E+00	1.3813E+00	1.4754E+00	1.2769E+00
35	3.9443E-01	5.9609E-01	8.2643E-01	1.1360E+00	1.4276E+00	1.5506E+00	1.3395E+00
36	3.9655E-01	6.0464E-01	8.2843E-01	1.1586E+00	1.5132E+00	1.6775E+00	1.4348E+00
37	4.1953E-01	6.4951E-01	8.7222E-01	1.2243E+00	1.6466E+00	1.8497E+00	1.5641E+00
38	5.0365E-01	7.6277E-01	1.0095E+00	1.3839E+00	1.8442E+00	2.0544E+00	1.7028E+00
39	6.9449E-01	1.0666E+00	1.4006E+00	1.7635E+00	2.1418E+00	2.2287E+00	1.7592E+00
40	1.1179E+00	1.8612E+00	2.3945E+00	2.6835E+00	2.6538E+00	2.2198E+00	1.3438E+00

IMPURITY MASS DEPOSITED IN BOTTOM, G.

NODE	1	2	3	4	5	6	7	8	9	10	11	12	13	14
HMBOT	0.0000	0.0000	0.0000	0.0000	0.0000	0.0000	0.0000	0.0000	0.0000	0.0000	0.0000	0.0000	0.0000	0.0000

IMPURITY MASS DEPOSITED IN THE CENTER, G.

NODE	1	2	3	4	5	6	7
1	0.0000E+00	0.0000E+00	0.0000E+00	0.0000E+00	0.0000E+00	0.0000E+00	0.0000E+00
2	0.0000E+00	0.0000E+00	0.0000E+00	0.0000E+00	0.0000E+00	0.0000E+00	0.0000E+00
3	0.0000E+00	0.0000E+00	0.0000E+00	0.0000E+00	0.0000E+00	0.0000E+00	0.0000E+00
4	0.0000E+00	0.0000E+00	0.0000E+00	0.0000E+00	0.0000E+00	0.0000E+00	0.0000E+00
5	0.0000E+00	0.0000E+00	0.0000E+00	0.0000E+00	0.0000E+00	0.0000E+00	0.0000E+00
6	0.0000E+00	0.0000E+00	0.0000E+00	0.0000E+00	0.0000E+00	0.0000E+00	0.0000E+00
7	0.0000E+00	0.0000E+00	0.0000E+00	0.0000E+00	0.0000E+00	0.0000E+00	0.0000E+00
8	0.0000E+00	0.0000E+00	0.0000E+00	0.0000E+00	0.0000E+00	0.0000E+00	0.0000E+00
9	0.0000E+00	0.0000E+00	0.0000E+00	0.0000E+00	0.0000E+00	0.0000E+00	0.0000E+00
10	0.0000E+00	0.0000E+00	0.0000E+00	0.0000E+00	0.0000E+00	0.0000E+00	0.0000E+00
11	0.0000E+00	0.0000E+00	0.0000E+00	0.0000E+00	0.0000E+00	0.0000E+00	0.0000E+00
12	0.0000E+00	0.0000E+00	0.0000E+00	0.0000E+00	0.0000E+00	0.0000E+00	0.0000E+00
13	0.0000E+00	0.0000E+00	0.0000E+00	0.0000E+00	0.0000E+00	0.0000E+00	0.0000E+00
14	0.0000E+00	0.0000E+00	0.0000E+00	0.0000E+00	0.0000E+00	0.0000E+00	0.0000E+00
15	0.0000E+00	0.0000E+00	0.0000E+00	0.0000E+00	0.0000E+00	0.0000E+00	0.0000E+00
16	2.2654E-05	0.0000E+00	0.0000E+00	0.0000E+00	0.0000E+00	0.0000E+00	0.0000E+00
17	5.6103E-05	0.0000E+00	0.0000E+00	0.0000E+00	0.0000E+00	0.0000E+00	0.0000E+00
18	9.1613E-05	1.0886E-04	0.0000E+00	0.0000E+00	0.0000E+00	0.0000E+00	0.0000E+00
19	1.2649E-04	2.4437E-04	0.0000E+00	0.0000E+00	0.0000E+00	0.0000E+00	0.0000E+00
20	1.6581E-04	3.8032E-04	0.0000E+00	0.0000E+00	0.0000E+00	0.0000E+00	0.0000E+00
21	2.1117E-04	5.2429E-04	1.8016E-04	0.0000E+00	0.0000E+00	0.0000E+00	0.0000E+00
22	2.5692E-04	6.8400E-04	5.2028E-04	0.0000E+00	0.0000E+00	0.0000E+00	0.0000E+00
23	3.0897E-04	8.6040E-04	8.9027E-04	0.0000E+00	0.0000E+00	0.0000E+00	0.0000E+00
24	3.6594E-04	1.0538E-03	1.2753E-03	0.0000E+00	0.0000E+00	0.0000E+00	0.0000E+00
25	4.3249E-04	1.2710E-03	1.6936E-03	6.5243E-04	0.0000E+00	0.0000E+00	0.0000E+00
26	5.0980E-04	1.5056E-03	2.1620E-03	1.4894E-03	0.0000E+00	0.0000E+00	0.0000E+00
27	5.9858E-04	1.7781E-03	2.6708E-03	2.3757E-03	0.0000E+00	0.0000E+00	0.0000E+00
28	7.0296E-04	2.0784E-03	3.2492E-03	3.3726E-03	0.0000E+00	0.0000E+00	0.0000E+00
29	8.2356E-04	2.4317E-03	3.9108E-03	4.4408E-03	1.5601E-03	0.0000E+00	0.0000E+00
30	9.6878E-04	2.8571E-03	4.6481E-03	5.6544E-03	3.5478E-03	0.0000E+00	0.0000E+00
31	1.1364E-03	3.3510E-03	5.5173E-03	7.0107E-03	5.7388E-03	0.0000E+00	0.0000E+00
32	1.3369E-03	3.9382E-03	6.5234E-03	8.5864E-03	8.2190E-03	0.0000E+00	0.0000E+00
33	1.5692E-03	4.6367E-03	7.7462E-03	1.0390E-02	1.0987E-02	2.8361E-03	0.0000E+00
34	1.8533E-03	5.5043E-03	9.1760E-03	1.2508E-02	1.4148E-02	7.7928E-03	0.0000E+00
35	2.1953E-03	6.5481E-03	1.0923E-02	1.5025E-02	1.7787E-02	1.3499E-02	0.0000E+00
36	2.6101E-03	7.8160E-03	1.3070E-02	1.8116E-02	2.2065E-02	2.0165E-02	0.0000E+00
37	3.1194E-03	9.4020E-03	1.5702E-02	2.1922E-02	2.7197E-02	2.7969E-02	1.9997E-03
38	3.7682E-03	1.1357E-02	1.8979E-02	2.6665E-02	3.3488E-02	3.7219E-02	1.6587E-02
39	4.6040E-03	1.3880E-02	2.3209E-02	3.2660E-02	4.1690E-02	4.8457E-02	3.6110E-02
40	5.7029E-03	1.7202E-02	2.8791E-02	4.0460E-02	5.2024E-02	6.2239E-02	6.2111E-02

TOTAL MASS IN THE ANNULUS = 3.9962E+02 G.

TOTAL MASS IN THE CENTER SECTION = 1.0805E+00 G.

TOTAL MASS IN THE BOTTOM SECTION = 0.0000E+00 G.

TOTAL MASS IN THE WHOLE TRAP = 4.0070E+02 G.

MASS CALCULATED, FLOW X DELTA-C = 4.0396E+02 G.

FOLLOWING IS THE PERCENT OF NODE VOLUME USED.

NODE	1	2	3	4	5	6	7	8	9	10	11	12	13	14
1	0.0	0.0	0.0	0.0	0.0	0.0	0.0	21.9	4.7	1.1	0.8	1.6	6.3	23.2
2	0.0	0.0	0.0	0.0	0.0	0.0	0.0	27.4	10.0	2.9	2.0	4.2	13.2	29.7
3	0.0	0.0	0.0	0.0	0.0	0.0	0.0	28.4	14.6	5.1	3.6	7.6	18.7	31.3
4	0.0	0.0	0.0	0.0	0.0	0.0	0.0	28.7	17.9	7.7	5.8	11.2	22.6	32.0
5	0.0	0.0	0.0	0.0	0.0	0.0	0.0	28.7	20.3	10.4	8.4	14.6	25.4	32.2
6	0.0	0.0	0.0	0.0	0.0	0.0	0.0	28.5	21.9	12.8	11.1	17.6	27.5	32.1
7	0.0	0.0	0.0	0.0	0.0	0.0	0.0	28.1	23.1	15.2	13.8	20.1	28.9	31.6
8	0.0	0.0	0.0	0.0	0.0	0.0	0.0	27.3	23.8	17.0	16.2	21.9	29.6	30.8
9	0.0	0.0	0.0	0.0	0.0	0.0	0.0	26.4	24.0	18.2	17.9	23.2	29.9	29.8
10	0.0	0.0	0.0	0.0	0.0	0.0	0.0	25.3	23.8	19.2	19.3	24.1	29.6	28.7
11	0.0	0.0	0.0	0.0	0.0	0.0	0.0	24.1	23.2	19.7	20.4	24.3	29.1	27.4
12	0.0	0.0	0.0	0.0	0.0	0.0	0.0	22.8	22.7	19.8	20.8	24.3	28.3	26.0
13	0.0	0.0	0.0	0.0	0.0	0.0	0.0	21.4	21.8	19.8	20.8	24.0	27.3	24.6
14	0.0	0.0	0.0	0.0	0.0	0.0	0.0	20.1	20.9	19.5	20.7	23.6	26.3	23.3
15	0.0	0.0	0.0	0.0	0.0	0.0	0.0	18.9	20.1	19.2	20.4	23.0	25.2	21.9
16	0.0	0.0	0.0	0.0	0.0	0.0	0.0	17.8	19.1	18.8	20.0	22.4	24.0	20.7
17	0.0	0.0	0.0	0.0	0.0	0.0	0.0	16.7	18.3	18.4	19.7	21.8	23.0	19.6
18	0.1	0.0	0.0	0.0	0.0	0.0	0.0	15.7	17.5	18.0	19.3	21.1	22.0	18.6
19	0.1	0.1	0.0	0.0	0.0	0.0	0.0	14.8	16.7	17.7	18.9	20.5	21.0	17.6
20	0.1	0.1	0.0	0.0	0.0	0.0	0.0	14.0	16.1	17.2	18.3	19.8	20.1	16.7
21	0.2	0.1	0.0	0.0	0.0	0.0	0.0	13.2	15.5	16.8	17.8	19.2	19.2	15.9
22	0.2	0.2	0.1	0.0	0.0	0.0	0.0	12.5	14.8	16.3	17.5	18.7	18.5	15.1
23	0.2	0.2	0.1	0.0	0.0	0.0	0.0	11.8	14.3	16.0	17.2	18.2	17.7	14.4
24	0.3	0.3	0.2	0.0	0.0	0.0	0.0	11.2	13.8	15.6	16.8	17.6	17.1	13.8
25	0.3	0.3	0.2	0.1	0.0	0.0	0.0	10.7	13.3	15.1	16.3	17.1	16.4	13.2
26	0.4	0.4	0.3	0.2	0.0	0.0	0.0	10.3	12.8	14.7	16.0	16.7	15.9	12.7
27	0.4	0.4	0.4	0.2	0.0	0.0	0.0	10.0	12.4	14.3	15.6	16.3	15.3	12.2
28	0.5	0.5	0.5	0.3	0.0	0.0	0.0	9.8	12.1	14.0	15.3	15.9	14.8	11.7
29	0.6	0.6	0.6	0.5	0.1	0.0	0.0	9.5	11.8	13.8	15.1	15.5	14.4	11.4
30	0.7	0.7	0.7	0.6	0.3	0.0	0.0	9.3	11.5	13.4	14.8	15.2	14.1	11.1
31	0.8	0.8	0.8	0.7	0.5	0.0	0.0	9.1	11.2	13.1	14.5	14.9	13.9	10.9
32	1.0	0.9	0.9	0.9	0.7	0.0	0.0	8.9	10.8	12.8	14.3	14.8	13.8	10.8
33	1.1	1.1	1.1	1.1	0.9	0.2	0.0	8.8	10.6	12.4	14.2	14.8	13.9	10.9
34	1.3	1.3	1.3	1.3	1.1	0.5	0.0	8.6	10.4	12.2	14.1	15.1	14.3	11.2
35	1.6	1.6	1.6	1.5	1.4	0.9	0.0	8.5	10.3	12.0	14.1	15.6	15.1	11.7
36	1.9	1.9	1.9	1.9	1.8	1.3	0.0	8.6	10.5	12.0	14.4	16.5	16.3	12.6
37	2.2	2.2	2.3	2.2	2.2	1.8	0.1	9.1	11.3	12.6	15.2	18.0	18.0	13.7
38	2.7	2.7	2.7	2.7	2.7	2.4	0.9	10.9	13.2	14.6	17.2	20.1	19.9	14.9
39	3.3	3.3	3.3	3.3	3.3	3.2	2.0	15.0	18.5	20.3	22.0	23.4	21.6	15.4
40	4.1	4.1	4.1	4.1	4.1	4.1	3.4	24.1	32.3	34.7	33.4	29.0	21.6	11.8
BOTTOM	0.0	0.0	0.0	0.0	0.0	0.0	0.0	0.0	0.0	0.0	0.0	0.0	0.0	0.0

**********PRESSURES AND FLOWS AFTER 5.0400E+07 SEC, BELOW.******

********** ITERATION NUMBER 6**********

BOTP = 0.63313E+01 PINLET = 0.14265E+02 DPANN = 0.62502E+01 VFRA = 0.47950E+02 VFRC = 0.62500E+02

BOTP = 0.63313E+01 PINLET = 0.14349E+02 DPANN = 0.79337E+01 VFRA = 0.60877E+02 VFRC = 0.62500E+02

BOTP = 0.63313E+01 PINLET = 0.14400E+02 DPANN = 0.80176E+01 VFRA = 0.61519E+02 VFRC = 0.62500E+02

BOTP = 0.63313E+01 PINLET = 0.14430E+02 DPANN = 0.80685E+01 VFRA = 0.61911E+02 VFRC = 0.62500E+02

BOTP = 0.63313E+01 PINLET = 0.14449E+02 DPANN = 0.80991E+01 VFRA = 0.62144E+02 VFRC = 0.62500E+02

BOTP = 0.63313E+01 PINLET = 0.14460E+02 DPANN = 0.81176E+01 VFRA = 0.62289E+02 VFRC = 0.62500E+02

BOTP = 0.63312E+01 PINLET = 0.14466E+02 DPANN = 0.81287E+01 VFRA = 0.62374E+02 VFRC = 0.62500E+02

BOTP = 0.63312E+01 PINLET = 0.14470E+02 DPANN = 0.81352E+01 VFRA = 0.62423E+02 VFRC = 0.62500E+02

PRESSURE CONVERGENCE ERROR WAS 0.8628E-03 , DIMENSIONLESS

NUMBER OF ITERATIONS DURING LAST CONVERGENCE WAS 550

ANNULUS PRESSURE DROP WAS 8.1392E+00 LB/FT**2

CENTER SECTION PRESSURE DROP WAS 6.3302E+00 LB/FT**2

TOTAL COLD TRAP PRESSURE DROP WAS 1.4469E+01 LB/FT**2

THE NUMBER OF PRESSURE/FLOW CYCLES WAS 9

TOTAL NUMBER OF CYCLES THROUGH INNER PRESSURE LOOP WAS 9550

Distribution for ANL-83-36

Internal:

E. S. Beckjord
C. E. Till
R. Avery
L. Burris (2)
D. W. Cissel
D. R. Ferguson
B. R. T. Frost
L. G. LeSage
R. A. Lewis
R. J. Teunis
R. S. Zeno
C. S. Abrams
R. L. Breyne
P. A. Finn
S. Greenberg
D. R. Hamrin
J. E. Harmon
T. F. Kassner
V. M. Kolba (5)
L. Larsen
R. A. Leonard
R. F. Maharry
V. A. Maroni
J. M. McKee
C. C. McPheeters (5)
W. E. Miller
B. Misra
W. H. Olson
D. J. Raue (5)
W. E. Ruther
W. R. Simmons
C. R. F. Smith
F. A. Smith
M. J. Steindler (2)
R. A. Washburn
R. D. Wolson (5)
G. R. Yerbich
ANL Patent Dept.
ANL Contract File
ANL Libraries (3)
TIS Files (3)

External:

DOE-TIC, for distribution per UC-79Ta (118)
Manager, Chicago Operations Office, DOE
Director, Technology Management Div., DOE-CH
R. Tom, DOE-CH
Dep. Asst. Secretary, Breeder Reactor Programs, DOE-Wash. (2)
Chemical Technology Division Review Committee Members:
C. B. Alcock, U. Toronto
S. Baron, Burns and Roe, Inc., Oradell, N. J.
W. N. Delgass, Purdue U.